

Sara Angell Bakke
Amina Ettayebi
Ina Renate Haufe

A Stochastic Programming Approach to Optimal Operation of Low-Temperature District Heating

Master's thesis in Industrial Economics and Technology Management
Supervisor: Ruud Egging-Bratseth

June 2020

Sara Angell Bakke
Amina Ettayebi
Ina Renate Haufe

A Stochastic Programming Approach to Optimal Operation of Low- Temperature District Heating

Master's thesis in Industrial Economics and Technology Management
Supervisor: Ruud Egging-Bratseth
June 2020

Norwegian University of Science and Technology
Faculty of Economics and Management
Dept. of Industrial Economics and Technology Management

Preface

This thesis represents the completion of our Master of Science degree in Industrial Economics and Technology Management. It is written as the result of the course TIØ4905: Managerial Economics and Operational Research, Master's Thesis at the Department of Industrial Economics and Technology Management. The thesis is a continuation of our specialization project in the fall of 2019.

The thesis's motivation is related to the ongoing Low-temperature thermal grids with surplus heat utilization (LTTG+) project at SINTEF Energy Research, which looks at optimization models for local District Heating Grids. District Heating is becoming an increasingly important energy distribution system, and one research area is Demand Side Management. The assignment was to look at how District Heating Grids can benefit from Demand Side Management and Storage.

We would like to express our sincerest gratitude towards the people who have contributed to the content of this thesis. First and foremost, we thank our supervisor, Ruud Egging-Bratseth, for his support and guidance. He has granted us a high degree of autonomy while providing feedback and academic insights, which have been essential for the completion of this work. We would also like to thank Brage Rugstad Knudsen and Hanne Kauko at SINTEF Energy Research for their interesting discussions and appreciated feedback.

Trondheim, June 2020

Abstract

The growing energy demand in the world, together with the increasing challenges related to climate change, has sparked an ongoing restructuring of energy systems towards renewable energy. The variability of non-dispatchable renewable energy sources and the increasing power demand caused by increasing electrification have triggered the development of new smart energy systems. Currently, electricity covers a large part of the heating demand in Norway. Low-temperature District Heating Grids (DHGs) can contribute substantially to more efficient use of energy resources as well as better integration of renewable energy and surplus heat to cover heating demand. This thesis studies an optimization problem regarding the cost-effectiveness of utilizing waste heat, Demand Side Management (DSM) and Thermal Energy Storage (TES) in low-temperature DHGs. To solve the optimization problem, we first present a deterministic model, before expanding it to two stochastic models with uncertain Space Heating demand.

Another significant contribution of this work is the comparison of the deterministic and stochastic models and assessing the value of including uncertainty in Space Heating demand. This thesis presents both a traditional scenario tree-based model and a multi-horizon structure model. The size of the traditional stochastic model increases exponentially with the number of periods with uncertainty. By decoupling the periods with uncertainty, the multi-horizon approach reduces the problem size extensively and overcomes the computational challenges faced by the traditional stochastic model. Calculation times are reduced from about 9 hours for each problem instance to 25 seconds. In most cases, the multi-horizon model provides a satisfactory solution close to the one provided by the traditional stochastic model.

The methodology is evaluated in a planned residential area at Leangen, in Trondheim. Considering seasonal TES and DSM, the analysis in this thesis shows that a TES has the most significant impact on the annual operational cost as it allows the largest reduction of heat production from expensive heat technologies in winter months. If there is a large surplus of heat from waste incineration in the summer, the larger the TES capacity, the more production from the most expensive production technologies can be reduced, which results in a significant reduction in total operational cost. DSM is valuable both with and without TES, but with a moderately lower impact on operational cost. The availability of TES and application of DSM provides savings of up to 22% in CO₂ emissions, 11% in peak production, and 9% lower operational cost. Even if the current development of the DHG at Leangen does not consider a TES, our results indicate that the payback time for storage may be as low as 9 to 11 years, and suggest that further research should be carried out of including TES in the DHG.

Sammendrag

Den økende energietterspørselen i verden sammen med økende utfordringer knyttet til klimaendringer har ført til en omstilling av dagens energisystemer mot fornybar energi og smarte energisystemer. I dag blir en stor andel av oppvarmingsbehovet i Norge dekket av elektrisitet. Lavtemperatur fjernvarmenett kan bidra vesentlig til mer effektiv bruk av energiresurser, samt bedre integrering av fornybar energi og overskuddsvarme for å dekke oppvarmingsbehovet. Denne masteroppgaven studerer et optimaliseringsproblem som minimerer total forventet operasjonell kostnad gjennom bruk av spillvarme, styring av etterspørsel og termisk energilager i lavtemperatur fjernvarmenett. For å løse problemet presenterer denne oppgaven en deterministisk modell som utvides til to stokastiske modeller som inkluderer usikkerhet i romoppvarmingsbehov.

Et annet viktig bidrag i denne masteroppgaven er sammenligningen av den deterministiske og de stokastiske modellene, hvor verdien av å inkludere usikkerhet i romoppvarmingsbehovet blir vurdert. Oppgaven presenterer både en tradisjonell, scenario tre modell og en modell med multi-horizon struktur. Scenario treet i den tradisjonelle stokastiske modellen øker betraktelig med antall perioder med usikkerhet som inkluderes i problemet. Ved å frakoble perioder med usikkerhet klarer multi-horizon modellen å redusere størrelsen på problemet betydelig og overkomme beregningsutfordringene som den tradisjonelle stokastiske modellen har. Beregningstiden for hver probleminstans blir redusert fra rundt 9 timer til 25 sekunder. For de fleste probleminstansene gir multi-horizon modellen en tilfredsstillende løsning som er nær løsningen til den tradisjonelle stokastiske modellen.

En case-studie, som inkluderer et termisk sesonglager og styring av etterspørsel, av et planlagt boligområdet på Leangen, i Trondheim, er også gjennomført. Analysen i denne oppgaven viser at et termisk lager har størst innvirkning på den årlige driftskostnaden, da det bidrar til å redusere produksjonen fra dyre varmeproduksjonsteknologier i vintermånedene, mer enn reduksjonen som er mulig gjennom styring av etterspørsel. Styring av etterspørsel er verdifullt både med og uten et termisk lager til stede, men har en lavere innvirkning på den totale driftskostnaden. Sesonglageret og mulighet til styring av etterspørsel gjør det mulig å spare opptil 22% i CO₂ utslipp, 11% i maksimal produksjon og 9% i total driftskostnad. I tillegg, hvis det er et stort overskudd av spillvarme fra søppelforbrenning om sommeren, gjør et lager med høy kapasitet det mulig å eliminere produksjon fra de dyreste produksjonsteknologiene, noe som resulterer i en betydelig reduksjon i total driftskostnad. Selv om det per dags dato ikke foreligger noen plan om å installere et lager på Leangen indikerer resultatene våre at tilbakebetalingstiden kan være så lav som 9 til 11 år for det termiske lageret. Basert på resultatene foreslår vi at ytterligere analyse av lager i fjernvarmenettet på Leangen bør utføres.

Table of Contents

Preface	i
Abstract	ii
Preface	iii
Table of Contents	vi
List of Tables	viii
List of Figures	x
Acronyms	xi
1 Introduction	1
2 Background	3
2.1 District Heating Grids	3
2.2 The market for District Heating in Norway	5
2.3 Supply of District Heat	6
3 Literature Review	11
3.1 District Heating Grids	11
3.2 Thermal Energy Storage	14
3.3 Demand Side Management	16
3.4 Stochastic Programming	18
3.5 Time Series Analysis	26
3.6 This Work	28
4 Problem Description	29
5 Model Formulation	32
5.1 Assumptions and Explanations	32
5.2 Deterministic Model	34
5.3 Expanding the Model to Incorporate Uncertainty	41
5.4 Traditional Stochastic Model	43

5.5	Multi-horizon Stochastic Model	47
6	Data Analysis	49
6.1	Datasets	50
6.2	Parameters	53
6.3	Regression Model for Space Heating Demand	61
7	Scenario Generation	65
7.1	The Scenario Generation Algorithm	65
8	Comparative Analysis	71
8.1	Hardware and Software	72
8.2	Evaluation of the Stochastic Method	72
8.3	Evaluation of Decisions Made in the Models	75
9	Case Study - Leangen	80
9.1	The Base Case	82
9.2	The Base Case with TES	83
9.3	Different Deficit and Curtailment Costs	85
9.4	Different SH Demand Requirements	90
9.5	Different HW Demand Requirements	94
9.6	Increased Waste Heat and Larger TES	97
9.7	Investment Cost Analysis of TES	100
9.8	Comparison of DSM and TES	102
9.9	Data Limitations	103
10	Concluding Remarks and Future Research	105
10.1	Concluding Remarks	105
10.2	Future Research	107
	Bibliography	116
	Appendices	117
A	Traditional Stochastic Model	118
A.1	Indices, sets, parameters and variables	118
A.2	Objective function	120
A.3	Constraints	121
B	Multi-horizon Stochastic Model	124
B.1	Indices, sets, parameters and variables	124

B.2	Objective function	126
B.3	Constraints	127
C	Averaged electricity price	129
D	Production mix in Trondheim	130
E	Production mix at Leangen	131
F	Regression	132
F.1	Optimal lag length for apartments	132
F.2	Regression functions	132
G	Temperature scenarios	135

List of Tables

- 3.1 Overview of DHG generations. 12
- 3.2 Article overview: Selected articles addressing grid optimization. 28

- 6.1 Peak hours during a typical day for nine user profiles at Leangen. 52
- 6.2 Peak hours during a typical day for five user profiles at Leangen. 52
- 6.3 Production costs for different production technologies. 54
- 6.4 Monthly production technology capacities in kWh. 56
- 6.5 Hourly lower and upper bounds for SH demand fulfillment at Leangen. . . 60
- 6.6 Lower and upper interval bounds for SH demand fulfillment at Leangen. . 60
- 6.7 Coefficients in the regression functions for the five building types. 63
- 6.8 R-squared values for the five building types. 64

- 7.1 Probabilities for temperature scenarios from September to April. 69

- 8.1 Abbreviations used in this chapter and Chapter 9. 71
- 8.2 Details of computer and solver for the traditional stochastic model. 72
- 8.3 Details of computer and solver for the deterministic and multi-horizon model. 72
- 8.4 Production capacities in kWh for the production technologies in the summer. 74
- 8.5 VSS calculated for the multi-horizon model and traditional stochastic model
for the four problem instances with fixated TES level at the end of August. 75
- 8.6 The BC for the multi-horizon and the traditional stochastic model. 76
- 8.7 Total operational cost and maximum TES level for the four problem instances. 77

- 9.1 Settings for the cases analyzed. 81
- 9.2 The BC for the two model types. 82
- 9.3 The BC with a TES. 83
- 9.4 Cost for different DSM decisions. 86
- 9.5 Results from different deficit and curtailment costs without TES. 86
- 9.6 Results from different deficit and curtailment costs with TES. 89
- 9.7 Results from changing SH demand requirements. 91
- 9.8 Change of HW demand requirements with no TES. 94
- 9.9 Models analyzed with three different storage sizes. 98

9.10 Profitability analysis of the different TES sizes.	101
F.1 Optimal lag length for apartments.	132

List of Figures

1.1	Global consumption of energy divided by sectors in 2015.	1
2.1	A DHG with two parallel heating centrals and three consumers.	4
2.2	Average price rate for DH in Norway, excluding VAT.	5
2.3	Distribution of consumption of district heating.	6
2.4	Net production of district heating in Norway in 2018 given in TWh.	7
3.1	Stochastic scenario tree.	19
3.2	Independent deterministic problems.	19
4.1	An example of a DHG layout with nodes.	30
4.2	Operational distribution of DH.	31
5.1	Multistage scenario tree.	42
5.2	Scenario tree with multi-horizon structure.	43
6.1	Layout of the DHG at Leangen.	50
6.2	Layout of nodes at Leangen.	51
6.3	The difference in total delivered heat with five and nine user profiles.	53
6.4	Hourly averaged local waste heat supply at Leangen.	58
6.5	Hourly averaged heat demand for HW at Leangen.	59
6.6	The difference in SH demand for load profile generator and regression model.	64
7.1	Clusters for September to April.	68
7.2	Low, medium and high-temperature scenario for September.	69
8.1	Problem instance: DSM & TES.	78
8.2	Problem instance: EL boiler.	78
8.3	Problem instance: Bio boiler.	78
8.4	Problem instance: Natural Gas.	78
9.1	Storage level for the deterministic model and the multi-horizon model.	84
9.2	Production mix for the BCs with and without TES.	84
9.3	Production mix for the deterministic model.	88

9.4	Production mix for the multi-horizon model.	88
9.5	Production mix for the deterministic model with a TES.	90
9.6	Production mix for the multi-horizon model with a TES.	90
9.7	TES level for changed SH demand requirements.	92
9.8	Difference in production mix from BC.	92
9.9	Total delivered heat versus target demand.	93
9.10	Delivered HW versus target HW demand in the multi-horizon model.	96
9.11	Electricity used in January for the multi-horizon cases.	97
9.12	Electricity used by HPs and EL boiler in January for Case 28.	97
9.13	Production mix for cases with increased waste heat and different TES sizes.	99
9.14	TES level for cases with increased waste heat and different TES sizes.	100
C.1	Electricity price (NOK/kWh).	129
D.1	Production mix in Trondheim for 2019 in MWh.	130
E.1	Proposed production mix at Leangen in kWh.	131
G.1	Scenarios for September.	135
G.2	Scenarios for October.	135
G.3	Scenarios for November.	135
G.4	Scenarios for December.	135
G.5	Scenarios for January.	136
G.6	Scenarios for February.	136
G.7	Scenarios for March.	136
G.8	Scenarios for April.	136

Acronyms

BC Base Case.

CHP combined heat and power plant.

COP Coefficient Of Performance.

DH District Heat.

DHG District Heating Grid.

DHO District Heating Operator.

DR Demand Response.

DSM Demand Side Management.

EL Electricity.

GHG Greenhouse Gas.

HP Heat Pump.

HW Hot Water.

LPG Liquefied Petroleum Gas.

LTTG+ Low-temperature thermal grids with surplus heat utilization.

NG Natural Gas.

SH Space Heating.

TES Thermal Energy Storage.

Chapter 1

Introduction

The world's energy demand is expected to rise by 1% annually through 2040 (IEA 2019). Industrialization, urbanization and digitization have been forming the modern energy consumption trends. Consumers have an increasing environmental focus and the demand for clean energy is high, putting pressure on reducing fossil energy consumption. Buildings account for about 30% of the current global energy consumption (Figure 1.1) and heating accounts for roughly half of the buildings' energy consumption (Kauko 2018). Electricity alone can not meet the increasing energy demand that follows the increasing population in the world but should be met by a combination of smarter electricity, natural gas, and thermal heating grids based on the utilization of waste heat and renewable sources.

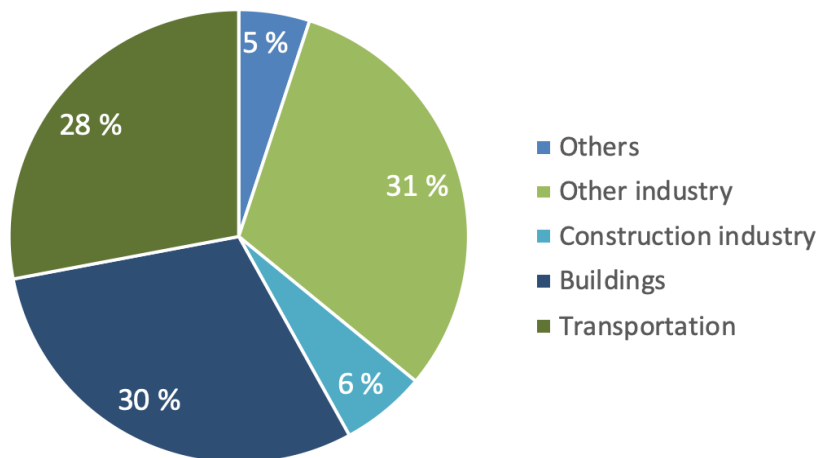


Figure 1.1: Global consumption of energy divided by sectors in 2015.
Source: Own illustration based on UN-Environment (2017).

The European Technology and Innovation Platform on Renewable Heating & Cooling has an ambition that heating and cooling demand in Europe should be covered by 100% renewable energy by 2050 (Lettenbichler and Provaggi 2019). At the same time, new buildings in the EU are required to have low energy consumption (Council of European

This introduction is a moderately revised version of the one in our specialization project.

Union 2018). New apartment buildings in Norway are required to have a lower net energy demand than 95 kWh/m^2 , while the net energy demand in new office buildings must be below 115 kWh/m^2 (*Byggteknisk forskrift [TEK17]* 2017). In 2007, these requirements were 120 and 165 kWh/m^2 , respectively (*Byggteknisk forskrift [TEK07]*). These ambitions require rethinking and redesign of the current energy systems and transitioning to smart energy systems. To this end, low-temperature District Heating Grids (DHGs) and Demand Side Management (DSM) can play a central role in reducing CO_2 emissions from the heating of buildings.

District Heat (DH) is advantageous because it enables economic utilization of energy sources that otherwise would be wasted. Today's DHGs operate with high temperatures causing high heat losses. Modern heating grids, often referred to as 4th generation DHG, will be designed with lower distribution temperatures to reduce losses and enable the grid to use lower temperature heat sources, such as urban waste heat (e.g., heat recovered from data centers, metro stations). In the future, low-temperature DHGs will be essential to enable smart energy systems. Integrating and utilizing several types of energy sources in the DHG increases the complexity, and challenges the cost-effective management of the DHG, including efficient use of waste heat and storage to reduce fossil fuels that cover peak demands.

In this project, we have worked with SINTEF Energy Research, who leads the research project Low-temperature thermal grids with surplus heat utilization (LTTG+). The project tests the possibilities and advantages of implementing smart heating solutions that provide heat with low heat losses (Kauko 2018). The purpose of this thesis is to develop an optimization model to support a cost-minimizing operation of low-temperature DHGs. The thesis will analyze how to optimally manage consumers' demand using waste heat, controllable energy sources, DSM techniques, and TES. With this, contribute to making DHGs more profitable and preferable as a heating source for buildings.

This thesis is divided into ten chapters. Chapter 2 describes the background for the problem in this thesis with an introduction to District Heating Grids. In Chapter 3, a review of related literature is given before describing the problem in detail in Chapter 4. Chapter 5 presents the deterministic and stochastic mathematical formulations of the problem. Next, in Chapter 6, we document and present the data from the DHG at Leangen (Trondheim) before presenting the scenario generation for the stochastic models in Chapter 7. The models are evaluated in the comparative analysis in Chapter 8, while the models are used to analyze the Leangen case study in Chapter 9. Lastly, the thesis concludes and suggests future work in Chapter 10.

Chapter 2

Background

In this chapter, the background of the thesis is presented. The chapter starts with describing District Heating Grids (DHGs) and how the market and production for District Heat (DH) work in Norway. Next, we present an introduction to 4th generation District Heating Grid (DHG) and its main differences with conventional DHG.

2.1 District Heating Grids

The description of DHGs in this section will apply to most DHGs used today in the western world. Later in the chapter, a description of several generations of DHGs will follow.

District Heating Grids distributes heat from supply sources to end-users. From a heating central, hot water is provided to buildings through a system of pipes called supply pipelines. The heating central can produce heat (e.g., from boilers), or operate as a gathering point for produced heat (e.g., renewable energy or thermal energy developed as a by-product). Heat is distributed to heat substations that connect the main grid to the consumers' heating system. The temperature of the hot water is lowered as heat is emitted to the substations. The grid also contains return pipelines that transport the cooled water back to the heating central. At the heating central, the cooled water is reheated and injected into the supply pipelines again (Sarbu and Sebarchievici 2016). The temperature of supply water generally ranges from 70°C to 150°C, while the return temperature is generally between 45°C and 60°C (Rutz et al., 2019; Zinko et al., 2005).

A consumer in a DHG can be a single household, groups of households, or a large complex building such as a factory or an office building. When hot water is supplied through supply pipelines, it can be used directly or indirectly. Directly means that the water from the supply pipeline also flows through the heating pipelines in the building. Heat is used indirectly when a heat exchanger captures and transfers it to the heating system inside

This background is a moderately revised version of the one in our specialization project.

the building (Sarbu and Sebarchievici 2016). Figure 2.1 shows an example of a DHG with two heating centrals, two TESs, and three consumers (two residential buildings and one factory). In the figure, supply pipelines are indicated with red and return pipelines with blue.

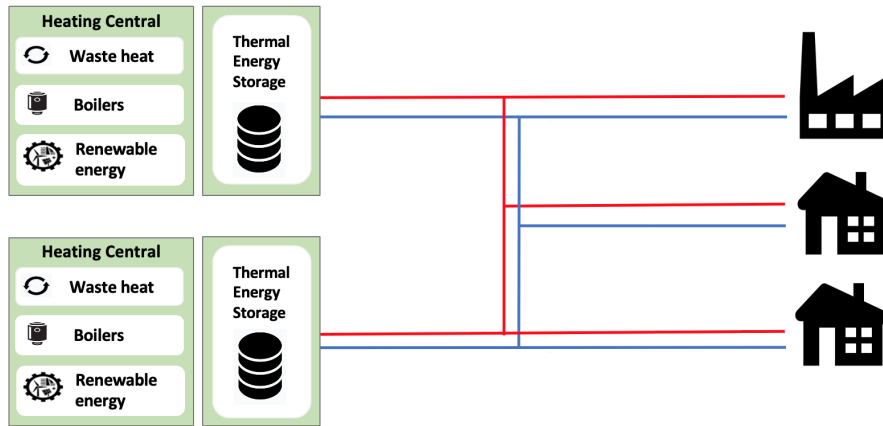


Figure 2.1: A DHG with two parallel heating centrals and three consumers.
Source: Own illustration.

The fundamental idea behind the development of newer DHGs is to use local waste heat and fuel sources that under normal circumstances would be wasted or remain unused. Energy recovery of waste heat from industrial activities is an example of available surplus heat sources in cities. Smart DH technology is a new technology that enables efficient use of CO₂ neutral energy sources to cover the heating demand of buildings (Gao et al. 2017). Also, it contributes to reducing primary energy demand and CO₂ emissions (Kauko 2018). Smart DHGs are suited for the integration of renewable and low-carbon energy sources in addition to waste heat. In periods with high heat consumption, the peak demand can be covered by electric or fossil-fuelled boilers. However, fossil energy sources have a huge negative environmental impact and are gradually replaced by bio-energy and waste heat. According to Norsk Fjernvarme (2015), by 2020, all DH in Norway should be supplied from CO₂ neutral energy sources.

District Heat strengthens the security of energy supply. DHGs in Oslo and Trondheim are well developed and cover up to 40% of the total energy demand in Norwegian buildings on the coldest days (Norsk Fjernvarme 2015). Thus, by constructing district heating infrastructure, the need for investments in the electric grid is reduced. Additionally, DHGs are energy flexible systems that utilize the most affordable and cost-effective energy sources. Resulting in a low production cost and a supply competition between District Heat and other energy carriers such as electricity, gas, and oil (Norsk Fjernvarme 2015).

2.2 The market for District Heating in Norway

In Norway, the price of District Heat is always stated by law to be less than the price of electric heating (*Norwegian Energy Act § 5-5* 1990, June 29). District Heat is similar to electricity in the degree that it is not economically rational to have more than one DHG in a geographic area, which means that the DH has a natural monopoly. In the electric power market, only the distributors have a monopoly, while there is an open market for power suppliers. Therefore, power prices are established in the competitive market. In contrast, the supply and distribution of DH are normally sold as one product in Norway (NVE 2015). The monopoly on DH gives the District Heating Operators (DHOs) an advantage when setting the price, as it is mostly up to each distributor to set the price. However, they are subjected to laws and regulations like the *Norwegian Energy Act § 5-5*.

The average price rate for DH in Norway, excluding VAT, is presented in Figure 2.2. Due to the *Norwegian Energy Act § 5-5*, the DHO has to provide a lower price for DH than the power price. The DH tariff consists of the power spot price provided by Nordpool, electricity certificate cost, administrative surcharge, grid cost, electricity fee, and a discount rate (Fortum 2019). As an example, Fortum Varme has a 2% discount on the DH tariff rate for detached and town-houses, while commercial buildings and housing cooperatives have a discount of 5% (Fortum 2019).

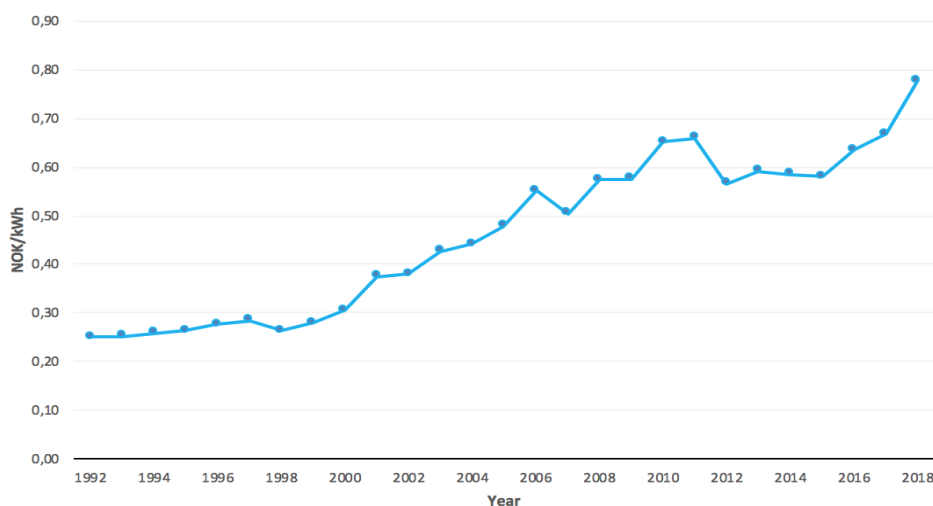


Figure 2.2: Average price rate for DH in Norway, excluding VAT.

Source: Own illustration based on SSB (2018).

2.3 Supply of District Heat

Here we discuss the supply and production in Norwegian District Heating Grids and describe some typical grid components.

2.3.1 Supply of District Heat in Norway

In Norway, the use of District Heat has doubled since 2007. Excluding Svalbard, the heat supply from DHGs in 2018 was 5.7 TWh (Bøeng 2019). Still, District Heat only contributes to 3% of the total energy consumption in Norway, and approximately 10% to the heating of buildings (Olje- og energidepartementet 2019). Figure 2.3 shows the distribution of DH in Norway from 1992 to 2018. The service industry accounted for the largest share of consumption with 62%, households accounted for 22%, while the rest went to the industry and other businesses (Bøeng 2019). The service industry is the group that has increased consumption the most over the last 20 years.

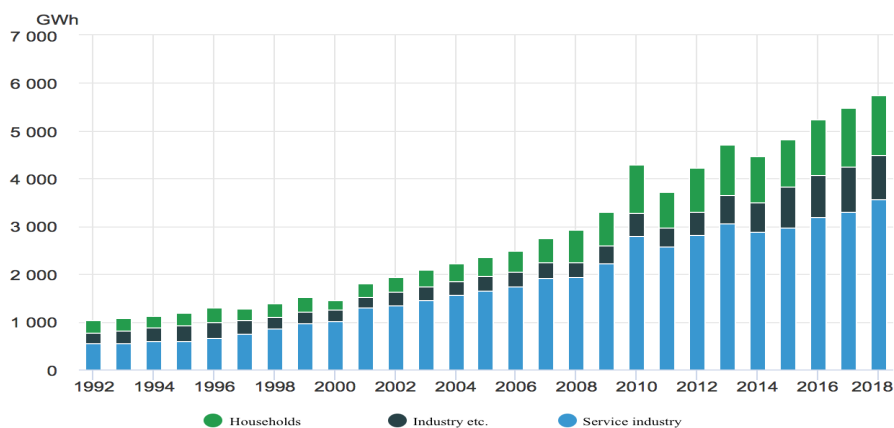


Figure 2.3: Distribution of consumption of district heating.
Source: Bøeng (2019).

Generally, the composition of energy sources in DHGs varies with availability and energy price. In 2018, the net production of District Heat was 6.5 TWh. The transmission losses account for about 12% of the net production, and therefore 5.7 TWh was distributed to the consumers. Figure 2.4 presents the net production of District Heat in 2018 from various energy sources in Norway. The figure shows that 2.9 TWh of the net production came from waste incineration, and 1.5 TWh from burning wood chips (Bøeng 2019). Other energy sources for the DHGs include urban waste heat, while boilers based on electricity, gas, and oil are used to cover peak loads. The use of oil boilers in DHGs has decreased in recent years, and in 2018, oil boilers provided less than 1% of the total DH supply.

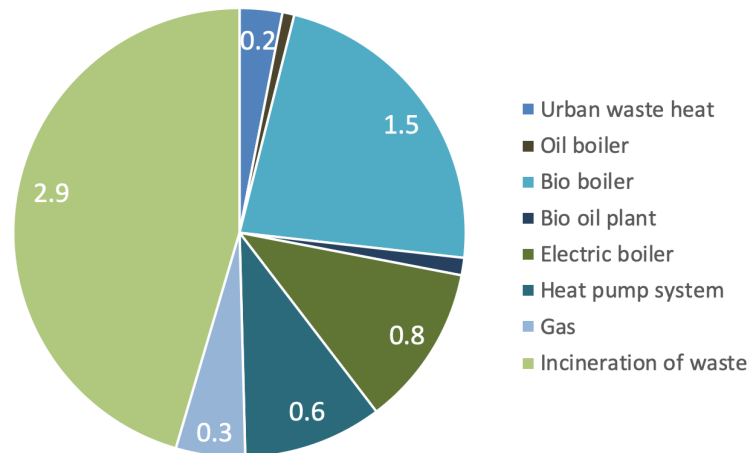


Figure 2.4: Net production of district heating in Norway in 2018 given in TWh.
Source: Own illustration based on SSB (2018).

One important distinction between the different heat sources is their controllability. Managing the consequences of using uncontrollable sources is one aspect that needs to be addressed in low-temperature DHGs.

2.3.2 Uncontrollable Energy Technologies

Renewable energy, such as heat harvested by solar collectors, is an intermittent (uncontrollable and irregular) energy supply source. Waste heat from discontinuous processes is also an intermittent heat source that is typically released to the environment and ignored as a by-product. In the context of smart DH, a better term for waste heat is resources that otherwise would be unused. The largest part of waste heat in Norway comes from waste incineration, while a small part comes from industrial waste heat. Only 3% of DH's net production in 2018 came from industrial waste heat (Figure 2.4). Local situations may allow more significant shares, and newer generations of DHGs can integrate excess heat from data centers, supermarkets, office buildings, ice rinks, and industry, hereafter referred to as urban waste heat.

The waste heat resource can be directly used when the temperature is higher than the return temperature of the DHG. Otherwise, the temperature must be lifted by a Heat Pump (HP). Industrial waste is an unstable heat source as it depends on the industry's operating hours and the season. The majority of energy in industrial processes is of high grade, such as steam and combustible gas. High-grade energy is generally used for internal power generation within the industry as the temperature is above 400°C. However, low-grade energy, mostly between 30°C and 200°C, is likely discarded to the environment if

not used as supply in DHGs. Another reason why industrial waste heat represents a low contribution to the supply of DH is the technical issues with integrating this heat source. The industry is usually far from the DHG, which can lead to significant investment costs in transmission grids and large heat losses due to long transmission distances (H. Li and Nord 2018).

2.3.3 Controllable Energy Technologies

The main contribution from controllable energy technologies to the DHGs is from peak load boilers. Boilers are closed containers where a fluid (usually water) is heated. There exist many types of boilers, e.g., boilers based on biomass, bio-oil, electricity, Natural Gas (NG), Liquefied Petroleum Gas (LPG), and oil. However, this section will cover two of the most commonly used boilers in Norwegian DHGs, boilers based on biomass and electricity (*ENØK i bygninger : effektiv energibruk* 2007).

A bio boiler produces heat from combusting wood chips, wood pellets, or firewood. Bio boilers that run on wood chips are the most common energy source after waste incineration in Norway (Figure 2.4). The main advantages of bio boilers are high energy efficiency and reduction of CO₂ emissions. According to ENOVA, a pellet boiler can be as efficient as 90%, and with energy recovery technology in DHGs, the efficiency can be even higher (Tereshchenko 2016). The costs of biomass fuels are typically lower than for fossil fuels and can, therefore, reduce operational costs.

Electric boilers convert electrical energy into heat, and there exist several different types (*ENØK i bygninger : effektiv energibruk* 2007). They are often used when the power price is lower than combustible fuels. Therefore, they are used to some extent in countries that occasionally have low power prices, such as Norway. Electric boilers have a short start-up time and are easy to control as electricity is the only input needed, and no fuel feeding is required. Electric boilers are very efficient as they only have a minuscule heat loss (*ENØK i bygninger : effektiv energibruk* 2007). Consequently, they often work as back-up sources to cover peak demand and extreme operation situations (Tereshchenko 2016).

2.3.4 Thermal Energy Storage

TES's primary purpose is to store heat when production exceeds consumer demand and make it available in peak periods. TES can be short-term (e.g., hot water tanks) or long-term. Seasonal TES is long-term storage designed to collect heat during the summer when the heat demand is low and preserve the stored heat for consumption during the winter (Dinçer and Rosen 2010).

District Heating Grids can benefit from TES to avoid costly, usually fossil-fired boilers to cover peak demand. Implementing TES in a DHG can help the DHO to better schedule its production and improve its operational efficiency. Since the DH demand can vary on a daily, weekly and seasonal basis, TES contributes significantly to reducing peak demand, reducing the environmental burden from fossil fuels, and exploiting CO₂ neutral energy sources.

2.3.5 Heat Pumps

Large scale HPs can be used in DHGs to utilize free heat from the surroundings. A HP uses electricity to lift the temperature from the ambient heat temperature to the desired temperature (NOVAP 2018). Ambient heat can be waste heat from industry and buildings, heat from seawater, river water, or geothermal heat. The heat from these sources rarely have high enough temperatures to be used directly in DHGs; therefore, HPs are usually needed (Norsk Fjernvarme 2018).

A simple HPs consists of an evaporator, a compressor, a condenser, and an expansion valve. A working fluid is circulating inside the HPs, switching between liquid and gas state. In the evaporator, the working fluid absorbs heat from the heat source with relatively low temperature (ambient heat). The compressor uses electricity to run the process of increasing the pressure before heat is delivered through the condenser at the desired temperature.

Each HP has an efficiency, which is most commonly evaluated by the Coefficient Of Performance (COP), which describes the ratio between delivered heat at the desired temperature and the electricity used to run the process (NOVAP 2020). The COP usually lies between 2 and 5, dependent on the temperature lift (NOVAP 2018). A COP of 3 signifies that 3 kWh heat is delivered from 1 kWh electricity, which is possible due to the free ambient heat absorbed by the HP (Norsk Fjernvarme 2018). In comparison, if no HPs is present, 3 kWh of electricity will be used to supply 3 kWh of heating.

The COP for a HP is needed to find the amount of power required to provide the desired heat output. COP is calculated based on temperature parameters (in Kelvin units), and the general equation for COP is shown in Equation 2.1. The power amount (W) that is needed to lift the incoming heat's temperature to the desired output temperature can be found by dividing the heat output ($Q_{condenser}$) by the COP.

$$COP = \frac{Q_{condenser}}{W} = \frac{T_{condenser}}{T_{condenser} - T_{evaporator}} \longrightarrow W = \frac{Q_{condenser}}{COP} \quad (2.1)$$

Chapter 3

Literature Review

This chapter provides an introduction to the existing literature on topics related to District Heating Grids (DHGs), Thermal Energy Storage (TES) and Demand Side Management (DSM). There is to our understanding limited research on applying optimization models to the operation of low-temperature DHGs, which include TES and DSM. Therefore, this literature review's main focus is on the operation of both conventional DHGs and power grids, which share many characteristics with modern DHGs. The first part of this chapter presents the evolution of District Heating Grids, followed by an introduction to Thermal Energy Storages and Demand Side Management. In the second part of this chapter, we introduce the main ideas and definitions of stochastic programming as well as different solution methods for stochastic problems, including multi-horizon stochastic programming. The definition of stochastic programming and multi-horizon stochastic programming forms the basis for the stochastic models proposed in Chapter 5. Lastly, a brief introduction to scenario generation and time-series analysis is done before placing our work in the context of existing literature.

3.1 District Heating Grids

District Heat has an important role in improving indoor thermal comfort and saving primary energy consumption (Jie et al. 2015). The characteristics and design of DHGs have changed in relatively large steps at a time, referred to as DHG generations. The most apparent trend throughout the generations is the decrease in the heat carrier's supply temperatures in order to reduce transmission heat losses (Lund et al. 2014). Kauko, Kvalsvik, et al. (2017a) claim that sufficiently low supply temperatures makes it possible to reduce transmission heat losses by up to one third. The 1st generation DHGs used steam as a heat carrier, while the 2nd and 3rd use pressurized hot water. The supply temperatures associated with the 2nd generation are high, mostly over 100°C, while the supply temperatures in the 3rd generation DHGs are lower, often below 100°C (Lund et al.

The literature review is based on the same topics as in our specialization project, but extended with literature on stochastic programming, scenario generation, and time series analysis.

2014). Today, most DHGs in Europe, the US, China, Korea, and Canada belong to the 3rd generation, which was introduced in the 1970s (Lund et al. 2014). According to Lund et al. (2014), 4th generation DHGs can supply low-temperature DH for Space Heating (SH) and Hot Water (HW) to existing and new buildings. Table 3.1 summarizes the main technical characteristics and objectives of the four DHG generations.

Table 3.1: Overview of DHG generations.

Generation	Technical characteristics	Target
First	Steam as the heat carrier	Reduce the use of individual boilers
Second	Pressurized hot water as the heat carrier (above 100°C)	Fuel savings and better comfort
Third	Pressurized hot water as the heat carrier (below 100°C)	Increase energy efficiency and minimize fuel cost
Fourth	Lower distribution temperatures and integration of sustainable energy sources	Cost minimization, reduce emissions and heat losses

Source: Lund et al. (2014).

The primary motivation behind the 1st generation of DHGs was to replace individual boilers in buildings to increase comfort and reduce the risk of boiler explosions. However, there were many challenges related to 1st generation DHGs. The main challenge for authorities was to provide proper planning and market regulation, causing the transition to 2nd generation in the 1930s, where the focus shifted to fuel cost savings and consumer comfort (Lund et al. 2014).

The transition from 2nd to 3rd generation DHGs caused problems due to the old grids' lack of monitoring systems, which made it challenging to optimize the new grids, primarily because the target heat load values for the older grids were overestimated (Lefter et al. 2014). A technical and costly challenge with 3rd generation DHGs is transmission heat losses. To address this, researchers and grid operators focus on the optimal design of new grids and refurbishment of existing grids (e.g., Adamo et al. (1997)). The results obtained by Adamo et al. (1997) show that significant savings can be achieved by optimizing the diameter and the wall thickness of the pipes. The best solution for the specific case discussed in the paper is to reduce the diameter and increase the wall thickness. Another concern with the current operation of 3rd generation DHGs is the peaks that often occur during cold seasons. Energy systems are usually dimensioned to cover peak load, which implies that the systems are built to exceed the capacity necessary to meet peak load. Therefore, peak reduction is an effective measure to reduce investment costs.

The development of modern District Heating Grids (e.g., 4th generation DHGs) has proved to be a major contribution to reducing Greenhouse Gas (GHG) emissions in many countries. The most significant advantage of 4th generation DHGs is the possibility to combine heat from renewable energy sources (e.g., solar energy) with recycled heat from low-temperature sources, such as urban waste heat. From an economic point of view, utilizing low-temperature recycled heat can lead to reduced resource consumption and, therefore, lower fuel costs. Moreover, it is an extremely flexible energy source that can make use of any fuel, which ultimately can increase price stability and contribute to providing heat at competitive prices (Schmidt et al. 2017). The transition to 4th generation District Heating Grids is a challenging issue, and in the future, DHGs still face issues such as transmission heat losses, although less than in 3rd generation DHGs.

Another aspect of the transition from 3rd generation to 4th generation DHGs is the potential of decreasing heat demand in newer buildings (H. Li and Nord 2018). Lower heat demand makes the established pipelines in 3rd generation DHGs over-dimensioned, which generally implies higher loss rates. Therefore, it will be important to focus on system design, integrating cheap heat sources, and customize operations in different areas. Newer buildings do not have heat supply problems from 4th generation DHGs, as they can be designed to utilize low-temperature DH. However, as indicated by Rønneseth and Sartori (2019), the problem lies with existing high-grade heat consumers. Therefore, a natural transition to 4th generation DHGs will start in new building areas consisting of modern buildings with low heat demand (SINTEF 2018).

There exists limited research on minimizing operational costs for 4th generation DHGs. Vesterlund et al. (2017) analyze a complex, multi-source high-temperature DHG to find out how supply temperature, pressure, the thermal efficiency of heat production, and thermal losses affect operational costs. Wahlroos et al. (2017) investigate how excess heat can increase the effectiveness of DHGs by reducing boilers' operating hours and other controllable sources through a simulation. The results were a reduction in operational costs and fuel savings. In the study, utilization of waste heat had the potential to reduce the operational costs by up to 7%, depending on the level of waste heat. Dorotić et al. (2019) emphasize the importance of integrated heating and cooling systems in 4th generation DH by proposing a multi-objective optimization model for combined district heating and cooling systems. One objective in the paper is to minimize the total system cost, including both investment and operational costs, while the second objective is to minimize CO₂ emissions. Another possibility is to allow heat exchange between buildings (i.e., surplus heat is transferred to other buildings). The model was implemented in an urban area in Risch Rotkreuz, Switzerland, by Sameti and Haghghat (2019). The

case study focuses on the potential cost reduction when there is heat exchange between buildings in a 4th generation DHGs, but does not consider the case when there is no heat exchange between buildings. The results show that allowing heat exchange among the buildings leads to a 25% reduction in total annualized cost and a 5% reduction in emission compared to conventional DHGs.

Similar to 4th generation DHGs, there exists a concept about 5th generation DHG, which has even lower supply temperatures. The goal of reducing supply temperature further enables even lower temperature waste heat usage and better facilitates prosumers, buildings that act as both consumer and producer (Von Rhein et al. 2019). This thesis focuses on low-temperature DHGs, which can be either 4th or 5th generation DHGs.

Smart energy grids are needed in the future to implement more renewable energy sources and facilitate the interaction of prosumers. Electric smart grids require a significant expansion of the existing power grid and significant investment in storage technology. In contrast, smart energy systems (consisting of smart electric, thermal, and natural gas system) can be implemented with fewer investments as it requires minor expansion in existing grids and storage (Lund 2018). A study on different alternatives, such as smart power grids and smart energy systems in Denmark, is done by Lund (2018). In Denmark, the infrastructure for DHGs is already built, which results in smart energy systems being the most affordable option due to its high efficiency and ability to recycle low-temperature heat. In the study, smart energy systems show great potential to cover future energy demand compared to power grids alone. To achieve this, the focus of the future energy systems should be on integrating electricity, heating (e.g., through low-temperature DHGs), cooling, natural gas, flexible demand and various storages (H. Li and Nord 2018).

3.2 Thermal Energy Storage

Thermal Energy Storage systems have become an important part of many DHGs. TESs can be filled when the District Heat demand is low (e.g., in the night) and used for heating and cooling applications when the request is high (e.g., in the morning) (Sarbu and Sebarchievici 2018). In particular, the use of TES systems increase in buildings and industrial processes because of their advantages, as TES enables heat storage to meet demand in later periods. The advantages are more prominent in the winter when the heat demand is high, and the use of peak heating boilers is necessary. TESs allows for a reduction in heat produced by boilers and contribute to reductions in operational costs and less pollution of the environment (Dinger and Rosen 2010). E.g., for electric boilers,

this can potentially save money as it is possible to take advantage of fluctuating power prices by producing and storing heat when it is cheap and using the stored heat to meet demand when power prices are high (de Oliveira et al. 2016).

TESs play a big part in improving the thermal reliability and performance of DHGs, and therefore, designing efficient and economical TESs is an essential focus of the existing literature. A TES system can be described in terms of numerous characteristics that highly depend on the form of energy stored (e.g., water, liquid nitrogen). Capacity primarily depends on the size of the storage device and defines the energy stored in the system. Power is how fast the energy stored in the system can be added and withdrawn while the efficiency ratio defines the energy loss during the storage period and the adding/withdrawing cycle (IRENA 2013). When designing the optimal TES, the trade-off and correlation between thermodynamical quality and cost must be evaluated. Both capacity costs and operational costs (e.g., production costs, adding/withdrawing costs) should be considered (IRENA 2013). The combination of different characteristics for TES (e.g., size, location) in a DHG is researched by Leško et al. (2018), to maximize flexibility at the lowest possible cost. Out of the TES options researched in the paper, hot water tanks were the most profitable solution from an operating cost perspective.

The storage period is a property that defines the period when energy is stored before consumption is withdrawn (IRENA 2013). TES types can be categorized as long-term and short-term. For instance, the long-term can be a seasonal storage that allows the use of heat some months after storing it. Another valuable property is the locations of TESs in the DHGs, which can either be decentralized or centralized. In the latter, the TES is located in a central location serving the entire grid, while decentralized TESs are smaller and can be located anywhere in the grid (e.g., co-located with the consumers). Bachmaier et al. (2015) analyze the flexibility of a centralized and decentralized TES in a DHG. The results from the investigated case show that operating decentralized TESs is nearly as efficient as operating a centralized TES.

Water is the most common heat carrier in TES, and hot water tanks are well-used for short-term storage in DHGs (Basecq et al. 2013). The most promising and economically feasible solutions for long-term thermal storage can be divided into two main categories, systems separated and insulated from the ground and systems integrated with the ground. Examples of systems belonging to the first category are large underground tanks, with water as a storage medium, and pit thermal energy storage. The latter is an artificial pool with a lid, filled with water or a water gravel-mixture. Systems integrated with the ground are borehole thermal energy storage and aquifer thermal energy storage. Hot water is pumped in/out from boreholes in the ground, while aquifer storage utilizes natural

deposits of groundwater (Mangold and Deschaintre 2015). Storing heat in a long period incur heat losses to the environment. Nordell (1994) explains that seasonal TES based on borehole technology has high losses during the first years of operation. However, the losses decrease significantly over the years of operation when the ground temperature stabilizes.

3.3 Demand Side Management

Demand Side Management considers activities and behaviors related to control and modification of energy consumption (D. Li et al. 2016). The activities aim for energy conservation and energy efficiency, and can, for instance, involve energy storage. Behaviors are ways of acting that support the execution of the activities (e.g., device installations, policies, regulations, and education). DSM originated from the energy crisis in 1970 when the Western world faced substantial petroleum shortages. Today, DSM techniques are an important tool in optimizing energy consumption, in terms of GHG emissions and energy system reliability (D. Li et al. 2016).

Demand Side Management is best explored in the electricity sector (D. Li et al. 2016). It is often less expensive to implement a form of DSM control than to build new power plants and energy infrastructures. Therefore, DSM can be especially useful for grids with capacity challenges (Palensky and Dietrich 2011). Several of the DSM techniques, like Demand Response (DR), aim to reduce consumer energy demand, primarily during peak load periods (Boshell and Veloza 2008). DR in the electricity sector is described by Balijepalli et al. (2011) as changes in consumers' normal consumption patterns in response to incentive payments or changes in the price of electricity.

Some of the services DR techniques provide to the electricity market are also relevant in the District Heating market, e.g., peak shaving, which reduces energy demand during peak periods (Zhou et al. 2008). This technique will result in lower energy consumption, as the energy demand is permanently removed, often referred to as curtailment load. Another DR technique, which can be used to reduce peak load, is load shifting. This technique involves moving a certain amount of load from a period to another, for instance, from peak time to off-peak time. For load shifting to be possible, the load needs to be deferrable (capable of being postponed) or adjustable (the consumption can be adjusted to a different level) (D. Li et al. 2016). It could, for instance, be possible to start Space Heating of an office building night to Monday (off-peak time) instead of Monday morning (peak time). Although load shifting can reduce demand in critical periods, it must be emphasized that the total energy consumption in a longer period (e.g., a day) will remain relatively unchanged, as the load is moved and not curtailed.

The body of literature on optimization models using DSM has been growing rapidly in recent years. The majority of these studies focus on power grids and the power electricity market. Optimization models for DHGs share many characteristics with models for the power market, and it can be assumed that DSM implementation in a DHG will give many of the same benefits as DSM in a power grid. A study done by Ottesen and Tomasgard (2015) shows that benefits from DSM in the electricity market are linked to reductions in cost, peak load, and CO₂ emissions. The study uses DSM in a decision support model that seeks to find an optimal strategy for utilizing flexible units in buildings. In general, energy-flexible units in buildings can react to an external signal that it receives from outside the building, and in that sense, it can be used to provide DSM and DR based on grid requirements. The authors categorize load units into inflexible, shiftable, and curtailable. They find a net cost saving of 12% in the case study considering a Norwegian university building. Based on electricity price fluctuations during the day, decisions are made on the utilization of flexible sources (e.g., electric versus fuel-fired water heaters), flexible load units, and small hot water storage units. In a later study, Ottesen, Tomasgard, and Fleten (2016) present a model with an aggregator that gathers and manages groups of prosumers. The load units are again categorized as inflexible, shiftable, and curtailable. The aggregator trades in a spot market by selling electricity to the prosumers and by buying back their surplus electricity. The value of flexibility in this paper is 12%, as the total cost decreases by 12%. Marañón-Ledesma and Tomasgard (2019) also consider DSM by allowing shiftable and curtailable load in a large-scale stochastic European energy market model. The paper focuses on integrating renewable energy into the European power system from 2010 until 2050. According to the paper, DSM will lead to an 11% reduction in the peak plant capacities and a 86% reduction in storage capacity. The results indicate that flexible loads reduce the need for (investment in) storage infrastructure.

Studies about DSM techniques in DHGs typically consider potential cost reductions or peak load reduction where scheduling flexibility takes a producer perspective, DSM considers the consumer perspective. From a cost minimization perspective, they are essentially the same. Cai et al. (2018) consider comfort zones for space heating, indicating how much the temperature is allowed to deviate from the target temperatures. Temperature adjustments within the comfort zone are not penalized, while outside the space heating comfort zone, the deviations are penalized with a cost. The results indicate a potential of an 11% reduction in energy costs for a real urban DHG, located in Copenhagen's Nordhavn area. Kontu et al. (2018) investigate how DSM decisions affect production in a DHG in Finland. The obtained results show that the value of DSM for the DHO remains low (2% in cost savings). The larger the share of heat from base production plants, the less profitable DSM techniques are. The savings are most significant when a high proportion

of the production mix is peak sources, e.g., boilers. Thus, the value of DSM techniques is highly dependent on the production sources available in the DHGs.

Other studies focus more explicitly on using DSM to reduce peak loads in DHGs. The use of varying thermal demand profiles of consumers has been investigated by Guelpa et al. (2019) and Capone et al. (2019). The papers use the variation in heat demand requests to flatten the demand and reduce peak loads in a case study of the Turin DHG, the largest DHG in Italy. Capone et al. (2019) found the peak reduction to be between 20% and 42%, depending on the flexibility of the demand. The results indicate that DSM can have a significant impact on peak reduction and operational costs. In Guelpa et al. (2019), both the supply and return networks are included in the optimization process. Consequently, they found the peak reduction to vary between 15% and 37% depending on how many buildings in the DHG has flexible heat demand (heating system schedule that can be modified) and the maximum allowed schedule modifications. The results show how the potential for peak reduction in DHGs increase with the number of consumers with flexible demand.

3.4 Stochastic Programming

Many real-life decisions are affected by uncertainty. This section gives an introduction to stochastic programming, which is one way to handle uncertainty. A traditional method for solving stochastic problems is then discussed before introducing the concept of multi-horizon modeling and why this method can be useful compared to traditional stochastic programming.

Stochastic programming is a framework for modeling optimization problems that involve uncertainty. In contrast to deterministic optimization problems, where all parameters are assumed to be known with certainty, and all relevant information is assumed to be available when making a decision, some parameters are unknown in stochastic programming. In reality, real-world problems almost inevitably include parameters that are unknown at the time when making decisions. Some decisions must be delayed until the relevant information is revealed so that they can be adapted to the specific observed outcome (Higle 2005). Stochastic recourse models distinguish between what decisions can be made now with the available data and what decisions can be delayed until more information is revealed. Recourse models were first introduced in 1955 by Dantzig (Dantzig 2004).

According to Kall (1997), deterministic models often provide reasonable solutions for stochastic problems. However, the respective stochastic model must be solved to conclude

whether the deterministic solution is eligible (Kall 1997). Stochastic programming seeks to find a feasible and optimal policy for almost all the possible data instances (Shapiro and Philpott 2007). When the probability distributions for the uncertain parameters are discrete and the number of possible outcomes in each stage (i.e., the time at which information will be available) is finite, different realizations of the future can be created. Each possible combination of outcomes for a stochastic problem is a scenario that can be represented in a scenario tree (Shapiro and Philpott 2007). Figure 3.1 shows a scenario tree with five stages, two branches, and eight scenarios. Nodes with the same tree level are in the same stage, while branches are points in time where new information is revealed. Each scenario in the tree corresponds to a path from the root node to one of the leaves. The root node is the initial decision stage before obtaining any information about future conditions. The leaf nodes represent where all available information has been revealed (Shapiro and Philpott 2007).

In some stochastic optimization models, it may be necessary to include specific constraints to ensure that the decision was taken at a specific stage only depends on the information revealed up to that stage and not on future information. These conditions are known as non-anticipativity constraints. Each scenario in Figure 3.1 can be solved as an independent deterministic problem, which results in eight independent deterministic problems, as presented in Figure 3.2. The nodes within the ellipses have equivalent decision variables since they possess identical levels of information, which is ensured by the non-anticipativity constraints (Higle 2005).

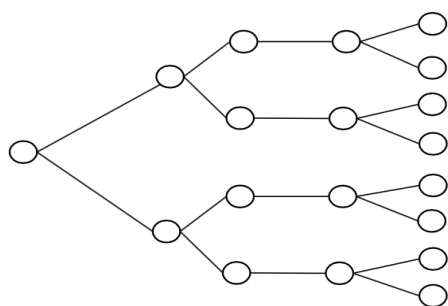


Figure 3.1: Stochastic scenario tree.
Source: Own illustration.

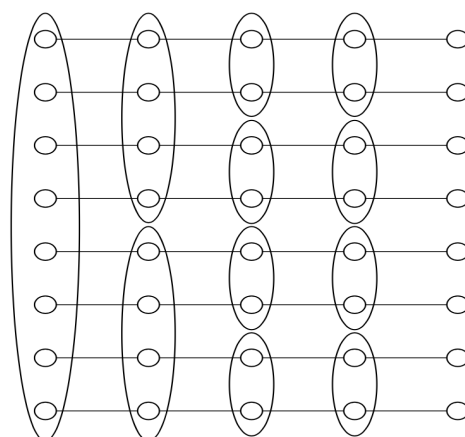


Figure 3.2: Independent deterministic problems.
Source: Own illustration.

3.4.1 Formulation of the Stochastic Model

The two-stage recourse problem is an example of a stochastic problem where each stage represents a new level of information. The first stage is before obtaining any information. Therefore, all decisions in the first stage are made under uncertainty. In the second stage, the information is revealed, and new decisions can be made by adapting the solutions from the previous stage to fit the new information (Shapiro and Philpott 2007). The general form of a two-stage problem is presented below. This formulation is also called a two-stage recourse problem.

$$\begin{aligned} \min_x \quad & cx + E[h(x, \tilde{\omega})] & (A) \\ \text{s.t.} \quad & Ax \geq b \\ & x \geq 0 \\ \text{where} \quad & h(x, \omega) = \min g_{\omega} y & (B) \\ \text{s.t.} \quad & W_{\omega} y \geq r_{\omega} - T_{\omega} x \\ & y \geq 0 \end{aligned}$$

x is the first-stage decision variable, where no information regarding the uncertain data $\tilde{\omega}$ is available. The second-stage variable y , on the other hand, depends on $\tilde{\omega}$ and is decided after observations of $\tilde{\omega}$ is obtained. The second-stage problem (B) exploits the outcomes and tries to find an optimal solution for the second stage, while the solutions from the first stage are considered. The entire model (A) minimizes the first stage cost cx and the expected costs from the second stage problem. This two-stage stochastic formulation could also be implemented by using the deterministic equivalent formulation. Then problem (B) would be included in problem (A), and a scenario index ω would be added to the y variable. The objective function then becomes $\min cx + \sum_{\omega \in \Omega} p_{\omega} c_{\omega} x_{\omega}$, where p_{ω} is the probability of each scenario (Higle 2005).

For a linear multistage problem, uncertainty is resolved at several points in time. The model (C) show a formulation of a linear multistage problem where x_{ω} represents the decision in each scenario and c_{ω} is the objective function coefficients in scenario ω .

$$\begin{aligned}
\min_x \quad & \sum_{\omega \in \Omega} p_\omega c_\omega x_\omega & (C) \\
\text{s.t.} \quad & x_\omega \in X(\omega) \quad \forall \omega \in \Omega \\
& \{x_\omega\}_{\omega \in \Omega} \in \mathcal{N}
\end{aligned}$$

The set of constraints for each scenario is denoted by $x_\omega \in X(\omega)$. \mathcal{N} represents the set of non-anticipative solutions. In order for the solutions to be non-anticipative, we must ensure that the decision variables associated with node n produce identical values. One way to do this is to include non-anticipativity constraints (Higle 2005). These are not explicitly formed here, but the formulation corresponds to Figure 3.2. The ellipses are groups of decisions equal in \mathcal{N} .

In general, formulating and solving stochastic problems is a challenging task. For stochastic problems with a small number of scenarios, a linear programming solver can be used (Shapiro and Philpott 2007). However, for real-world problems with numerous stages and scenarios, the scenario tree may become explosively large and increase the solution time for linear programming solvers. The explosion of scenario tree size can cause linear programming to be invalid, and new approaches must be utilized to solve the stochastic problems (Birge and Louveaux 2011).

3.4.2 Stochastic Models in the Literature

Several parameters can be uncertain when modeling energy systems. Both generation and demand uncertainty is often connected to short-term uncertainty, such as fluctuations in energy prices and weather conditions. Several authors have used a two-stage scenario tree to illustrate the chain of scenarios when considering uncertainty related to energy systems. The first stage is often characterized by the possibility to invest in production technologies and infrastructure, while the second stage is about making operational decisions. Seljom and Tomasgard (2015) take the uncertainty of wind availability and electricity prices into account. The first stage is considered as an investment stage, where investments in new wind power capacity can be set for future time periods. The second stage is where operational decisions are made, and the decisions are constrained by the capacity installed in the first stage. Huang et al. (2016) aim to find the optimal investment in various power generation technologies in the first stage while accounting for electricity demand uncertainty in the second stage.

In the stochastic variation of the energy scheduling model developed by Ottesen and Tomasgard (2015), uncertainty in load forecasting is captured. A day is illustrated by a two-stage scenario tree, the first 12 hours represented by the first stage and the last 12 by the second stage. All information is assumed to be known with certainty for the first stage, while the load parameter is uncertain for the second stage. The results indicate that the stochastic model is best in cases with limited flexibility in the energy systems in the building. In the study by Ottesen, Tomasgard, and Fleten (2016), the aggregator problem is modeled as a two-stage stochastic linear program that accounts for uncertainty in electricity prices and electrical loads. Bidding decisions are made in the first stage and scheduling decisions in the second stage. In the case study, the value of stochastic planning is a 1% decrease in the total cost with Norwegian electricity prices. The stochastic planning results in a 1.7% decrease with German electricity prices due to higher price fluctuations.

Liu et al. (2014) present a multistage mixed-integer stochastic programming model for optimal operation of energy-efficient building systems. The aim is to minimize the daily production cost for buildings while satisfying their various physical operation restrictions. The uncertainty factors come from the randomness of non-controllable electric and thermal loads and solar power generations. The scheduling horizon of one day is discretized into three stages, where the first stage is at hour 1, the second stage is from hour 2 to 6, and the third stage is from hour 7 to 24. The paper concludes that the multistage model contributes to the optimal operation of energy-efficient building systems.

Stochastic programming has also been used to optimize DHGs in the existing literature. Hohmann et al. (2019) present a polynomial two-stage stochastic program for DHGs with uncertain demand. The focus is on finding high-performance operating strategies concerning the expected operational cost incurred by hydraulic and thermal losses. In the paper, three different operating strategies for change in heat supply are evaluated (first, constant supply temperature and variable mass flow, second, variable supply temperature and constant mass flow, and last variable supply temperature and variable mass flow). In the first stage, the optimal set point for the constant control variable is selected. In the second stage, the other control variable and remaining variables (pressure drops and temperatures) are adjusted to optimize the heat supply to consumers. Lambert et al. (2016) consider a sequential problem faced by a decision-maker in the phasing of long-term investments into district heating networks. The paper suggests a model that determines the annual capital expenditure that maximizes the expected net present value. The type of uncertainty taken into consideration is heat demand and fuel cost, which affect production operating costs. The model is formulated as a multistage stochastic programming problem

to address the problem of heat demand and fuel price uncertainty. The use of a sequential decision-making approach allows for optimal phasing and expansion of DHGs that might not have been identified by arbitrary incremental network expansion.

3.4.3 Multi-horizon Stochastic Programming

Some optimization problems, like investments in energy systems, can contain uncertainty on the strategic and operational levels. In addition, uncertainties at the strategic level are generally influenced by the operational level. Stochastic problems tend to become large and unmanageable, and thus extensive research has been done to manipulate the structure of the problem to make the size more manageable (Su et al. 2015).

Kaut et al. (2014) study a type of stochastic problem called infrastructure-planning models, and they propose a restructuring of the problem formulation that significantly reduces the problem size. This approach is called multi-horizon stochastic programming. The idea is to distinguish between uncertainty on the strategic level and the operational level to reduce the size of the traditional stochastic problems (Kaut et al. 2014). The multi-horizon model implies that, if strategic decisions are not directly dependent on a specific operational situation and the strategic uncertainty is independent of operational uncertainty, the operational stages can be modeled as embedded in the respective strategic node. Kaut et al. (2014) also emphasize that for the approach to be exact, there should be no dependency between the decisions taken in the operational scenarios of two consecutive strategic nodes. However, ignoring the connection between operational nodes with succeeding nodes has its limitations. For example, electricity in a battery from one period to the next cannot be captured accurately with this approach. This is the price for improving the problem size (Su et al. 2015).

Relevant to the problem in this thesis, Kaut et al. (2014) suggest that many areas, such as the energy planning sector and the design of supply chains, can benefit from multi-horizon stochastic programming. They present the multi-horizon optimization approach illustrated on a simple example of installing photovoltaic (PV) panels on a building. A more complex case is studied by Hellemo (2016), where a multi-horizon stochastic approach is used to optimize the design and operation of the infrastructure for natural gas production. Marañón-Ledesma and Tomasgard (2019) also use a multi-horizon stochastic approach in their study considering the role of DR in the European power system.

3.4.4 Evaluation of the Stochastic Method

Stochastic programming is proven to be an effective framework for handling decision problems that involve uncertainty. Stochastic problems tend to be more computationally demanding than their deterministic counterparts, and they often require specific solution methods. Therefore, it can be useful to evaluate the real value of solving the stochastic model, or whether the deterministic approach can provide a nearly optimal solution (Birge and Louveaux 2011).

The expected value of perfect information (EVPI) and the value of the stochastic solution (VSS) are commonly applied to compare the solutions obtained from the stochastic program with simpler deterministic alternatives (Birge and Louveaux 2011). The EVPI finds the value of knowing the future with certainty and can for example be seen as an estimate of the maximum amount one would pay for more accurate forecasts of uncertain parameters. The VSS can give reasonable indications of whether stochasticity in a model brings additional value or if the deterministic counterpart is good enough (Birge and Louveaux 2011).

EVPI

Equation (3.4) defines the expected value of perfect information (EVPI) as the difference between the wait-and-see solution (WS) and the recourse problem solution, also known as the stochastic solution (SP) (Birge and Louveaux 2011).

$$EVPI = SP - WS \tag{3.4}$$

VSS

The value of the stochastic solution measures the value of using a stochastic approach instead of a deterministic approach. The difference between the value of the optimal solution of the stochastic problem (SP) and the expected value of using the expected value solution (EEV) is calculated to determine the VSS. Computation of the EEV involves solving the expected value problem, EV, and then solving the SP with some fixed values. The value of the stochastic solution can then be determined, as indicated in Equation (3.5) (Birge and Louveaux 2011).

$$VSS = EEV - SP \tag{3.5}$$

For a minimization problem we have the general property:

$$SP \leq EEV \tag{3.6}$$

If Condition (3.6) does not hold, the SP is not the optimal solution to the stochastic problem, and a better solution can be obtained by using the expected value solution (Birge and Louveaux 2011).

3.4.5 Scenario Generation

It is difficult or impossible to realistically capture all information about future uncertainty in order to solve a stochastic programming model. Therefore, it is necessary to create scenarios to represent the uncertainty and incorporate them into the stochastic model (Tanaka and Ohmori 2016). The accuracy of a stochastic problem depends on the number of scenarios (Shapiro and Philpott 2007). In reality, the true distribution of scenarios would be infinite, which is impossible to generate. Therefore, the proper generation of scenarios is crucial in order to obtain accurate stochastic models. There exist many approaches to scenario generation (Dupačová et al. 2000). Some common approaches are statistical methods, sampling, and simulations. Statistical methods involve the determination of statistical properties (e.g., mean and variance) for data distribution. Sampling generally provides scenario values from historical data, while simulation approaches give scenario values by simulating the stochastic process (Di Domenica et al. 2009). Other widely used scenario generation methods in optimization problems are clustering algorithms which help reduce the number of scenarios (Jain 2010).

The choice of scenario generation method is problem-dependent. Therefore, it is interesting to investigate the choice of method in similar problems as ours. Skar et al. (2016) construct scenarios on hourly profile loads by dividing the year into four seasons. Similarly, in the paper by Seljom and Tomasgard (2015), scenarios are constructed based on historical data because the aim is to represent realistic operational situations in the model and not to forecast the future. When dealing with historical weather, the number of observations is often very high, and the scenario tree can become very large. Under this situation, clustering analysis, such as the k-means clustering algorithm, can be used to aggregate the historical data into a smaller scenario tree. Seljom and Tomasgard (2015) use the k-means clustering algorithm to reduce the number of scenarios from historical data by arranging original scenarios of demand and wind into clusters according to the similarities. They also check if the number of scenarios is enough to obtain a stable result.

Sachs and Sawodny (2016) also use k-means clustering to divide load profiles into days and to find the amount of representative daily load profiles that accurately portrays the system load behavior. Using historical data, as Skar et al. (2016) and Seljom and Tomasgard (2015) do, it is possible to avoid incorrect assumptions about the distribution of the stochastic process. Correlation within a day is automatically ensured since the same set of hours is sampled for all the random variables. Similarly, auto-correlations between hours within each scenario are preserved as each sample is a set of consecutive hours.

Stochastic programming is dependent on the modeling of uncertainties expressed through scenarios, which includes the approximation of random variables (input that can vary) by a discrete distribution (King and Wallace 2012). Thus, the quality of the output from the optimization model is heavily dependent on the scenario generation. Kaut (2003) state that a "bad" scenario tree can lead to a "bad" solution. It is also important to find the best trade-off between a realistic and simple model. A model with many scenarios can result in a large and complex problem that might increase computation time and may even be infeasible. In contrast, a model with few scenarios may lead to a simple and insufficient picture of reality (Kaut 2003).

3.5 Time Series Analysis

In this section, time series analysis, with particular emphasis on regression models, is introduced for prediction of uncertain parameters based on historical data. Time series analysis is a statistical framework for assessing the behavior of time series, and typically it consists of measurements or observations on variables made over a time interval (Hansen 2017). Time series have interesting properties compared to other data types; for example, the order of data occurrence is essential. Data values observed at time t in a time series are often affected by the data values observed in preceding times. Thereby, the ordered set of time t and data values represent the dependencies between the collected data in a time series (Lee and Elmasri 1998).

Regression models are widely used for addressing associations among sets of variables. The overall idea of regression models is to determine a relationship between a single dependent variable and one or multiple independent variables. A regression model with one independent variable is known as a simple regression model. When there are two or more independent variables, it is called multiple regression models. The regression analysis yields a predicted value for the dependent variable, and a good regression model must yield predicted values that are very close to the actual values (Palmer and O'Connell 2009). According to Pedhazur (1982), there are two main reasons for using regression

models in the scientific literature. The first reason is the purpose of the explanation. Here the regression model is used to study the effect of adjusting independent variables and how they affect the input variables. The second reason is for forecasting purposes, as the regression model provides an estimate of the expected value based on the regression function. Ciulla and D'Amico (2019) state that regression models can be useful tools for predicting energy consumption in buildings based on weather conditions.

The optimal lag length should be determined before the calculation of the regression function. There exist several model selection criteria in the literature (Sinha et al. 2015). The first information-theoretic criterion to gain acceptance was the Akaike Information Criterion, AIC. Many other criteria have since been introduced, including the well-known measure by Schwartz (1978), known as the Bayesian Information Criterion, BIC, or Schwartz Information Criterion, SIC. The criterion is widely used due to its computational simplicity and effective performance in many models (Neath and Cavanaugh 1997). The information criteria for estimating the optimal lag length is dependent on the number of observations. According to Liew (2004), the AIC is more appropriate when the number of observations is less than 60, while the so-called Hannan-Quin (HQ) criteria, is more efficient when the number of observations is above 120.

In order to determine if the model generates values that are close to the observed values, the goodness of fit measure can be used. One well-known approach for evaluating a regression model is the R-squared (R^2) method, which measures how well the regression predictions approximate the real values. The R-squared value describes the relationship between the predicted and observed data, and the closer the value of R-squared is to 1, the better the prediction (1 indicates that the regression predictions perfectly fit the data) (Henseler et al. 2009).

3.6 This Work

A selection of the previously mentioned literature representing the broad focus in research on optimization of power grids and DHGs are included in Table 3.2. The table helps place our contribution in context with existing research and literature.

Table 3.2: Article overview: Selected articles addressing grid optimization.

Authors	Det/Stoc	Components	Objective
Cai et al. (2018)	Det	DH/DSM/4GDHG	Min energy cost
Capone et al. (2019)	Det	DR/DH/TES	Min thermal peak
Dorotić et al. (2019)	Det	DH/4GDHG/TES	Min total cost & CO ₂ emission
Guelpa et al. (2019)	Det	DSM/DH	Min thermal peak
Hohmann et al. (2019)	Stoc (two-stage)	DH	Min operational cost
Leško et al. (2018)	Det	DH/TES	Min operational cost
Liu et al. (2014)	Stoc (multi-horizon)	EL/Battery/Solar	Min production cost
Marañón-Ledesma and Tomasgard (2019)	Stoc (multi-horizon)	DSM/Storage/EL	Min total cost
Ottesen and Tomasgard (2015)	Stoc (two-stage)	DSM/Storage/EL/Smart grid	Min operational cost
Ottesen, Tomasgard, and Fleten (2016)	Stoc (two-stage)	DSM/Storage/EL/Smart grid	Min total cost
Sameti and Haghighat (2019)	Det	DH/4GDHG/EL/PV/CHP	Min total cost
Vesterlund et al. (2017)	Det	DH	Min operational cost
Our contribution	Det & Stoc	DH/DSM/4GDHG/TES	Min operational cost

To the best of our knowledge, the literature remains relatively unexplored on optimization models that combine Demand Side Management and Thermal Energy Storage in low-temperature District Heating Grids with local waste heat. Similarly, few studies account for uncertainty in demand when modeling the operation of DHGs. Our problem seeks to minimize the total operational cost of a DHG by considering the operational decisions made based on costs from production technologies, DSM techniques, TES, and local waste heat. Two stochastic optimization models are established, in addition to a deterministic model to support a cost-minimizing operation of low-temperature District Heating Grids with uncertain SH demand. The first stochastic model can be categorized as a traditional scenario tree-based stochastic model, while the second is a multi-horizon stochastic model, which is an approximation of the traditional scenario-tree based stochastic model. The deterministic model is also investigated in order to evaluate the value of uncertainty in our work. In addition, the models are compared against each other in terms of solution and computational complexity.

Chapter 4

Problem Description

In this chapter, the research question and scope are presented and described in detail. The problem description provides the starting point for formulating the mathematical problem that will be used to address the research question.

The research question in this thesis is: *How can a District Heating Operator (DHO) minimize operational costs and manage consumer demand in a low-temperature District Heating Grid (DHG) with local waste heat and uncertain heat demand?* As Demand Side Management (DSM) mechanisms and seasonal Thermal Energy Storage (TES) are resources that can be used to reduce grid loads and manage consumer demand, an important part of the research question is to find out when it is optimal to store heat in a TES and use DSM, and what value it brings the DHO. To answer the research question, this thesis will determine optimal operational scheduling strategies for low-temperature DHGs, which minimize the total operational cost and allow for optimal and efficient use of local waste heat, DSM and TES, considering Space Heating demand uncertainties.

While the low-temperature DHG at Leangen is the target area for investigation in this thesis, the resulting problem formulation can also be used to optimize the operation of other DHGs with low- or high-temperature settings. The heat supply area can consist of buildings with different characteristics and heat demand, for instance, residential and office buildings, classified as consumer nodes. The grid is allowed to have several heating centrals, each represented by a heating central node. In addition, it should be possible to have TESs and Heat Pumps (HPs) included in the grid, which can be co-located with any node. Supply pipelines connect the heat central nodes to branching nodes and consumer nodes, while return pipelines are ignored. Furthermore, each node has to satisfy energy balance equations. As a consequence of ignoring the return pipelines, the grid can be viewed as a non-cyclic connected graph with nodes and edges. Figure 4.1 is an example of a small DHG with two heat central nodes (1 and 2), two branching nodes (3 and 4) and three consumer nodes (5, 6 and 7). The arrows indicate the water flow directions in

This problem description is a revised version of the one in our specialization project.

the supply pipelines. The layout of the DHG is exogenously given and depends on the case study in the area of investigation.

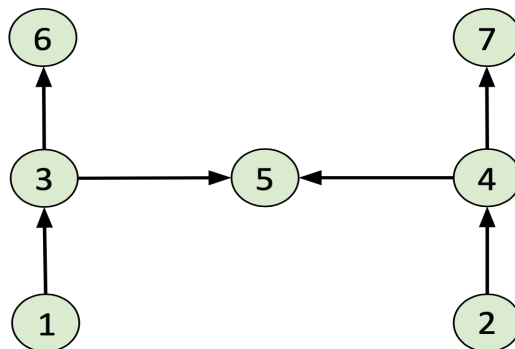


Figure 4.1: An example of a DHG layout with nodes.
Source: Own illustration.

The heating centrals can supply heat from different heat technologies that may have different production costs, capacities, and CO₂ emissions. The heat technologies can be split into uncontrollable technologies (e.g., renewable energy and waste heat) and controllable technologies (e.g., boilers). The heat production in each operational period is restricted by the total available capacity of the installed technologies. Maximum limits on total storage capacity for each TES and pipeline capacities should also be included. The heat storage levels in the TESs are assumed known at the beginning and end of the planning horizon. Adding heat to a TES must happen before withdrawing heat, and it is assumed that it is only possible for a TES to store heat from controllable heat technologies. The amount of heat added and withdrawn to and from the TES also depend on the available adding/withdrawing capacity, as well as the amount of heat currently stored and the storage efficiency. Heat losses also occur in the pipelines, resulting in related efficiencies.

HPs are required to lift the temperature of the supplied heat to the desired temperature level. One centralized HP is needed to lift the temperature of the local waste heat to the grid temperature, while smaller HPs, at each consumer node, ensure the correct temperature for the Hot Water. The COPs of the HPs is exogenously given. Power costs associated with the HPs should also be included in the model.

The consumer heat demand is divided into Space Heating (SH) and Hot Water (HW). One consumer node consists of one or several user profiles, with a specific consumption pattern for SH and HW. To ensure consumer comfort, the DHO needs to meet exogenously specified demand requirements for each user profile. These requirements are allowed as upward and downward deviations from the target demand over single and multiple

consecutive periods for each consumer. For instance, the latter can be 24 hours in a day or four hours in the evening (from 16:00 to 20:00). Hence, it is possible to deliver less heat than the target demand in some periods, resulting in a deficit or a surplus if the delivered heat exceeds the target demand. Deficit and surplus in consecutive periods can be interpreted as demand shifting. The under-delivered heat in consecutive periods can be classified as curtailment.

The decisions to be made in every period of the planning horizon are heat production levels of controllable heat technologies, amount of heat to add or withdraw from the TESs, and amount of heat to deliver to each consumer. Figure 4.2 shows an example of how the operational distribution decisions for a specific DHO can be combined to cover consumer target demand in a given time period.

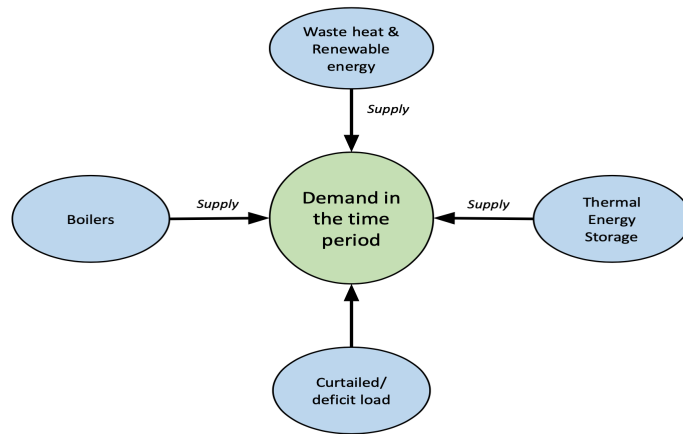


Figure 4.2: Operational distribution of DH.
Source: Own illustration.

The operational costs, which are to be minimized, consist of heat production costs from controllable energy technologies, power costs for the operation of HPs, heat transportation costs, and costs related to adding and withdrawing heat from the TES. In addition, CO₂ emissions, deficit, and curtailment loads are charged with a penalty fee, which is considered an operational cost. The amount of delivered HW determines the power cost for the HPs at each consumer node, while waste heat supply determines the power cost for the centralized HP.

It is assumed that the entire infrastructure is already established, so the problem does not consider investment costs. Neither maintenance costs are included as part of the operational costs. In general, several input parameters, such as future fuel cost and target demand, can be uncertain and unknown. Whereas in this thesis, there is only operational uncertainty related to SH target demand.

Chapter 5

Model Formulation

In this chapter we present a deterministic and two stochastic models based on the problem description in Chapter 4. The mathematical models are constructed to support operational decisions for conventional and modern District Heating Grids (DHGs) with different layouts and production mixes. The models can be used for grids with one or several heating centrals alongside one or several Thermal Energy Storages (TESs). The problem is uncertain and complex, with many variables. Therefore, a set of assumptions is included in 5.1 in order to model the problem. A deterministic version of our model is presented in Section 5.2, before we expand the formulation to a traditional stochastic model (Section 5.4) and a multi-horizon stochastic model (Section 5.5).

5.1 Assumptions and Explanations

Time Periods

To facilitate the comparison with the multi-horizon stochastic model results in later chapters, we divide the time horizon into strategic time periods and operational time periods. Each strategic time period contains several operational time periods.

Production from different Technologies

Heat central nodes can produce heat from controllable technologies and uncontrollable technologies. The amounts of available hourly heat from uncontrollable technologies are exogenously given parameters. The models endogenously determines production from controllable technologies.

Compared to the specialization project, the deterministic model is modified by diving the planning horizon into strategic and operational time periods, in addition to adding HPs.

Heat Demand

Heat demand is divided into types for different purposes, e.g., Space Heating (SH) and Hot Water (HW). Therefore, some parameters and variables must account for different demand-types, e.g., target heat demand, delivered heat demand, and deficit load.

Costs

We ignore any fixed costs connected to start-up and shutting down of the production technologies to avoid binary variables, as they reduce the scalability of the model. We assume that all production costs are variable costs that only depend on the amount of heat produced. All costs for adding heat to and withdrawing heat from the TES are accounted for when adding heat.

User Profiles

Requirements regarding consumer comfort can be modeled in several ways. In this thesis, a solution with user profiles is chosen. Each consumer node can contain one or multiple user profiles with different heat requirements for SH and HW. Sensitivity to DSM can vary with user profile and time.

Thermal Energy Storage

It is assumed that at most one TES can be co-located with any node. Additionally, low-temperature heat can be unfit to feed directly into a TES due to temperature differences. Therefore, it is assumed that heat from uncontrollable technologies, e.g., waste heat, cannot be added to TESs. Only heat production from the controllable heat technologies can be stored in TESs.

Heat Losses

Heat losses occur in the pipelines, in the TESs, and when adding heat to or withdrawing heat from the TESs. Both heat losses related to adding to and withdrawing from TESs are accounted for when adding heat. Heat losses related to pipelines are dependent on the supply temperature levels, the ambient temperatures of the pipelines, the heat transport volumes, the pipeline lengths, and the insulation levels in the pipelines. However, we assume fixed operating temperatures in different parts of the system, which results in fixed loss rates in the pipelines.

Heat Pumps

Heat Pumps (HPs) lift the temperature of the heat carrier to the desired temperature needed in another part of the grid, or for the end-users. The models distinguishes between the COP of centralized and decentralized HPs. In real life, the COP of HPs varies considerably (and not linearly) with the HP's evaporator and condenser temperature. Since we assume fixed operating temperatures, this non-linear variability can be ignored. Therefore, we assume a fixed COPs and needed electricity input per unit of delivered heat. However, the costs of electricity can vary over time.

5.2 Deterministic Model

In this section, the deterministic model is presented. The model consists of indices, sets, parameters, and variables and is formulated as a linear programming model.

5.2.1 Indices, sets, parameters and variables

Let N be defined as a set of all nodes, $N = \{N^P, N^B, N^C\}$, and is referred to with indices by i, j . The subset N^P is the set of all heat central nodes, N^B is the set of all branching nodes and N^C is the set of all consumer nodes. E is the set of all heat production technologies indexed by e . $E = \{E^C, E^U\}$, where E^C is the set of all controllable heat technologies, and E^U represents all the uncontrollable heat technologies. The two demand-types are defined in the set, $G = \{SH, HW\}$, indexed by g .

The set of strategic time periods is defined as $T^S = \{1, 2, \dots, t_{last}^S\}$ and is indexed by t . The set of operational periods is defined as T^O , and indexed by h, h' . T^O is defined as $T^O = \{1, 2, \dots, t_{last}^O\}$. The set of different user profiles is defined as P and is indexed by p .

Indices and Sets:

$e \in E$	Set of all heat production technologies.
$E^C \subset E$	Subset of heat technologies of type controllable.
$E^U \subset E$	Subset of heat technologies of type uncontrollable.
$g \in G$	Set of demand-types.
$i, j \in N$	Set of all nodes.
$N^P \subset N$	Subset of nodes of type heat central.
$N^B \subset N$	Subset of nodes of type branching.
$N^C \subset N$	Subset of nodes of type consumer.
$t \in T^S$	Set of strategic time periods.
$h, h' \in T^O$	Set of operational time periods.
$p \in P$	Set of all user profiles.

All parameters and variables that are used in the model are listed below. Parameters are defined as uppercase letters, while variables are defined as lowercase letters. The indices relating the parameters and the variables to the various sets are added as subscripts. Superscripts are used to increase the comprehensibility of the model.

Parameters:

$C_{ghh'p}$	Unit deficit cost for not meeting demand-type g in the operational period from h to h' for user profile p [NOK/kWh].
C^A	Unit cost for adding heat to the TES [NOK/kWh].
C_e^E	CO ₂ emission cost for technology e [NOK/ kg CO ₂].
C_{eth}^F	Unit fuel costs of technology e in strategic period t in operational period h [NOK/kWh].
C_{ij}^T	Pipeline transportation costs from node i to node j [NOK/kWh].
COP^C	Coefficient of Performance for the centralized HP.
COP^D	Coefficient of Performance for the decentralized HPs.
D_{githp}	Target heat demand of type g at node i in strategic period t in operational period h for user profile p [kWh].
F_{ij}^{MAX}	Capacity limit for the pipeline from node i to j [kWh].
$L_{gihh'p}$	Minimum percentage of demand-type g at node i that must be satisfied in the operational period from h to h' for user profile p .
O_e	CO ₂ factor for technology e [kg CO ₂ /kWh].
Q_{it}^{-MAX}	Capacity limit for adding heat to the TES at node i in strategic period t [kWh].
Q_{it}^{+MAX}	Capacity limit for withdrawing heat from the TES at node i in strategic period t [kWh].

S_i^{START}	Initial storage level in the TES at the beginning of the planning horizon [kWh].
S_i^{MAX}	Capacity limit for stored heat (total inventory) in the TES at node i [kWh].
S_i^{END}	Planned storage level in the TES at the end of the planning horizon [kWh].
R_{ip}	Percentage of target demand at node i that user profile p stands for.
$U_{gihh'p}$	Maximum percentage of demand-type g at node i that must be satisfied in the operational period from h to h' for user profile p .
X_{eith}	Uncontrollable heat from technology e available at node i in strategic period t in operational period h [kWh].
X_{eith}^{MAX}	Production capacity limit for technology e at node i in strategic period t in operational period h [kWh].
η_{ij}	Efficiency ratio (1-loss rate) for heat flow from node i to node j .
η^A	Efficiency ratio for adding heat to the TES.
η_t^S	Efficiency ratio for the TES from strategic period t to strategic period $t + 1$.

Variables:

f_{ijth}	Heat amount that is transported from node i to node j in strategic period t in operational period h [kWh].
q_{ith}^-	Heat amount that is added to the TES at node i in strategic period t in operational period h [kWh].
q_{ith}^+	Heat amount that is withdrawn from the TES at node i in strategic period t in operational period h [kWh].
s_{ith}	Heat amount stored in the TES at node i in strategic period t at the end of operational period h [kWh].
x_{eith}	Heat amount produced by technology e at node i in strategic period t in operational period h [kWh].
y_{githp}	Delivered heat amount for demand-type g in node i in strategic period t in operational period h for user profile p [kWh].
$z_{githh'p}$	Amount of deficit load for demand-type g in node i in strategic period t in the operational period from h to h' for user profile p [kWh].

5.2.2 Objective function

The objective is to minimize the total operational costs in Equation (5.1). The first term describes the heat production costs from controllable heat technologies, which include the fuel cost and CO₂ emission cost. The second term describes the transportation cost of transporting heat in the pipelines between nodes, while the third term handles the sum of deficit cost for Space Heating and Hot Water, respectively. The fourth term represents

the cost associated with adding and withdrawing heat to and from the TES. The two last terms are the electric power costs associated with the HPs, where the last term is a fixed cost associated with HPs for uncontrollable heat technologies.

$$\begin{aligned}
 \min \sum_{t \in T^S} \sum_{\substack{h, h' \in T^O \\ \wedge h' \geq h}} & \left(\sum_{e \in E} \sum_{i \in N} (C_{eth}^F + C_e^E O_e) x_{eith} \right. \\
 & + \sum_{i \in N} \sum_{j \in N} C_{ij}^T f_{ijth} \\
 & + \sum_{i \in N^C} \sum_{p \in P} C_{ghh'p} z_{githh'p} \\
 & + \sum_{i \in N} C^A q_{ith}^- \\
 & + \sum_{i \in N} \sum_{p \in P} C_{(EL),th}^P \frac{y^{(HW),ithp}}{COPD} \\
 & \left. + \sum_{i \in N} C_{(EL),th}^P \frac{X_{eith}}{COPC} \right) \tag{5.1}
 \end{aligned}$$

5.2.3 Constraints

Demand

A variable representing the delivered heat to a node in a given time period (y_{githp}) is defined alongside a variable for the amount of deficit load for a single time period or consecutive time periods ($z_{githh'p}$). We have not defined any variables for shifted heat load nor curtailed heat load. The amount of heat that is shifted or curtailed from one time period to another can be interpreted from the results obtained after running the model.

Constraint (5.2) defines the deficit load for demand-type g in consumer node i in strategic period t in the consecutive operational period from h to h' for user profile p as the difference between the target heat demand and the delivered heat in the consecutive operational periods from h to h' for user profile p . (Larger than or equal, because over-deliveries cause the right-hand side to become negative.)

$$z_{githh'p} \geq \sum_{\tau=h}^{h'} (R_{ip} D_{git\tau p} - y_{git\tau p}), \quad \forall g \in G, i \in N^C, t \in T^S, (h, h') \in T^O \wedge h' \geq h, p \in P \tag{5.2}$$

Constraint (5.3) ensures that the delivered heat covers the minimum demand requirements over the consecutive operational periods from h to h' for user profile p .

$$\sum_{\tau=h}^{h'} y_{git\tau p} \geq L_{gihh'p} R_{ip} D_{githp}, \quad \forall g \in G, i \in N^C, t \in T^S, (h, h') \in T^O \wedge h' \geq h, p \in P \quad (5.3)$$

Constraint (5.4) ensures that delivered heat does not exceed the maximum deliverable amount in the consecutive operational periods from h to h' for user profile p .

$$\sum_{\tau=h}^{h'} y_{git\tau p} \leq U_{gihh'p} R_{ip} D_{githp}, \quad \forall g \in G, i \in N^C, t \in T^S, (h, h') \in T^O \wedge h' \geq h, p \in P \quad (5.4)$$

Production

Production from a controllable heat technology cannot exceed its production capacity limit.

$$x_{eith} \leq X_{eith}^{MAX}, \quad \forall e \in E^C, i \in N^P, t \in T^S, h \in T^O \quad (5.5)$$

Nodal heat balance

The heat balance for each node i in the strategic period t in the operational period h is given in Constraint (5.6). The heat sources and inflows are found on the left side, and the outflows and sinks, on the right. The sources in Constraint (5.6) consist of produced heat from controllable heat technologies and uncontrollable heat technologies, the heat inflow from connected nodes (corrected for heat losses), and withdrawn heat from the TES. The sinks consist of delivered heat, heat outflow to connected nodes, and heat added to the co-located TES.

$$\sum_{e \in E^C} x_{eith} + \sum_{e \in E^U} X_{eith} + \sum_{j \in N} \eta_{ji} f_{jith} + q_{ith}^+ = \sum_{g \in G} \sum_{p \in P} y_{githp} + \sum_{j \in N} f_{ijth} + q_{ith}^-, \quad \forall i \in N, t \in T^S, h \in T^O \quad (5.6)$$

Pipeline

Constraint (5.7) secures that the heat sent from node i to j in strategic period t at operational period h does not exceed the capacity limit of the pipeline from i to j .

$$f_{ijth} \leq F_{ij}^{MAX}, \quad \forall (i, j) \in N, t \in T^S, h \in T^O \quad (5.7)$$

Storage

The initial storage level in an operational period depends on the initial storage level, and additions and withdrawals in the previous operational period (and corrections for losses where appropriate). In most operational periods, the previous operational period is within the same strategic period (Constraint (5.8)). However, if the operational period under consideration is the first operational period in a strategic period, the previous operational period is the last operational period in the previous strategic period (Constraint (5.9a)).

Constraint (5.8) ensures that the amount of heat at the end of the operational time period h equals the amount stored at the end of the preceding operational time period $h-1$ plus the net addition and withdrawal of heat at current time h . Stored heat and heat addition are corrected for heat losses.

$$s_{ith} = s_{it(h-1)} + \eta^A q_{ith}^- - q_{ith}^+ \quad \forall i \in N, t \in T^S \setminus \{1\}, h \in T^O \quad (5.8)$$

Constraint (5.9a) states that the amount of stored heat at the end of the first operational time in each strategic period t equals the amount stored in the last operational period, t_{last}^O , of the preceding period $t-1$, and the net addition and withdrawal of heat at the first operational time 1. The heat addition is corrected for heat losses.

$$s_{it,1} = \eta_t^S s_{i(t-1)t_{last}^O} + \eta^A q_{it,1}^- - q_{it,1}^+ \quad \forall i \in N, t \in T^S \quad (5.9a)$$

Constraint (5.9b) is a special case of Constraint (5.9a). It ensures that the storage level at the end of the first operational period in the first strategic period in the planning horizon is equal to the initial storage level at the start of the planning horizon, S_i^{START} , and the net addition and withdrawal of heat in the first time period.

$$s_{i,1,1} = \eta_1^S S_i^{START} + \eta^A q_{i,1,1}^- - q_{i,1,1}^+ \quad \forall i \in N \quad (5.9b)$$

Constraint (5.10) ensures that a TES can only store heat from controllable heat technologies.

$$\sum_{e \in EU} X_{eith} \geq q_{ith}^+, \quad \forall i \in N, t \in T^S, h \in T^O \quad (5.10)$$

Capacity Constraint (5.11a) ensures that the amount of heat stored in a TES respects the TES's capacity limit. Constraint (5.11b) applies for the last operational time period in the last strategic period. The constraint ensures that the planning horizon's storage level does not exceed the planned storage level at the end, S_i^{END} .

$$s_{ith} \leq S_i^{MAX}, \quad \forall i \in N, t \in T^S \setminus \{t_{last}^S\}, h \in T^O \setminus \{t_{last}^O\} \quad (5.11a)$$

$$s_{i,t_{last}^S, t_{last}^O} \leq S_i^{END}, \quad \forall i \in N \quad (5.11b)$$

Capacity constraints (5.12) and (5.13) ensure that the added heat (including heat losses) and withdrawn heat do not exceed the respective capacity limits.

$$\eta^A q_{ith}^- \leq Q_{it}^{-MAX}, \quad \forall i \in N, t \in T^S, h \in T^O \quad (5.12)$$

$$q_{ith}^+ \leq Q_{it}^{+MAX}, \quad \forall i \in N, t \in T^S, h \in T^O \quad (5.13)$$

Non-negativity

All variables are non-negative:

$$f_{ijth}, q_{ith}^-, q_{ith}^+, s_{ith}, x_{eith}, y_{githp}, z_{githh'p} \geq 0, \quad (5.14)$$

$$\forall (i, j) \in N, e \in E, t \in T^S, (h, h') \in T^O, p \in P, g \in G$$

5.3 Expanding the Model to Incorporate Uncertainty

In the following sections, the deterministic model is expanded to incorporate uncertainty through a scenario-tree based stochastic model and a multi-horizon model. However, first a review of the chosen model designs is presented.

5.3.1 Model Structure

The problem is modeled as a stochastic program in this chapter, due to operational uncertainty in SH target demand. Only SH target demand is modeled as uncertain because it is highly dependent on outdoor temperature and weather, while HW target demand remains relatively unchanged by this and mostly depends on consumption patterns. The model includes optimization over several horizons, i.e., strategic and operational horizons, as seen in Section 5.2. The model consists of indices, sets, parameters, and variables and is formulated as a linear programming model.

The problem has uncertainties at the operational level. To include this, we first present a stochastic model based on scenario trees. It is important to determine when relevant information (i.e., SH target demand) is revealed in order to construct the scenario tree. The first stage represents the first strategic time period and marks the beginning of the first stage of operational decisions. Information about the operational periods in a strategic period is assumed to be revealed before the beginning of the first operational period. The second stage is the second strategic period where new information is revealed, and operational decisions are made, the third stage represents the third strategic period, and so on. There are no strategic decisions in the model.

If we solve the problem using a traditional scenario tree structure, we get a scenario tree as illustrated in Figure 5.1. The figure shows when information is revealed and how decisions are made. The figure shows the first three strategic periods in the planning horizon. From the strategic time periods, two branches are representing two scenarios for each strategic period. Two operational scenarios are illustrated in the figure for practical purposes. The operational scenarios are sequences of operational decisions. Only the two first operational periods are shown in the figure for simplicity, and dotted lines illustrate the others. To exemplify, the scenario tree in Figure 5.1 could represent a planning horizon of three months, where the strategic periods are months, while the operational periods are hours in each month. At the beginning of each month, a new branching on operating conditions takes place.

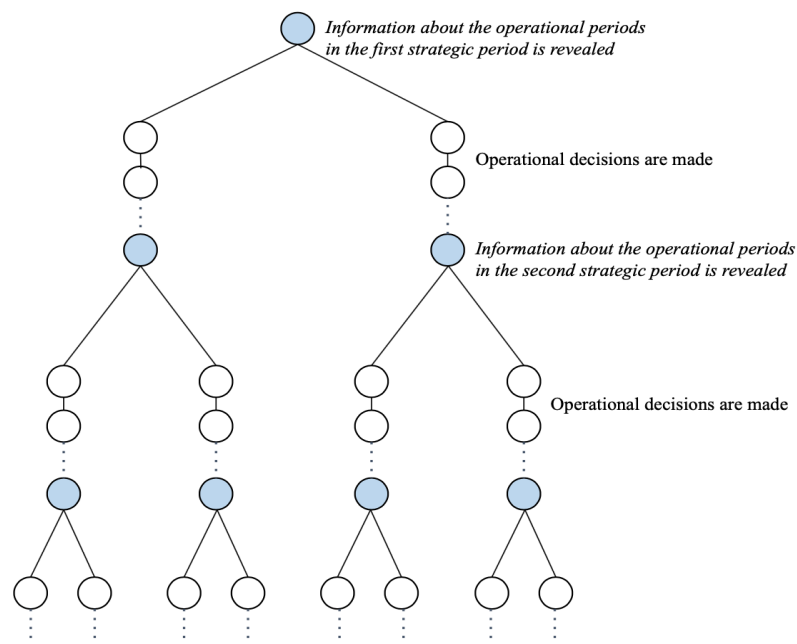


Figure 5.1: Multistage scenario tree.
Source: Own illustration.

The figure illustrates the growth of scenarios as the number of strategic periods increases. With three strategic periods and two scenarios for each period, the scenario tree comprises 2^3 (8) scenarios. In real-life problems, the actual number of scenarios is often much higher, e.g., in a problem with 12 strategic periods and three scenarios for each period, the number of scenarios would increase to 3^{12} (531 441). Hence, this scenario tree structure represents an explosion in the number of scenarios.

Multi-horizon modeling could be an alternative way to solve the stochastic problem (Kaut et al. 2014). The model size in a multi-horizon model grows linearly instead of exponentially, but at the expense of being an approximation. The multi-horizon scenario tree separates the strategic and operational period, and thereby avoid extensive branching. The scenario tree only consists of strategic periods as the operational periods are subtrees embedded in the strategic periods, as illustrated in Figure 5.2. At the beginning of the strategic periods, information about the embedded operational periods is revealed.

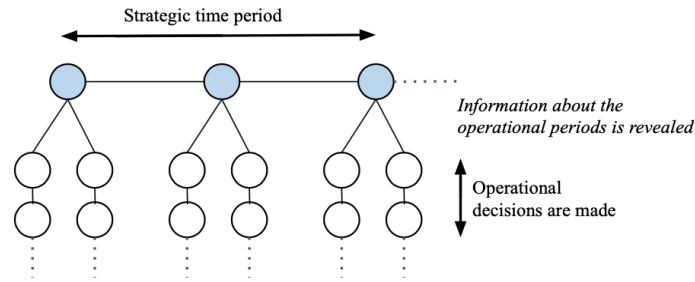


Figure 5.2: Scenario tree with multi-horizon structure.
Source: Own illustration.

As seen in Figure 5.2, the number of scenarios decreases compared to Figure 5.1. With this scenario tree structure, the total number of scenarios goes from 2^3 (8) to $2 \cdot 3$ (6). If we look at the problem with 12 strategic periods and three scenarios for each period, then the total number of scenarios would decrease from 3^{12} (531 441) to $3 \cdot 12$ (36). The massive reduction of scenarios shows the huge impact a multi-horizon structure has on the size of the scenario tree.

As mentioned in Chapter 3, the structure of the multi-horizon scenario tree is based on the assumption that the strategic decisions are independent of a specific operational decision (Kaut et al. 2014). In our model, this is not a problem since there are no strategic decisions. The model also assumes that the first operational decisions in a strategic period do not depend on the last operational decisions in the previous strategic period (Kaut et al. 2014). This is challenging for our problem because of the seasonal storage, where the storage level at the beginning of the first operational period in each strategic period is approximated from the last operational period in the preceding strategic period. The multi-horizon model is, therefore, an approximation of the traditional scenario tree model.

5.4 Traditional Stochastic Model

In this section, the deterministic model is expanded to a stochastic model. In the deterministic model, one decision plan for the entire planning horizon was found. In a stochastic model, decisions must be adapted to the realizations of different uncertain parameters and thereby allowing the decision variables to vary with the different scenarios.

Uncertainty in SH target demand is represented in the model, and different realizations of SH target demand are represented as operational scenarios. The operational scenario set is defined as $\Omega = \{1, 2, \dots, \omega_{last}\}$ and is indexed by ω . $|\omega_{last}|$ gives the number of operational scenarios related to each operating time horizon. In the traditional scenario-tree based stochastic model, each combination of realizations over the modeling horizon accounts for a scenario in the scenario tree. All variables and the parameter for SH target demand are scenario dependent, resulting in an extra index, ω , for all variables. The uncertain parameter SH demand becomes $D_{(SH)ith\omega}$, but all other parameters are unchanged from the deterministic model.

The main difference from the deterministic model is the need for non-anticipativity constraints, in addition to the constraints from the deterministic model. As described in Section 3.4, non-anticipativity constraints are added to ensure that the information structure associated with the decision process is honored. In other words, decisions are made strictly based on known information. The full traditional stochastic model formulation can be found in Appendix A.

5.4.1 Objective function

The objective is still to minimize the total expected operational costs, as shown in Equation (5.15). The terms for operational costs in the traditional stochastic model are the same as the operational costs in the deterministic model. However, all variables are dependent on operational scenarios; therefore, the cost terms are multiplied by the probability of each scenario π_ω . Furthermore, the scenario dependent costs are summed for all scenarios $\omega \in \Omega$. The last term is not scenario dependent as it is a fixed cost associated with HPs for uncontrollable heat production, which is a parameter.

$$\begin{aligned}
\min \sum_{\omega \in \Omega} \pi_{\omega} \sum_{t \in T^S} \sum_{\substack{h, h' \in T^O \\ \wedge h' \geq h}} & \left(\sum_{e \in E} \sum_{i \in N} (C_{eth}^F + C_e^E O_e) x_{eith\omega} \right. \\
& + \sum_{i \in N} \sum_{j \in N} C_{ij}^T f_{ijth\omega} \\
& + \sum_{g \in G} \sum_{i \in N^C} \sum_{p \in P} C_{ghh'p} z_{githh'p\omega} \\
& + \sum_{i \in N} C^A q_{ith\omega}^- \\
& + \sum_{i \in N} \sum_{p \in P} C_{(EL),th}^P \frac{y^{(HW),ithp\omega}}{COPD} \\
& \left. + \sum_{i \in N} \sum_{t \in T^S} \sum_{h \in T^O} C_{(EL),th}^P \frac{X_{eith}}{COPC} \right)
\end{aligned} \tag{5.15}$$

5.4.2 Constraints

Excluding the non-anticipativity constraints, the constraints in the traditional stochastic model are the deterministic constraints with scenario dependent SH target demand and scenario dependent variables. This means that all the constraints in the traditional stochastic model apply to each operational scenario.

Non-anticipativity

Constraints (5.16) to (5.22) are the non-anticipativity constraints considering the scenario dependent decision variables. A new parameter, $\phi_{th\omega}$, is introduced to display whether scenario ω and scenario $\omega + 1$ at a given stage in the scenario tree have identical information.

$\phi_{th\omega}$ represents the scenario tree:

$$\phi_{th\omega} = \begin{cases} 1 & \text{if variables in strategic period } t, \text{ operational period } h \text{ and scenario } \omega \\ & \text{should equal the variables in scenario } \omega + 1 \\ 0 & \text{otherwise} \end{cases}$$

Constraint (5.16) ensures that the heat amount sent from node i to node j in strategic period t in operational period h is the same for the scenarios with identical information.

$$f_{ijth\omega} = f_{ijth(\omega+1)}, \quad \forall i \in N, j \in N, t \in T^S, h \in T^O, \omega \in \Omega \wedge \phi_{th\omega} = 1 \quad (5.16)$$

Constraint (5.17) and Constraint (5.18) ensure that the heat amount withdrawn from the TES or added to the TES at node i in strategic period t in operational period h is the same for scenarios with identical information.

$$q_{ith\omega}^+ = q_{ith(\omega+1)}^+, \quad \forall i \in N, t \in T^S, h \in T^O, \omega \in \Omega \wedge \phi_{th\omega} = 1 \quad (5.17)$$

$$q_{ith\omega}^- = q_{ith(\omega+1)}^-, \quad \forall i \in N, t \in T^S, h \in T^O, \omega \in \Omega \wedge \phi_{th\omega} = 1 \quad (5.18)$$

Constraint (5.19) ensures that the heat amount in the TES connected to node i in strategic period t at the end of operational period h is the same for scenarios with identical information.

$$s_{ith\omega} = s_{ith(\omega+1)}, \quad \forall i \in N, t \in T^S, h \in T^O, \omega \in \Omega \wedge \phi_{th\omega} = 1 \quad (5.19)$$

Constraint (5.20) ensures that the heat amount produced by technology e at node i in strategic period t in operational period h is the same for scenarios with identical information.

$$x_{eith\omega} = x_{eith(\omega+1)}, \quad \forall e \in E^C, i \in N^P, t \in T^S, h \in T^O, \omega \in \Omega \wedge \phi_{th\omega} = 1 \quad (5.20)$$

Constraint (5.21) ensures that the delivered heat amount of demand-type g in node i in strategic period t in operational period h for user profile p is the same for scenarios with identical information.

$$y_{githp\omega} = y_{githp(\omega+1)}, \quad \forall g \in G, i \in N^C, t \in T^S, h \in T^O, p \in P, \omega \in \Omega \wedge \phi_{th\omega} = 1 \quad (5.21)$$

Constraint (5.22) ensures that the amount of deficit load of demand-type g in node i in strategic period t in operational period from h to h' for user profile p is the same for scenarios with identical information.

$$z_{githh'p\omega} = z_{githh'p(\omega+1)}, \quad \forall g \in G, i \in N^C, t \in T^S, h \in T^O, p \in P, \omega \in \Omega \wedge \phi_{th\omega} = 1 \quad (5.22)$$

5.5 Multi-horizon Stochastic Model

In this section, we present the multi-horizon stochastic model as an alternative extension of the deterministic model. Only the differences between the deterministic model and the multi-horizon model will be presented. The full multi-horizon formulation can be found in Appendix B.

This problem is subject to operational uncertainty, and thereby a set of operational scenarios is included in the multi-horizon structured model, similar to the traditional stochastic model. However, one of the advantages of the multi-horizon structure is the reduction of the number of scenarios. The operational scenario set is defined as $\Omega = \{1, 2, \dots, \omega_{last}^M\}$ and indexed by ω . The number of operational scenarios is given by $|\omega_{last}^M|$. The only uncertain parameter in the multi-horizon model is target SH demand, $D_{(SH)ith\omega}$, same as for the traditional stochastic model. All other parameters remain unchanged from the deterministic model. All constraints in the multi-horizon model are scenario dependent and the objective function in the is the same as for the traditional stochastic model, see Equation (5.15) in Section 5.4.1.

5.5.1 Constraints

The one constraint that has significantly changed from the deterministic model is presented in this section. The main difference from the deterministic model is the first operational decisions in each strategic time period. As mentioned in Section 3.4.3, for the multi-horizon model to be accurate, the first operational decisions in a strategic period should be independent of the last operational decisions in the preceding strategic period. For our problem, ignoring the connection between periods has limitations on the accurate presentation of the storage level from one period to the next. In the multi-horizon model presented here, the storage level at the beginning of a strategic period is approximated to be the weighted average storage level for the scenarios in the last operational period in the preceding strategic period. Therefore, the operational decisions in a strategic period are indirectly dependent on all operational decisions in the preceding period. In the end, the multi-horizon model can be described as an approximation of the traditional stochastic model.

Constraint (5.23) ensures that for each scenario ω , the amount of heat at the end of the first operational period in each strategic period t equals the weighted average stored in the last operational period t_{last}^O of the preceding strategic period $t-1$ for all scenarios, plus the net addition and withdrawal of heat at the first operational period. The weighted average storage level in the last operational period of the preceding strategic period is given as the sum of stored heat in each scenario multiplied by the probability of each scenario ω , π_ω . The stored heat in the preceding strategic period and the heat addition are corrected for heat losses.

$$s_{it,1,\omega} = \eta_t^S \sum_{\omega \in \Omega} s_{i(t-1)t_{last}^O, \omega} \cdot \pi_\omega + \eta^A q_{it,1,\omega}^- - q_{it,1,\omega}^+ \quad \forall i \in N, t \in T^S, \omega \in \Omega \quad (5.23)$$

Chapter 6

Data Analysis

This chapter discusses the necessary data origins and starts by presenting the datasets before presenting the parameters that are given as deterministic input to the model. These include costs (CO₂, production, transportation), production capacities, other technical data such as capacity and efficiencies for the pipelines, storage and heat pumps, waste heat supply, HW demand for buildings (henceforth referred to as consumers) and demand requirements for HW and SH. Lastly, we present the regression models used to generate Space Heating (SH) demand. A large part of the data and assumptions in this chapter is compiled based on discussions with SINTEF Energy Research, while some of the input data were obtained from Norwegian data sources. The compilation and verification of the datasets have taken around one and a half months.

The model is applied to Leangen, which is located in the eastern part of Trondheim in Norway. A horse racecourse currently dominates the area, but the plan is to transform it into a residential area. The construction time is estimated to be between 15 and 20 years, starting in 2021 (Lund Hagem Arkitekter 2019). Approximately 75% of the building stock will consist of apartment blocks. Besides, shops, a kindergarten, a nursing home, and office buildings are planned in the residential area (Trondheim Kommune Byplankontoret 2018). The heat supply to the new area is planned to come from a local low-temperature District Heating Grid (DHG). The local heat source to the DHG will be waste heat generated from the cooling of the local ice rink (see Figure 6.1) (Asplan Viak 2018). Moreover, the local DHG will be connected to the main DHG in Trondheim. The main grid is a conventional high-temperature DHG with higher supply temperatures than the low-temperature grid at Leangen. The connection between the main DHG in Trondheim and the DHG at Leangen is planned by indirect connection through the use of heat exchangers. However, we do not consider the technical and cost aspects of heat exchangers in this thesis.

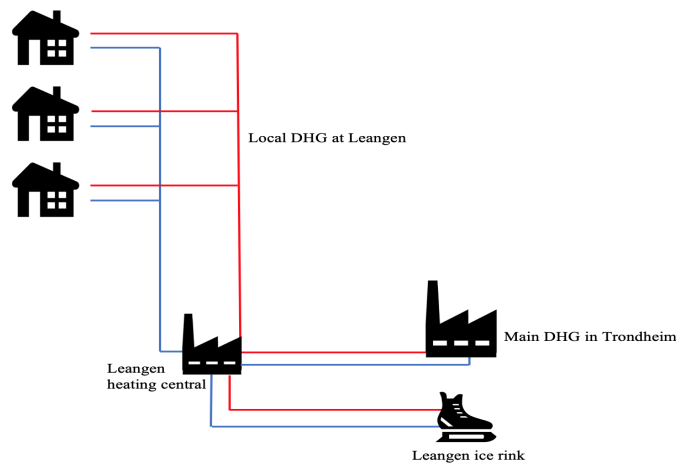


Figure 6.1: Layout of the DHG at Leangen.
Source: Own illustration.

The heating central for the main DHG in Trondheim is located at Heimdal, and the energy mix in 2019 consisted of heat from recovered waste heat (72%), fossil gas (14%), electric boilers (9%) and bioenergy (4%) (Norsk Fjernvarme 2019).

6.1 Datasets

6.1.1 Length of time periods

To capture the fluctuations in heat demand and available waste heat in a year, the model will run with a strategic time horizon of 12 days that represent the months in a year. Summer is represented by June, July, and August, fall by September, October, and November, winter by December, January, and February and spring by March, April, and May. The model will run with an hourly resolution for a planned operational time horizon of 24 hours embedded in each strategic period. The entire planning horizon is therefore 288 hours, and each set of 24 hours represents one month.

6.1.2 Nodes

The low-temperature DHG at Leangen is represented by 25 nodes, as depicted in Figure 6.2. The grid is modeled with one heating central node (node 1 in blue), five branching nodes (nodes 2-6 in orange), and 19 consumer nodes (nodes 7-25 in green). The heating central node receives waste heat from the local ice rink and serves as the connection to the main DHG in Trondheim. The production of heat from controllable technologies takes place in the main DHG, but it needs to be distributed through the heating central to reach

the consumer nodes at Leangen. The local waste heat, from the ice rink at Leangen, is also distributed from the heating central. The consumer nodes are divided between shops, kindergarten, nursing home, office, and apartments. Nodes 9, 16, 19, 21, and 23 are shops of different sizes. The office area is represented by node 14, the nursing home by node 15, and the kindergarten by node 17. The rest of the nodes in green are apartment nodes.

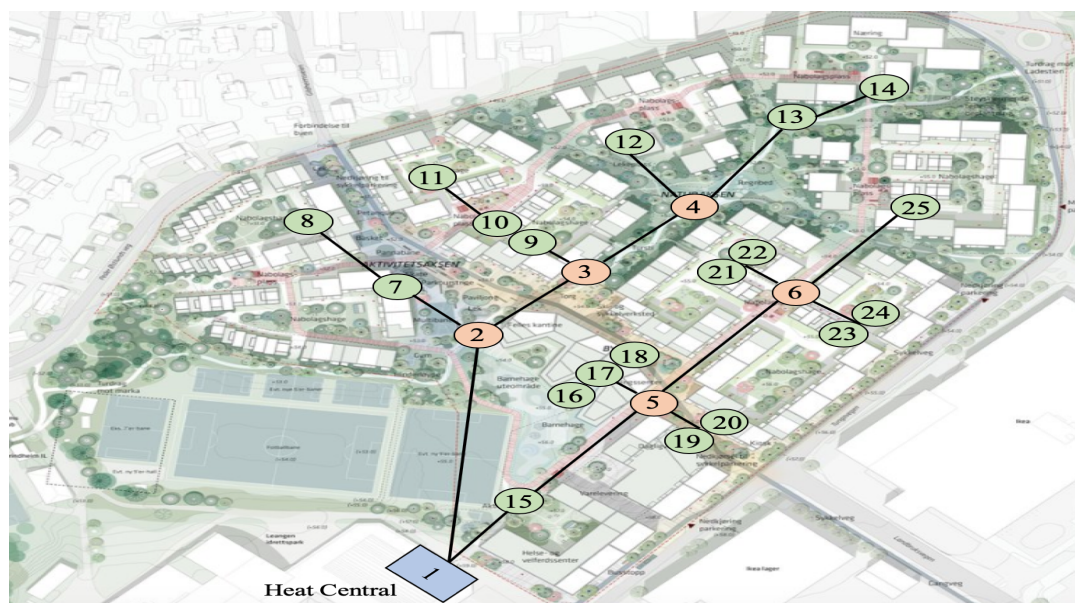


Figure 6.2: Layout of nodes at Leangen.
Source: Own illustration.

6.1.3 Selection of User Profiles

User profiles are designed to investigate the benefits of having consumers with different patterns of heat consumption. The user profiles are based on the different types of buildings that will be built at Leangen (Lindberg et al. 2019). Shops, kindergartens, nursing homes, offices, and apartments are considered as separate profiles. It may also be beneficial to divide the apartments into user profiles to distinguish the different consumption patterns between the residents. These user profiles are evaluated in this section. The user profiles for apartments are divided between singles (in work), couples (in work), families (with small children), students, and seniors (retired). We assume that it is possible to distinguish between these groups in terms of heat demand patterns. Table 6.1 presents the assumed peak hours for nine user profiles. A weekday is chosen, as the heat demand patterns are considered to be more identical on weekdays.

Table 6.1: Peak hours during a typical day for nine user profiles at Leangen.

Singles	Couples	Families	Students	Seniors	Shops	Kindergarten	Nursing home	Office
6-8 18-21	6-7 18-21	6-7 16-20	7-12 20-22	9-18 -	6-12 -	6-11 -	3-11 -	6-12 -

For five user profiles, we only distinguish between the different building types. As a result, we do not differentiate between the consumption patterns of the residents in the apartments. In order to identify the peak hours, the average target demand for each building type was analyzed based on linear regression of the data for target heat demand (SH and HW) generated from a load profile generator found in Lindberg et al. (2019). The subsequent peak hours for five user profiles are presented in Table 6.2.

Table 6.2: Peak hours during a typical day for five user profiles at Leangen.

Apartments	Shops	Kindergarten	Nursing home	Office
6-9 18-21	6-12 -	6-11 -	3-11 -	6-12 -

The deterministic model was run with both alternatives to determine if it is beneficial to have five or nine user profiles. The variables that depend on user profiles are delivered heat and deficit (SH and HW), which is dependent on the demand requirement for each user profile. Therefore, a comparison of the total delivered heat is done. The results can be seen in Figure 6.3 and show the absolute difference in each hour. The total delivered heat is very similar in both cases, with the total delivered heat for nine user profiles being 0.001% higher than for five user profiles. The average difference in delivered heat is 0.64% between five and nine user profiles. The total expected operational cost for five user profiles is 0.06% less than for nine user profiles. The difference in the variables and thereby, the total operational cost is so small that five user profiles (corresponding to each building type) are preferred to simplify the pre-processing of the model. In addition, the individual user profiles for people living in the apartments, as given in Table 6.1 are based on assumptions, while the user profiles corresponding to building types, as given in Table 6.2 are based on actual data on peak hours generated from the load profile generator (Lindberg et al. 2019).

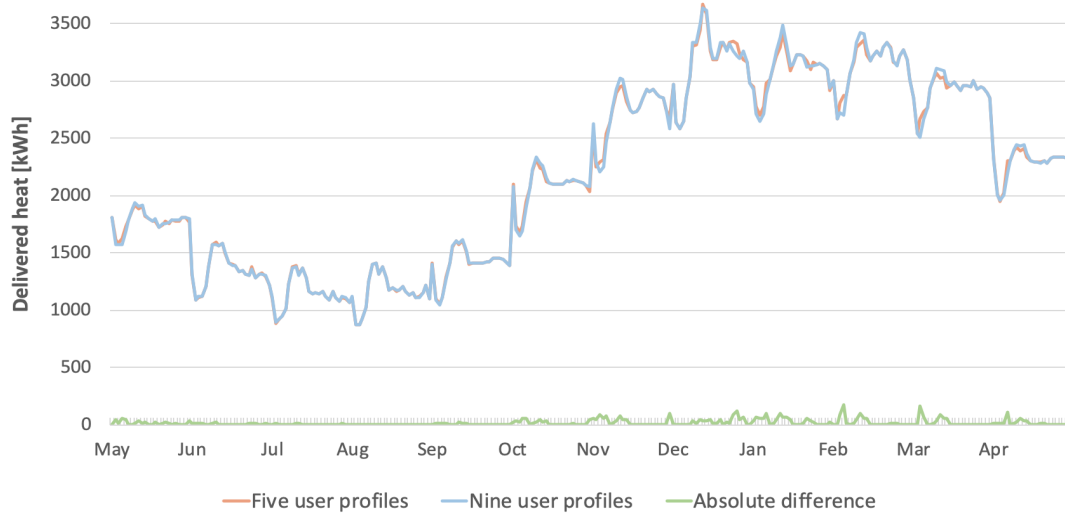


Figure 6.3: The difference in total delivered heat with five and nine user profiles.

6.2 Parameters

6.2.1 CO₂ emission Costs

The government in Norway has set a CO₂ fee to 0.5 NOK/kg CO₂ in order to reduce GHG emissions (Regjeringen 2018). Therefore, the CO₂ fee used in our model is set to 0.5 NOK/kg. Together with the carbon emission factor for each production technology, it makes up the cost associated with emitting CO₂. The carbon emission factor for the production technologies is given in Table 6.3, in which the carbon is given in kg CO₂ emissions per kWh heat produced (Kauko, Kvalsvik, et al. 2017b). The waste heat from the local ice rink is considered as CO₂ neutral since the heat is a by-product of the cooling process of the ice rink.

6.2.2 Production Costs

The production costs include fuel costs and carbon emission costs. We use production costs inferred from production technologies with capacities close to the real capacities of the main DHG in Trondheim. The production costs are listed in Table 6.3 for waste incineration, bio boiler, electric boiler, LPG, and NG. The fuel costs in the table also include fees if applicable, e.g., electricity fee for the electric boiler (Sidelnikova et al. 2015). For the bio boiler, the fuel costs depend on the type of biofuel. In Trondheim, the bio boiler is based on dry wood chips as fuel, which laid the foundation for finding the appropriate production cost. The waste heat supply from the local ice rink at Leangen

is considered free of charge as it is a by-product. In the model formulation described in Chapter 5, the fuel costs can vary from one period to the next. However, in the case study of Leangen, the costs for waste incineration, bio boiler, LPG and NG are considered constant for all periods.

Table 6.3: Production costs for different production technologies.

Production technology	Fuel cost [NOK/kWh]	Carbon emission factor [kg/kWh]	Emission cost [NOK/kWh]	Production cost [NOK/kWh]
Waste incineration	0.0153	0.0112	0.0056	0.0209
Bio boiler	0.3140	0.0198	0.0099	0.3239
Electric boiler	0.3186-0.4979	0.1100	0.0550	0.3736-0.5529
LPG	0.6140	0.2740	0.1370	0.7510
NG	0.2200	0.2430	0.1215	0.3415

Source: Sidelnikova et al. (2015) and Kauko, Kvalsvik, et al. (2017b).

The fuel cost for the electric boiler is the electricity cost, which is dependent on the power cost, fees, and the cost for grid rent (Sidelnikova et al. 2015). The power cost is time-dependent and based on historical power market data from Nord Pool. The hourly spot price for power in Trondheim is available for the years 2013-2019 (NordPool 2020). As described in Section 6.1.1, the model will run with 12 representative days. The hourly power price from Nord Pool (2013-2019) is averaged for each month to set data for the 12 representative days, and thus every hour of the representative day is the average of the month for the particular hour. The range of time-dependent fuel cost, the carbon emission factor and the emission cost for electricity is shown in Table 6.3. The production cost for the electric boiler is the sum of the fuel cost and the emission cost and varies by the hour and ranges from 0.3736 to 0.5529 NOK/kWh during the planning horizon. Appendix C shows the average electricity price for each hour in the planning horizon.

6.2.3 Transportation Costs

The transportation cost for delivering heat from the heating central to consumers is often associated with the pump work required to pump the heat carrier through the pipelines. The local DHG at Leangen will be developed as a compact grid, with short pipeline lengths. The total grid length will require little pumping work and will result in low transportation costs. Therefore, to simplify the analysis, we set the transportation cost between nodes at Leangen to zero.

6.2.4 Production Capacities

Trondheim DHG is a large heat source for the local DHG at Leangen, and covers the demand that exceeds the supply of local waste heat. The baseload of the main DHG in Trondheim is covered by averagely 78 MW waste heat from waste incineration in a year and heat produced from boilers based on biofuels, such as a bio, bio-oil or biogas. The peak load can be covered by an electric boiler, oil boiler, NG or LPG. The main DHG also has a small heat pump with 1 MW capacity, which is very small compared to the other technologies. Therefore, it is neglected in this case study.

The production mix for the DHG in Trondheim varies from year to year, due to an increasing number of consumers, variations in outdoor temperature, and operational technical matters. It is, therefore, difficult to find appropriate scaled-down capacities of the production technologies to cover the local heat demand at Leangen. The starting point for determining production capacities was the production mix for Trondheim in 2019 given by Statkraft, shown in Appendix D. The idea is that the bio boiler covers the minimum total heat demand (SH and HW) in the months from October to April. Waste incineration covers the maximum demand in the summer months (i.e., June, July, and August), assuming from the table in Appendix D that the waste incineration capacity for Trondheim is not fully utilized in the summer. Waste incineration is also utilized as the baseload in May and September, seen in Table 6.4, as the production technology in Trondheim has available capacity.

In order to find a capacity that makes use of DSM and TES, the capacity of peak load technologies is defined as the difference between average and minimum demand. The electric boiler is utilized to cover the peak loads from October to April. LPG is expensive compared to the other technologies, and therefore, it is only used as a buffer to cover peak load that might be caused by a scenario with very high demand. The buffer with high capacity makes the mathematical model feasible for all scenarios. The electric boiler and natural gas are used as buffers in May and September. In these months, the waste incineration only covers the average heat demand, and therefore it might be necessary with another production technology to cover the peak. Thus, buffers of an electric boiler and natural gas ensure the feasibility of the model. The production technologies that are not mentioned in Table 6.4 are assumed to be unused in the DHG, and their capacities are thereby zero. The proposed production mix for Leangen is given with more details in Appendix E.

Table 6.4: Monthly production technology capacities in kWh.

Month	Waste incineration	Bio boiler	Electric boiler	LPG	NG
January	0	1 733	688	10 000	0
February	0	1 684	516	10 000	0
March	0	1 900	507	10 000	0
April	0	1 636	413	10 000	413
May	1 568	0	10 000	0	10 000
June	1 468	0	0	0	0
July	1 317	0	0	0	0
August	1 162	0	0	0	0
September	1 043	0	10 000	0	10 000
October	0	1 179	522	10 000	522
November	0	1 397	565	10 000	565
December	0	1 521	552	10 000	0

6.2.5 Pipeline Capacities and Efficiencies

The pipelines in the local DHG at Leangen will be designed so as not to limit the operation of the DHG. The capacity limit for pipelines between nodes is set to a sufficiently large value in every hour as not to limit the distribution of heat at any time. The heat loss in the pipelines will be marginal since the grid is compact, with a total length of 1300 meters. Therefore, the efficiency ratio for heat flow from one node to another is set to 1, neglecting any small heat losses in the pipelines.

6.2.6 Storage Capacity and Efficiency

There is no current plan of installing a seasonal Thermal Energy Storage in the local DHG at Leangen. Nevertheless, there is potential for it, and analyzing its effect on the DHG can help the DHO make better decisions in the future regarding the design and operation of the DHG. The TES location will not affect the results since the heat loss in the pipelines is neglected. Therefore, the TES is arbitrarily placed in co-location with the heating central. It will only be possible to add heat to the TES during the summer (i.e., in June, July, and August). For this reason, maximum added heat for each hour in the summer is set sufficiently high (not restricting the amount of heat added), and maximum withdrawn heat is set to zero. Heat can be withdrawn in the fall, winter, and spring (i.e., September-May). Hence, maximum withdrawn heat for each hour in September-May is set sufficiently high, while maximum added heat is set to zero. The TES is assumed to be empty before the planning horizon starts, and since May is set to be the first day of 24

hours in the planning horizon of 12 representative days, the TES is assumed to be empty before May.

The unit cost for adding heat to the TES is set to zero, as the required cost for adding heat is negligible. The heat losses related to adding and withdrawing heat to and from the TES are also considered negligible. The heat loss for stored heat in the TES is assumed to be 40% in a year (Tvärne 2018). The TES is assumed to be almost empty six months after starting the withdrawing period (i.e., after February). This means that the heat amount in the storage is being affected by heat losses in the period June-February. The TES will have a total efficiency of 60% in a whole year, resulting in the efficiency ratio $\sqrt[8]{0.60} = 0.945$ for the year divided into eight efficiency periods. Consequently, the efficiency ratio is set to 0.945 in the transition between all months to capture this.

6.2.7 Heat Pump Cost, Efficiencies and Temperatures

It is decided to have one centralized heat pump, co-located with the heating central in the implementation of the Leangen case study. The centralized heat pump is responsible for lifting the local waste heat temperature to match the grid temperature. In addition, every consumer node will have a heat pump, which ensures the correct temperature of the HW.

According to Lund et al. (2014), comfortable room temperature can be maintained with the district heating supply temperature around 40°C. Concerning the hygienic risk of Legionella growth (with a reproductive temperature range of 25 to 45°C) in hot water storage systems, the HW storage tank should be held at a temperature of no lower than 55°C (European Committee for Standardization 2012). Following this, the desired temperature for HW should be above 55°C, and the desired grid temperature at Leangen is set to 40°C. The temperature of the waste heat from Leangen ice rink is assumed to be 35°C. Based on this, the Coefficient Of Performance (COP) could be very high, up to 25 for the heat pumps, but that is for theoretical loss-free heat pumps. Therefore, the COP is set to 5 for the decentralized heat pumps, which lifts the temperature from 40C to 55°C, while the COP is 10 for the centralized heat pump. The centralized heat pump has a higher COP because the temperature lift from waste heat to grid temperature is very small. A COP between 5 and 10 is only possible if the temperature lift is very low (Kemp 2012).

The power cost used for the operation of heat pumps is based on historical power market data from Nord Pool and is the same as the production cost for the electric boiler described in Section 6.2.2 and Appendix C. The production cost for electricity, described in Table 6.3, is considered as the only operational cost for the heat pumps, as start-up costs are disregarded.

6.2.8 Waste Heat Supply

The local ice rink generates the waste heat supply at Leangen. The heat supply was collected in an hourly time resolution from the 1st of January to the 31st of December in 2019. Figure 6.4 depicts the hourly averaged waste heat supply at Leangen through the year.



Figure 6.4: Hourly averaged local waste heat supply at Leangen.
Source: SINTEF Energy Research.

6.2.9 Demand Requirement for Hot Water

It is assumed that all consumer nodes have hot water storage tanks that the DHO is responsible to heat. It is also assumed that it is possible to utilize DSM by varying the hourly supplied heat for HW, due to a high number of hot water storage tanks that act as buffers. It is assumed that the hot water tanks are very well insulated, i.e., heat supplied during the night is kept at the supplied temperature during the day. The consumers are therefore indifferent to whether the tanks are heated at daytime or preheated during the night. Based on these assumptions, it is not important to distinguish between HW consumer patterns for different user profiles. Electricity is used to power the heat pumps

that are used in the process of heating the hot water storage tanks. It will be desirable for the DHO to heat the hot water storage tanks when the electricity price is low. To avoid huge peaks caused by the changes in electricity price, we introduce a lower bound of demand fulfillment for every hour and the whole day (hour 0-23). A default value for HW of 20% deficit and 20% surplus per hour is chosen for each user profile. In addition, daily deficits are not allowed, ensuring that the total HW demand during a day must be fulfilled. The reason for meeting the entire heat demand during a day is to ensure a sufficient supply of HW. The 20%-values is chosen to give the DHO some flexibility in the time of heat production and the opportunity to take advantage of the changes in the electricity price.

6.2.10 Target Hot Water Demand

The Hot Water target demand for the consumers at Leangen is generated in an hourly resolution from a load profile generator (Lindberg et al. 2019). The data is represented over a fictional year from 1st of January to 31st of December based on an averaged temperature profile for Trondheim (see Section 6.3 for more information about the load profile generator). The aggregated heat demand for all consumer nodes at Leangen is averaged by the hour and depicted in Figure 6.5. The figure shows that the HW demand pattern is independent of outdoor temperature and month but varies with the hour of the day, corresponding to the fact that HW demand is highly dependent on consumer patterns.

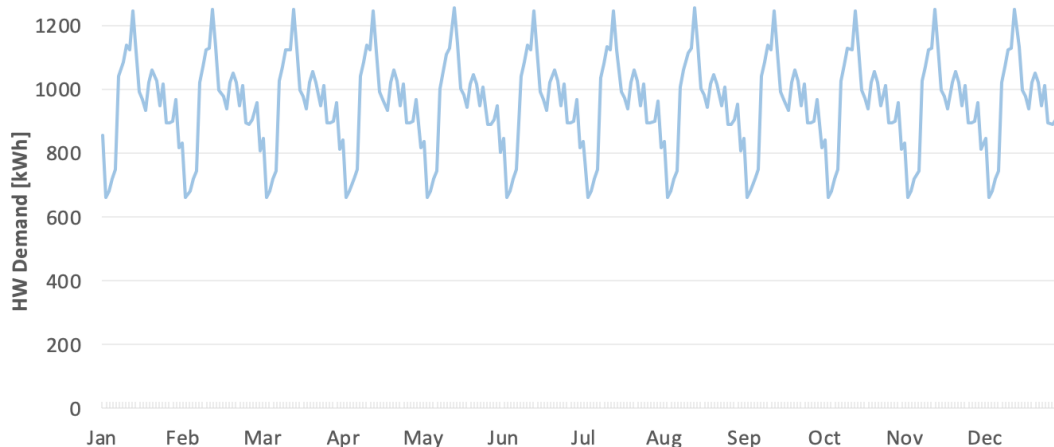


Figure 6.5: Hourly averaged heat demand for HW at Leangen.
Source: SINTEF Energy Research.

6.2.11 Demand Requirement for Space Heating

This section covers the demand requirements for SH. Hourly upper and lower bounds for SH demand fulfillment are depicted in Table 6.5. It should be possible to deliver a lower percentage of the SH demand during peak hours than in off-peak hours to reduce the delivered heat during peak hours. It should also be possible to deliver more surplus in off-peak hours than in peak hours to compensate for the deficit in peak hours. The kindergarten and the nursing home have stricter bounds than the other user profiles, as they are considered as the most sensitive user profiles.

Table 6.5: Hourly lower and upper bounds for SH demand fulfillment at Leangen.

Building type	Lower/Upper bounds [%]	
	<i>Off-peak</i>	<i>In-peak</i>
Apartments, shops & office	96/108	92/104
Kindergarten & nursing home	96/106	94/104

Table 6.6 shows the upper and lower bounds for demand fulfillment for intervals over several hours. Intervals are based on average peak hours for SH demand for the different user profiles through a year, which are found by a regression model based on data generated from the load profile generator (more about regression in Section 6.3). An interval covers both peak hours and some hours preceding the peak hours. The purpose of the intervals is to allow the District Heating Operator to reduce the production and delivery of heat in peak hours by delivering more heat in preceding hours. The idea is to under-deliver heat in the peak hours, but deliver surplus heat earlier in the day to smooth the curve for delivered heat. It is assumed that consumers will be dissatisfied if a large portion of their heat demand in the peak hours is delivered several hours after the peak hours.

Table 6.6: Lower and upper interval bounds for SH demand fulfillment at Leangen.

Buildings type	Interval [hours]	Lower/Upper bounds [%]
Apartments	3-9 & 16-22	96/108
Shops, office, kindergarten & nursing home	0-12	98/104

Apartments have one peak interval in the morning and one in the evening. The interval from hour 3 to 9, includes both hour 3 and hour 9 of the day (a full day consists of the hours 0-23). The shops, kindergarten, nursing home, and office have one long interval, starting at midnight. The long interval has a stricter lower and upper bound for demand fulfillment than the shorter intervals for apartments, to ensure consumer comfort. The

upper bounds of the intervals eliminate the risk of delivering a significant portion of the daily demand requirement to be delivered within one interval, ensuring customer comfort. In addition to the intervals in Table 6.6, the DHO has upper and lower bounds for demand fulfillment for a whole day (hour 0-23), and they are the same for all user profiles. In the case study of Leangen, we allow to curtail 2% of the total demand during a day and to deliver 2% more than the total demand, in order not to restrict the model. In Chapter 9, we do an analysis of the hourly, interval, and daily bounds for SH demand fulfillment.

6.3 Regression Model for Space Heating Demand

Space Heating and Hot Water demand for Leangen are originally generated from a load profile generator developed to forecast heat load and electric load in Norway. The generator is a simulator designed to simulate the SH and HW demand based on several characteristics. The SH demand from the load profile generator depends strongly on the shape, size, and physical properties of the building and outdoor temperatures. On the other hand, the HW demand mainly depends on the number of persons in the building and their behavior. The load profile generator also allows us to distinguish between regular and energy-efficient buildings. The generator explains load as a function of time (hour of the day, type of day, such as weekdays and weekends) and outdoor temperature. The resulting parameter is the SH or HW demand normalized per floor area unit. The original load profile generator used data points based on historical demand data for the years 2009-2011 (Lindberg et al. 2019), but it has since been upgraded with an expanded database. The present temperature data is based on Trondheim's weather profile from SIMIEN (ProgramByggerne 2020), a software used for energy simulations and building evaluations. The profile is a form of design profile, consisting of an average year with some extremely hot and cold days.

The load profile generator is manually run, and for the scenario generation in the stochastic models, this results in a time-consuming task. SH data for all consumer node combinations and possible outdoor temperature scenarios for the multi-horizon model require the load profile generator to run 57 times, resulting from having 19 consumer nodes with three scenarios. The traditional stochastic model must be run 124 659 times, based on 19 consumer nodes with 6 561 different scenarios each. Running the model manually 124 659 times is time-intensive work, and therefore, regressions models are developed alongside a Python program that generates the SH target demand for all scenarios. Based on the input and output data of the load profile generator, a time series analysis was done to find a linear relationship between the outdoor temperature and the SH target demand. The result is a linear regression function for each of the five building types.

To determine the optimal lag length for the outdoor temperature observations, we used Stata, a general-purpose statistical software. Stata has an economic package that calculates the optimal lag length based on eight criteria (see Section 3.5). To find the lag length, one must specify the maximum accepted length, and Hoffmann (1987) states that there is no a priori guide to what the maximum lag length should be. However, Wooldridge (2003) mentions that with annual observations, the number of lags is typically very small (one or two lags) to avoid losing the degrees of freedom. Since we are analyzing annual data, two lags were therefore chosen as the maximum length. The output results show that for almost all the eight criteria, including the HQ criterion, the optimal number of outdoor temperature observations that must be included in the regression analysis is one. Table F.1 in Appendix F shows the optimal number of lags that must be included in the regression analysis of the apartments. The tables for the remaining four buildings (shops, kindergarten, nursing home, and office) are very similar, and therefore not included in the appendix.

The last step was to conduct multiple regression analyses for the five different building types. In addition to the outdoor temperature variable for the current hour, dummy variables were introduced. Dummy variables are artificial variables that represent categorical data. According to Trochim (2007), dummy variables are useful because they enable a single regression equation to represent multiple groups. When defining dummy variables, if there are k categorical variables, only $k - 1$ dummy variables are needed (Trochim 2007). To avoid having regression functions for each month and hour, we introduce 34 dummy variables, 11 dummy variables for months, and 23 for hours. The result is that we only need to make five regression models, one for each building type. Table 6.7 shows the coefficients of the regression variables. The temperature variable *Temp* indicates the outdoor temperature observation, while D_1 - D_{34} are the dummy variables. Only variables with an absolute t-statistic value larger than one are part of the regression functions since a zero t-statistic value means that the sample results exactly equal the null hypothesis, which indicates that there is no difference between the obtained values and the expected results. As the difference between the sample data and the null hypothesis increases, the absolute value of the t-value increases (Kim 2015). The coefficients marked with – in Table 6.7 indicate that their corresponding variables have t-statistic values lower than one.

Table 6.7: Coefficients in the regression functions for the five building types.

Coefficient	Apartments	Shops	Kindergarten	Nursing home	Office
C_1	-0.6035	-0.9683	-1.1635	-0.9744	-0.84739
C_2	1.1546	-	-	0.2648	-
C_3	-0.7694	-0.3547	-	-	-
C_4	-0.8871	-0.4766	-	0.6292	-
C_5	-	-	-	0.7159	0.8785
C_6	-0.8039	-	0.6355	1.8527	1.9660
C_7	0.8696	1.5567	3.6276	2.5660	3.8097
C_8	1.3876	2.8659	7.1697	3.0431	5.4705
C_9	1.6830	4.1055	9.9623	4.4130	6.1393
C_{10}	1.5984	4.7388	8.9623	4.8592	6.3925
C_{11}	2.5046	5.4444	8.0376	5.0284	6.2753
C_{12}	3.2528	5.7972	8.2628	5.3328	6.3805
C_{13}	3.7098	5.7447	7.7871	5.2635	6.3890
C_{14}	3.9462	5.7350	7.1686	5.3412	6.2500
C_{15}	3.0721	5.5947	7.3883	5.3063	6.0930
C_{16}	3.0671	5.5239	7.3660	5.0394	5.8191
C_{17}	3.0459	5.0885	6.6103	4.7160	5.3324
C_{18}	3.6014	4.8151	4.5019	4.5064	4.7586
C_{19}	3.4388	4.2629	3.0142	3.6446	3.8588
C_{20}	3.8516	3.8893	2.8177	3.0852	2.7488
C_{21}	3.5184	3.1014	2.4715	1.8059	2.1137
C_{22}	2.8995	2.2050	2.3902	1.8059	1.6473
C_{23}	1.7998	1.1927	1.4415	1.3860	1.2139
C_{24}	1.5795	0.7377	1.1398	0.7026	-
C_{25}	-	-	-	-	-
C_{26}	-	-0.4701	-0.365	-0.2766	-0.3210
C_{27}	-0.3454	-1.7704	-1.0980	-0.1050	-1.1250
C_{28}	-1.3348	-2.2935	-1.2830	1.5811	-1.4547
C_{29}	-2.1126	1.8249	-1.2119	-1.7224	-1.3697
C_{30}	-2.4057	-0.5186	-0.6896	-1.6021	-0.8060
C_{31}	-1.9780	-0.5646	-0.5609	-1.5840	-0.8169
C_{32}	-2.0507	-2.1880	-1.5536	-1.9027	-1.5704
C_{33}	-2.4323	-1.8860	-0.9748	-1.2602	-1.1628
C_{34}	-1.6573	-0.6082	-	-0.4055	-0.2055
C_{35}	-1.6573	-	-	-	-
Constant	-0.6640	11.0999	14.0999	13.7175	9.6832

Equation (6.1) presents the general regression function for SH demand. The specific regression function for each building type can be found in Appendix F.

$$\begin{aligned}
Y = & C_1Temp + C_2D_1 + C_3D_2 + C_4D_3 + C_5D_4 + C_6D_5 + C_7D_6 + \\
& C_8D_7 + C_9D_8 + C_{10}D_9 + C_{11}D_{10} + C_{12}D_{11} + C_{13}D_{12} + \\
& C_{14}D_{13} + C_{15}D_{14} + C_{16}D_{15} + C_{17}D_{16} + C_{18}D_{17} + C_{19}D_{18} + \\
& C_{20}D_{19} + C_{21}D_{20} + C_{22}D_{21} + C_{23}D_{22} + C_{24}D_{23} + C_{25}D_{24} + \\
& C_{26}D_{25} + C_{27}D_{26} + C_{28}D_{27} + C_{29}D_{28} + C_{30}D_{29} + C_{31}D_{30} + \\
& C_{32}D_{31} + C_{33}D_{32} + C_{34}D_{33} + C_{35}D_{34} + C_{36}D_{35} + Constant
\end{aligned} \tag{6.1}$$

In Figure 6.6, the SH demand for apartments is depicted for the regression model and load profile generator, including the absolute difference in each hour. The total heat demand generated from the regression model and the load profile generator is similar, with only some deviation in the summer (i.e., June, July, and August). The heat demand generated by the regression model in the summer is almost zero because the regression model can not find a clear linear relationship between outdoor temperature and the total heat demand based on the given data for the summer months. However, this does not present a problem since the uncertainty is ignored in the summer.

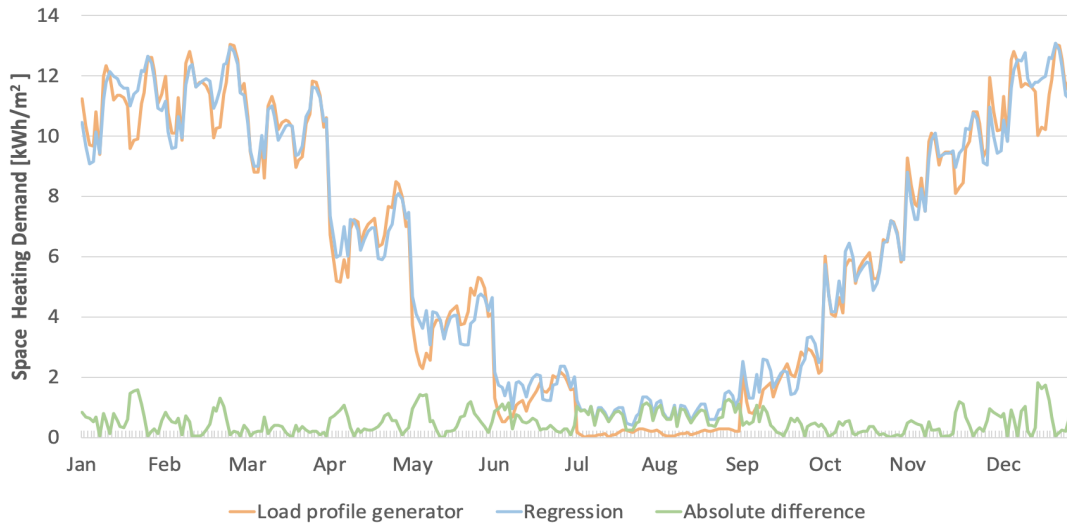


Figure 6.6: The difference in SH demand for load profile generator and regression model.

Table 6.8 shows the R-squared for the five building types, and all have values close to 0.9, which, together with Figure 6.6, indicates that the linear models provide a reasonable prediction of the SH demand for the different building types (see Section 3.5).

Table 6.8: R-squared values for the five building types.

	Apartments	Shops	Kindergarten	Nursing home	Office
R-squared	0.892	0.908	0.887	0.963	0.883

Chapter 7

Scenario Generation

This chapter intends to explain how stochasticity in the optimization problem is dealt with through scenario generation (Section 3.4.5). The chapter begins with the scenario generation algorithm used for the stochastic models in this thesis, followed by an evaluation and discussion of the scenario generation method.

7.1 The Scenario Generation Algorithm

In this thesis, scenarios for SH demand must be generated to solve the stochastic programming models. The selection of scenarios has a significant impact on model outcomes. A higher number of scenarios can capture more uncertainty, but they can also lead to a very complex model. On the other hand, a small number of scenarios may lead to an insufficient image of reality. Following this, three different scenarios for temperature (low, medium, and high) are generated for each month with uncertain SH demand (September-April). Three temperature scenarios for each month were chosen to have a moderate and realistic representation of reality without generating too many scenarios. In comparison, five temperature scenarios for each month will lead to 390 625 scenarios in the traditional stochastic model, while three temperature scenarios give 6 561 scenarios. The regression models are then used to approximate SH demand scenarios based on outdoor temperatures. From May to August, the demand for SH is very low due to high outdoor temperatures. Thereby, uncertainty in this period is not considered. A low-temperature scenario as input to the regression model results in a high-demand scenario for SH, and a high-temperature scenario results in a low-demand scenario for SH.

In order to use regression models to approximate SH demand, temperatures for Leangen are required for each hour in the planning horizon (see Section 6.3). The starting point for the generation of temperature scenarios is the hourly average temperatures for a year in Trondheim, with some extreme values collected from the building simulation software SIMIEN (ProgramByggerne 2020). These temperatures are then averaged for each day and used as input to the scenario generation algorithm. In this thesis, a deterministic

approach for scenario generation is chosen. If all input parameters to the scenario generation algorithm are held constant, the same scenario tree will be generated if we repeat the scenario generation procedure.

7.1.1 K-means Clustering

Clustering analysis is a method for distance measurement, where the primary goal is to classify and compress data in groups (Celebi et al. 2013). K-means clustering is the most commonly used version as it follows a heuristic algorithm, beginning with grouping data into clusters and integrating until a predefined termination criterion is met. The algorithm is suitable for scenario reduction as the number of cluster centers (i.e., centroids) can be set to the desired number of scenarios to avoid duplication of similar data series. In this thesis, the k-means clustering algorithm is used to divide each month with uncertain SH demand into three temperature clusters; low, medium, and high. The input data is the pre-processed average outdoor temperature for each day, and the length of the dataset is the n days in the month. The k-means clustering algorithm aims to assign similar data points to the same cluster. The clusters are created to be as different as possible, and thus one data point can only be assigned to one cluster (Lloyd 1982).

When the k-means clustering is applied to find the temperature scenarios, the algorithm chooses three random positions inside the data domain to be the initial centroids for the low, medium, and high-temperature clusters. All data points used as input are assigned to the cluster with the shortest Euclidean distance from the data point. In addition, the value of each centroid is set to the mean of all data points within the cluster to which the centroid belongs. The algorithm is repeated until the stopping criterion is met, i.e., until the centroids' values converge to the same value. Algorithm 1 shows the pseudocode of the applied k-means clustering algorithm.

Algorithm 1 K-means clustering algorithm.

Input: The outdoor temperature data $T = \{t_1, \dots, t_N\}$, the number of clusters $k = 3$

Output: 3 centroids $\{c_1, c_2, c_3\}$ dividing T into 3 clusters

Choose 3 initial centroids $C = \{c_1, c_2, c_3\}$ from T

Initialize all partition subsets as empty: $C_1 = C_2 = C_3 = \{\}$;

while For each cluster, the values of the centroids from the m previous iterations equal the value of the centroid from the current iteration **do**

 Assign each temperature observation to the closest centroid:

for $i \in \{1, \dots, N\}$ **do**

$l = \arg \min_{j \in \{1, 2, 3\}} \|t_i - c_j\|^2$;

$C_l = C_l \cup t_i$;

end

 Define new centroids based on current position:

for $j \in \{1, 2, 3\}$ **do**

$c_j = \sum_{i \in \{1, \dots, N\}, t_i \in C_j} t_i / |C_j|$;

end

end

Figure 7.1 shows the clusters found by the algorithm for the months with uncertain SH demand, which is from September to April. The blue color marks the clusters categorized as low-temperature scenarios, while green and orange represent clusters for the medium and high-temperature scenarios, respectively.

		Average temperature of the day									
Day	September	October	November	December	January	February	March	April			
1	13.8	3.0	-8.0	0.1	4.9	3.8	-0.1	-1.5			
2	14.3	2.4	-5.8	-4.4	2.4	3.1	-1.3	-0.7			
3	14.8	3.5	-3.8	3.6	2.6	0.6	-3.7	-2.4			
4	16.8	4.9	-2.8	3.4	1.8	-7.4	-5.1	-0.2			
5	15.8	6.0	-2.0	-0.6	0.3	-1.1	-4.4	5.8			
6	13.2	6.2	-1.6	-1.9	-1.4	-2.5	-2.5	5.1			
7	9.7	7.7	-0.4	-1.4	-0.3	-0.5	-2.8	8.3			
8	11.4	5.7	3.6	0.5	-2.0	-3.7	-7.0	7.4			
9	8.3	8.0	6.0	-2.5	-5.0	-8.7	-8.1	6.3			
10	7.5	11.8	7.0	-0.3	-4.4	-5.1	-5.8	9.3			
11	5.2	13.0	8.6	-6.2	-3.2	-4.1	-2.1	10.3			
12	6.4	10.5	4.0	1.2	-16.2	-6.2	-3.3	7.0			
13	7.0	9.9	1.6	-3.1	-10.9	-0.2	-1.7	3.7			
14	12.3	9.4	2.1	2.4	-10.0	-13.1	-0.8	4.0			
15	11.0	8.7	-0.7	3.0	-15.5	-11.3	0.7	2.8			
16	10.5	5.3	1.2	6.3	-4.0	-3.0	1.2	2.3			
17	4.5	7.0	2.6	2.2	-1.2	0.2	5.6	4.4			
18	10.1	6.6	0.5	5.3	1.7	-4.5	2.8	0.8			
19	8.6	4.2	7.7	4.7	4.1	-1.5	1.9	0.3			
20	8.0	8.3	6.5	4.2	1.2	2.0	-0.4	1.5			
21	9.9	7.4	4.4	-6.7	2.9	4.6	0.3	1.8			
22	7.8	4.5	5.0	1.6	3.9	5.6	3.0	3.4			
23	10.1	2.7	5.5	-5.5	0.8	1.2	1.6	4.0			
24	12.7	3.8	-1.1	-11.0	-5.6	1.5	2.5	3.1			
25	11.9	1.6	3.0	-14.6	-2.6	0.9	2.1	6.6			
26	9.4	-0.9	0.9	-12.8	4.0	-2.0	1.0	5.5			
27	9.1	0.4	0.0	-9.6	3.5	2.2	4.3	7.8			
28	5.8	-1.8	-2.4	-8.3	0.7	2.7	4.0	4.7			
29	9.6	1.0	-6.8	-3.8	1.9		3.4	2.1			
30	8.7	2.0	-4.8	0.9	3.2		3.7	1.1			
31		-0.2		-5.0	5.1		4.9				

Figure 7.1: Clusters for September to April.

7.1.2 Scenarios and Probabilities

After identifying the different clusters, the hourly data for the days in each cluster is used to find the scenarios for the representative day in each month with uncertainty. The temperature scenarios are found by taking the temperature average of the days belonging to the clusters (e.g., the low-temperature scenario is the temperature average of the days in the low-temperature cluster). This is done for all hours, resulting in three scenarios with hourly temperatures for each representative day in each month with uncertainty. Figure G.1 shows the scenarios with low, medium, and high-temperatures for September. Similar figures with temperature scenarios for October to April can be found in Appendix G.

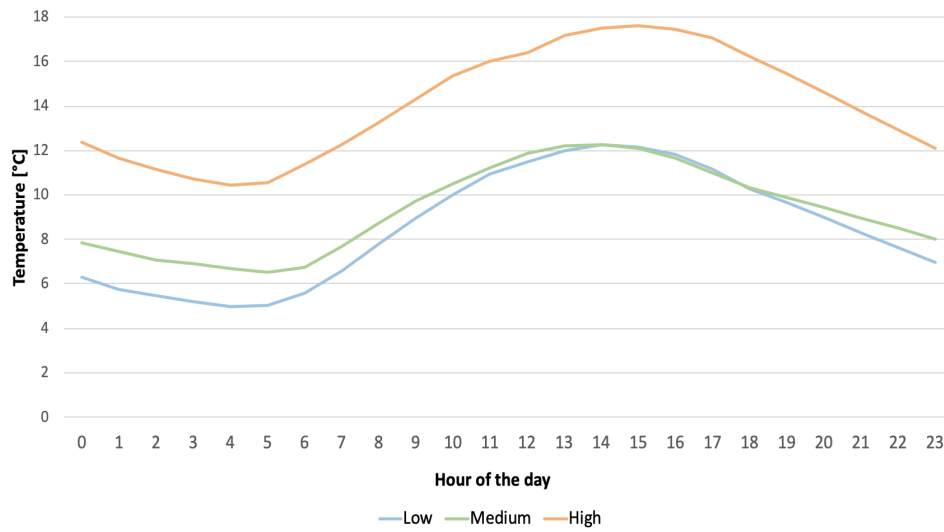


Figure 7.2: Low, medium and high-temperature scenario for September.

The number of days in each cluster is divided by the total number of days in each month to determine the probability of each scenario. Table 7.1 shows the probabilities for the scenarios with low, medium, and high-temperatures from September to April.

Table 7.1: Probabilities for temperature scenarios from September to April.

Month	Low	Medium	High
September	0.3667	0.4000	0.2333
October	0.3548	0.2581	0.3871
November	0.2000	0.4667	0.3333
December	0.3226	0.3871	0.2903
January	0.2581	0.5161	0.2258
February	0.3214	0.2500	0.4286
March	0.3548	0.2903	0.3548
April	0.1667	0.4667	0.3667

In the multi-horizon model, the scenarios and their corresponding probabilities are used directly. In the traditional stochastic model, different scenarios for each month with uncertainty are combined to make the scenarios in the traditional stochastic scenario tree. In this way, the probabilities for each scenario are found by using the general multiplication rule for probability, creating a total of 3^8 (6 561) scenario probabilities for the traditional stochastic model.

7.1.3 Evaluation and Discussion

King and Wallace (2012) suggest that a deterministic scenario generation method can be run repeatedly to create scenario trees with slightly different sizes for stability testing. For in-sample stability, the optimal objective value should not change significantly if more scenarios are added. If the objective value differs a lot by increasing the number of scenarios, this can indicate wrong modeling (King and Wallace 2012). Test cases were run for both the multi-horizon model and the traditional stochastic model. The latter was run with 2 187 and 6 561 scenarios (i.e., uncertainty from October and from September). The objective value increased by 0.7% when the number of scenarios increased from 2 187 to 6 156. Similarly, the multi-horizon model was tested with 25 and 28 scenarios, resulting in a 0.9% increase in the objective value when the number of scenarios increased. The obtained results signify minimal changes in the objective value function when the number of scenarios increases and are, therefore, an indication of correct modeling of the problem (King and Wallace 2012).

Clustering based on the k-means clustering algorithm ensures that the assigned days to each cluster are consecutive days from the input data. The k-means clustering algorithm is applied for each month individually to capture some of the seasonal correlation. Choosing the k-means clustering as a scenario generation method can be preferable for cases that do not investigate the best or worst-case scenarios. Selecting the average temperature of consecutive days in each cluster as scenarios is more moderate and perhaps realistic, instead of, for example, selecting the most extreme day with the highest and lowest temperature for the high and low-temperature scenarios. In addition, it is more moderate than taking the average of a predefined number of the most extreme days.

It should be noted that it is possible to find higher temperatures in the low-temperature cluster than in the medium and high-temperature clusters for the same representative day. The same applies to the medium and high-temperature clusters. Another aspect is that the probability for low and high-temperature scenarios for a representative day is allowed to be higher than the probability for a medium-temperature scenario. If the mentioned aspects are considered to be unfavorable to the investigation problem, other methods for scenario generation and probability setting should be applied. However, we do not perceive it as unfortunate for the problem considered in this thesis.

Chapter 8

Comparative Analysis

This chapter provides an evaluation of the performance of the three models presented in Chapter 5. The chapter begins with an introduction to the hardware and software used when running different problem instances. Then, the value of stochasticity will be analyzed, followed by an evaluation of models' decisions. In both this chapter and Chapter 9, the total operational cost in the multi-horizon and the traditional stochastic model refers to the model outcomes for the total expected operational cost (i.e., the weighted average operational cost). This also applies to all other output variables obtained by the two stochastic models. All problem instances in this chapter, unless otherwise specified, were run with the settings discussed in Chapter 6. As for the DSM costs, the hourly Space Heating (SH) deficit cost used in this chapter is 0.01 NOK/kWh, hourly Hot Water (HW) deficit cost is 0.001 NOK/kWh, while SH curtailment cost is 0.10 NOK/kWh.

A list of abbreviations is introduced in Table 8.1 to make it easier to follow the problem instances depicted in the tables and figures presented in this chapter and Chapter 9.

Table 8.1: Abbreviations used in this chapter and Chapter 9.

Abbreviation	Explanation
DET	Deterministic model
MH	Multi-horizon model
TRAD	Traditional stochastic model
TES	Thermal energy storage
x DC	Hourly SH deficit cost of x NOK/kWh
x CC	SH curtailment cost of x NOK/kWh
x TES	Thermal energy storage of size x MWh

8.1 Hardware and Software

The traditional stochastic model in this chapter is run on the Solstorm HPC cluster on an Intel[®] E5-2643v3 processor at 3.4 GHz and 512 GB RAM. The software used is FICO[®] Xpress Optimization Suite, with Xpress Optimization Suite version 8.8.1. All details are listed in Table 8.2.

Table 8.2: Details of computer and solver for the traditional stochastic model.

Console	Lenovo NextScale nx360 M5
Processor	CPU: 2x3.4GHz Intel [®] E5-2643v3 – 6 Core [™]
RAM	512 GB
Disk	120 GB SATA SSD
Operating system	CentOS 7.7.1908
Xpress Optimization Suite version	8.8.1

The deterministic and multi-horizon model in the comparative analysis study in this chapter and the case study (Chapter 9) is performed on an Intel[®] Core[™] i7-3770K processor at 3.5 GHz and 32 GB RAM. The software used is FICO[®] Xpress Optimization Suite, with Xpress Optimization Suite version 8.8.1. All details are listed in Table 8.3.

Table 8.3: Details of computer and solver for the deterministic and multi-horizon model.

Processor	CPU: 3.5GHz Intel [®] Core [™] i7-3770K
RAM	32 GB
Disk	500 GB
Operating system	Microsoft Windows 10 Education
Xpress Optimization Suite version	8.8.1

8.2 Evaluation of the Stochastic Method

In this section, the value of the multi-horizon model and the traditional stochastic model is evaluated. The evaluation methods used are the expected value of perfect information (EVPI) and the value of the stochastic solution (VSS), as described in Section 3.4.4. The EVPI is less relevant to our problem as weather data, and thus SH demand is subject to external uncertainty, which is challenging to eliminate. Hence, we will not provide a numeric value for the EVPI, but discuss its relevance to our problem. Our emphasis will be on the VSS, as the expected value of planning with uncertainties is more relevant to our problem.

8.2.1 EVPI

The parameter EVPI is estimated in the same manner for a multistage stochastic problem as for a two-stage stochastic problem. If each scenario in the stochastic problem is solved independently, then the wait-and-see solution (WS) is the expected value of the set of solutions to the scenario problems. The WS represents the expected solution if all uncertainty is resolved (Birge and Louveaux 2011).

In the multi-horizon model, the connection between consecutive periods is based on the weighted average storage level. Obtaining the WS requires us to solve all scenarios as independent deterministic problems. This implies that the simplicity of the multi-horizon model structure is eliminated, as all possible combinations of the scenarios must be tested. As a result, the WS calculation procedure for the multi-horizon and traditional stochastic problem is the same and requires the solution of 3^8 (6 561) independent problems, which is extensive and computationally demanding. The same calculation procedure for the WS results in the same EVPI for the multi-horizon model and the traditional stochastic model.

The EVPI indicates if it is worth making an effort to reduce the uncertainty in a model and can, in a way, provide a value for how much better forecasting technologies is worth. For our problem, this would require better forecasting of the outdoor temperature and thus the SH target demand. However, the weather is subject to external uncertainty that is difficult to eliminate, regardless of good forecasting methods. Considering the complexity of obtaining the EVPI and the relevance it has to our problem, we have decided not to examine the EVPI numerically in this thesis.

8.2.2 VSS

The VSS calculation for a multistage stochastic model is not straightforward since the decisions are made at multiple stages. Fixating the first stage decision variables is a trivial and well-known approach. This approach is more applicable to two-stage stochastic problems where investment decisions are made in the first stage and operational decisions in the second stage (Popela et al. 2014). In our models, fixating the first stage decision variables is not appropriate as there are no investment decisions, only operational decisions at every stage. Thus, the challenge is to choose which variables to fixate at which stage. Even though the traditional stochastic model and the multi-horizon model do not have investment decisions, we can distinguish between addition and withdrawal periods for the TES. Therefore, the approach used to calculate the EEV is to fixate the TES level variable

at the end of the adding period, i.e., the end of August, as there is no uncertainty from May to August.

Problem instances with different production capacities in the adding period (i.e., summer) were analyzed to observe how it affects the VSS. For the Leangen case study described in Chapter 6, waste incineration is the only available heat technology during the summer. This applies to the problem instance: DSM & TES. Based on this, we evaluate the models when additional production from other heat technologies are allowed in the adding period. The production technologies that we consider to be relevant based on production costs and CO₂ emissions are electric (EL) boilers, bio boilers, and natural gas. We assume that the amount of heat available from waste incineration from the main DHG in Trondheim is the same as described in Section 6.2.4. The models are run for three different problem instances, in addition to the DSM & TES problem instance. The production capacities for the summer months in the three additional problem instances are shown in Table 8.4. Production technologies that are not included in the table are assumed to have zero capacity in the summer, while for the remaining months, the production capacities are the same as presented in Section 6.2.4.

Table 8.4: Production capacities in kWh for the production technologies in the summer.

Problem instance Month	EL boiler			Bio boiler			Natural Gas		
	June	July	August	June	July	August	June	July	August
Waste incineration	1 468	1 317	1 162	1 468	1 317	1 162	1 468	1 317	1 162
EL boiler	10 000	10 000	10 000	0	0	0	0	0	0
Bio boiler	0	0	0	10 000	10 000	10 000	0	0	0
Natural Gas	0	0	0	0	0	0	10 000	10 000	10 000

First, the EV is calculated by running the deterministic model with the expected SH demand (i.e., the weighted average SH demand), then the EEV is found by solving the stochastic problem where the TES level is fixated at the end of August. The expected SH demand is found by calculating the expected value for the entire planning horizon from all scenarios, creating a single expected value scenario. Table 8.5 lists the EEV, SP, and VSS for the four problem instances. All four problem instances are analyzed with the multi-horizon model and the traditional stochastic model. In the last three problem instances, additional production technologies, other than waste incineration, are available in the summer (see Table 8.4).

Table 8.5: VSS calculated for the multi-horizon model and traditional stochastic model for the four problem instances with fixated TES level at the end of August.

Problem instance	Model	Max TES level [kWh]	EEV	SP	VSS	Δ
DSM & TES	MH	20 853	160 303	160 303	0	0.00%
DSM & TES	TRAD	20 853	160 575	160 575	0	0.00%
EL boiler	MH	20 853	160 303	160 040	263	0.16%
EL boiler	TRAD	20 853	160 575	160 401	174	0.11%
Bio boiler	MH	65 016	156 647	156 343	304	0.19%
Bio boiler	TRAD	65 016	157 801	157 726	75	0.05%
Natural Gas	MH	50 556	157 730	157 359	371	0.23%
Natural Gas	TRAD	50 556	158 896	158 593	303	0.19%

For each problem instance, the table lists the obtained EEV, SP, and VSS for the models. The table also includes the change in the objective value when going from the EEV to the SP. The EEV is almost equal to the SP for all problem instances, resulting in very low values for the VSS. The improvement in the stochastic problem solution (SP) compared to the expected value solution (EEV) is between 0-0.23% for the multi-horizon model. For the traditional stochastic model, the improvement is between 0-0.19%. The results obtained indicate that adding stochasticity to the SH demand is low compared to the added complexity. However, as mentioned above, VSS is not the best method to evaluate the values of the stochastic solutions for the multi-stage model. In addition, the VSS cannot distinguish between structural differences in the solutions from the deterministic and stochastic versions of the model. Even if the VSS is close to zero, there might be structural differences between the optimal decisions in the deterministic and stochastic models. These can not be identified by the VSS, but by exploring the differences in decisions made in the models. Therefore, the next section will investigate the storage decisions in the deterministic, multi-horizon, and traditional stochastic models.

8.3 Evaluation of Decisions Made in the Models

In addition to evaluating the two stochastic models against the deterministic model, it is also necessary to evaluate the multi-horizon model against the traditional stochastic model. The main difference between the multi-horizon and the traditional stochastic is how the TES is modeled. Therefore, it is important to investigate the TES decisions made in the two stochastic models as the TES modeling in the multi-horizon formulation achieves a massive decrease in complexity and computation time compared to the traditional stochastic model. Investigating the TES decisions will enable us to evaluate if

the multi-horizon model provides a reasonable approximation of the traditional stochastic model. Other decision variables are not analyzed in this chapter as they are affected by the TES level, e.g., the production mix is highly dependent on the amount of heat stored in the TES.

First, a Base Case (BC) without DSM and TES is analyzed for the three models. The two stochastic models are expected to yield the same outcomes when no TES is included since the only difference between them is rooted in the TES modeling. This can be seen in Table 8.6, where all the values are identical for the two stochastic models. On the other hand, the deterministic model has a lower total operational cost due to lower fuel costs. The deterministic model manages to produce heat from cheaper technologies as it has lower peak loads compared to the stochastic models.

Table 8.6: The BC for the multi-horizon and the traditional stochastic model.

Model	DET	MH	TRAD
Total production [kWh]	504 588	504 588	504 588
Peak production [kWh/h]	3 016	3 016	3 016
CO ₂ emissions [kWh]	26 063	27 411	27 411
Fuel cost [NOK]	139 847	143 435	143 435
Total operational cost [NOK]	172 982	176 571	176 571

The same four problem instances analyzed in Section 8.2.2 were analyzed in this section to observe the differences and similarities in TES behavior between the deterministic, multi-horizon, and traditional stochastic model. However, in this section, the maximum TES level is not fixated. Table 8.7 displays the results for the four problem instances for the three model types. The total operational cost for the multi-horizon model in Table 8.7 is, on average, 0.5% lower than the total operational cost for the traditional stochastic model. For the deterministic model, the total operational cost for the four problem instances is, on average, 2.4% lower than the traditional stochastic model. This indicates that the three models yield very similar operational costs. However, the storage level for each model in a problem instance is quite different. This is further discussed in the next paragraphs.

Table 8.7: Total operational cost and maximum TES level for the four problem instances.

Problem instance	Model	Total operational cost [NOK]	Max TES level [kWh]
DSM & TES	DET	156 358	20 853
DSM & TES	MH	160 303	20 853
DSM & TES	TRAD	160 575	20 853
EL boiler	DET	156 358	20 853
EL boiler	MH	160 040	33 864
EL boiler	TRAD	160 401	30 449
Bio boiler	DET	155 004	65 016
Bio boiler	MH	156 343	83 478
Bio boiler	TRAD	157 726	73 097
Natural Gas	DET	155 661	50 556
Natural Gas	MH	157 359	73 914
Natural Gas	TRAD	158 593	65 587

In the problem instance, DSM & TES, Figure 8.1 indicates that the three models store all of the heat produced from the waste incineration capacity surplus during the summer, which results in the same TES level. The deterministic model prefers to empty the TES before the stochastic models as it has lower peak loads than the stochastic models. On average, the multi-horizon model and the traditional stochastic model have almost identical TES behavior, with minimal variations in February and March. In the problem instance, with an EL boiler in Figure 8.2, the traditional stochastic model stores 46% more heat than the deterministic model, while the multi-horizon model stores 62% more than the deterministic model. The explanation is the high SH demand scenarios in the stochastic models, leading to higher peak loads than in the deterministic model.

Figure 8.3 and Figure 8.4 show the storage behavior in the problem instance with a bio boiler and natural gas, respectively. The traditional stochastic model stores 12% more heat than the deterministic model in the problem instance with a bio boiler and 30% more in the problem instance with natural gas. On the other hand, the multi-horizon model stores 28% more heat than the deterministic model in the problem instance with a bio boiler, and 46% more in the problem instance with natural gas. In the three problem instances with an extra production technology (i.e., EL boiler, bio boiler, and natural gas), the deterministic model stores less heat than the two stochastic models and tends to empty the storage before the traditional stochastic model. Figures 8.2 - 8.4 and Table 8.7 also show that the multi-horizon model stores more heat than the traditional stochastic model in the three problem instances, and the difference in maximum TES level is, on average, 11%.

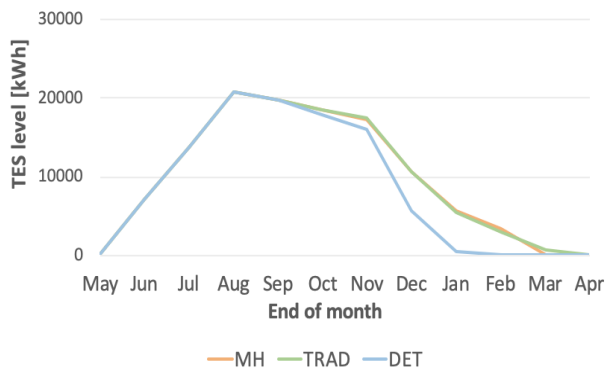


Figure 8.1: Problem instance: DSM & TES.

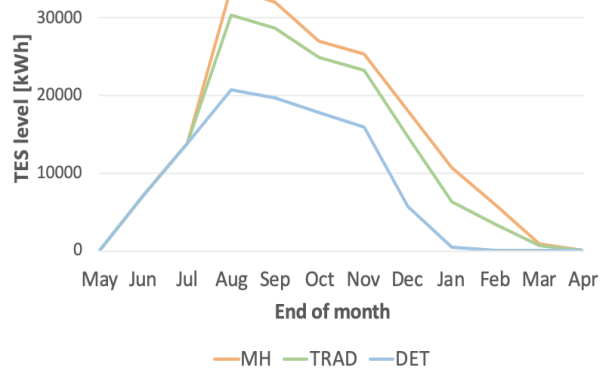


Figure 8.2: Problem instance: EL boiler.

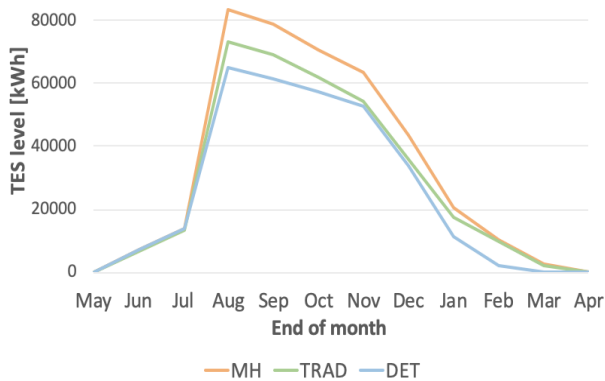


Figure 8.3: Problem instance: Bio boiler.

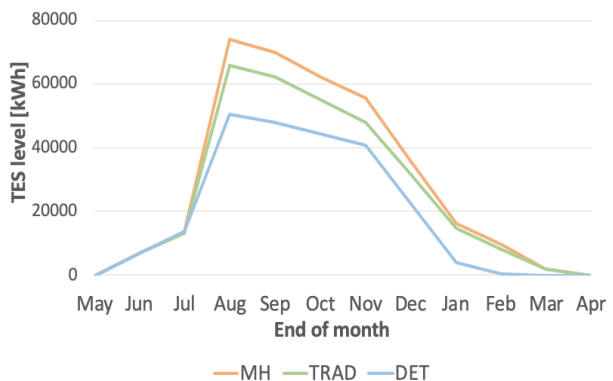


Figure 8.4: Problem instance: Natural Gas.

Figures 8.1 - 8.4 demonstrate the difference in decisions regarding the TES for the different models. The figures indicate that the multi-horizon model stores equally or more heat than the traditional stochastic model, which can be explained by the interaction between asymmetrical production costs and the difference in scenario structure. Fixating the TES level at the end of August in the multi-horizon model to be equal to the TES level at the end of August in the traditional stochastic model causes higher peak production in the multi-horizon model compared to when the TES level is not fixated. This indicates that a combination of asymmetrical production costs, production capacities, and how SH uncertainty is modeled in the multi-horizon model contributes to different storage decisions in order to reduce peak production technologies.

The computation time for the deterministic model is 8 seconds for the problem instance with DSM & TES, while it is 25 seconds for the multi-horizon model and 31 440 seconds (8 hours and 44 minutes) for the traditional stochastic model. Small differences in computation time occur for the different problem instances run by the same model. Still, these

are small when comparing the computation time for the models against each other. The memory usage by the models is also compared in the problem instance with DSM & TES. The deterministic model uses 89 MB RAM, the multi-horizon model uses 300 MB RAM, while the traditional stochastic model uses as much as 429 GB RAM. It becomes evident that the traditional stochastic model is the most computationally demanding. The reason is the high number of scenarios in the traditional stochastic model, which results from SH demand uncertainty from September to April. However, the multi-horizon model also includes SH demand uncertainty from September to April but has a significant advantage over the traditional stochastic model in computation time and memory use.

It is clear that the multi-horizon model is preferable in terms of computation time, and it provides a good prediction of the total operational cost. The difference in the modeling of the TES causes the multi-horizon model to store more heat than the traditional stochastic model when production technologies other than waste incineration are available in the summer. Even if this does not have huge effects on the total operational cost, a higher TES level requires higher investment costs. In our problem, waste incineration is much cheaper than the other production technologies, and the production capacity is limited. As a result, the TES level for the three models is similar, as seen in the problem instance with DSM and TES. It is also apparent that the multi-horizon model and the traditional stochastic model have a similar TES behavior compared to the deterministic model for this problem instance. Thereby, for our problem where waste incineration is the only technology available in the summer, and from an operational cost perspective, the multi-horizon model provides a good approximation of the traditional stochastic model. The multi-horizon model will, therefore, be used in the following analysis in Chapter 9. Additionally, the deterministic model will also be used to investigate the low-temperature DHG at Leangen as the effect of adding stochasticity to the SH demand, according to the VSS, is nearly insignificant (Table 8.5). This also enables us to do a comparative analysis between the deterministic model and the multi-horizon model for the case study at Leangen in Chapter 9.

Chapter 9

Case Study - Leangen

In this chapter, a case study of Leangen is performed for the deterministic model and the multi-horizon model. Specifically, we study how waste heat, Thermal Energy Storage (TES), and Demand Side Management (DSM) can add value to the operation of the low-temperature District Heating Grid (DHG) at Leangen. The analysis are done for a stylized planning horizon of 12 days representing 24 hours of a typical day each month. Target demands and allowed deviations are based on empirical demand data and assumptions for building insulation standards and comfort levels of different consumer groups. For full details, see Chapter 6. A case refers to a problem instance in this chapter.

The cases depicted in Table 9.1 are investigated in this chapter. The table presents the different settings in the cases, e.g., model type, if the case includes DSM or a TES, deficit costs. The x marks where the technique or change is applied. In all cases, unless otherwise specified, the production capacity of waste incineration in the summer (i.e., June, July, and August) is as defined in Section 6.2.4. The remaining settings are the same as presented in Chapter 6. The hourly Space Heating (SH) deficit and curtailment costs are presented in Table 9.1. In all cases, the hourly Hot Water (HW) deficit cost is set at 0.001 NOK/kWh, while HW curtailment cost is set at 10 NOK/kWh as daily HW curtailment is not allowed.

The actual results from the cases depicted in the table are further analyzed and discussed in the remaining sections of this chapter. All deterministic cases are analyzed with the weighted average SH demand. The results from the deterministic and multi-horizon model are analyzed to provide more insight into the differences and similarities between the two models. All output variables from the multi-horizon model are the expected values, as stated in Chapter 8.

Table 9.1: Settings for the cases analyzed.

Case	Model	DSM	TES	More waste heat	Change SH demand requirements	Change HW demand requirements	Hourly SH deficit cost [NOK/kWh]	Curtailement cost for SH [NOK/kWh]	Max TES level [kWh]
Base Case									
1	DET	-	-	-	-	-	-	-	-
2	MH	-	-	-	-	-	-	-	-
Base Case with TES									
3	DET	-	x	-	-	-	-	-	100 000
4	MH	-	x	-	-	-	-	-	100 000
Different Deficit and Curtailement Costs without TES									
5	DET	x	-	-	-	-	0.01	0.10	-
6	MH	x	-	-	-	-	0.01	0.10	-
7	DET	x	-	-	-	-	0.10	0.20	-
8	MH	x	-	-	-	-	0.10	0.20	-
9	DET	x	-	-	-	-	0.20	0.30	-
10	MH	x	-	-	-	-	0.20	0.30	-
11	DET	x	-	-	-	-	0.33	0.30	-
12	MH	x	-	-	-	-	0.33	0.30	-
Different Deficit and Curtailement Costs with TES									
13	DET	x	x	-	-	-	0.01	0.10	100 000
14	MH	x	x	-	-	-	0.01	0.10	100 000
15	DET	x	x	-	-	-	0.10	0.20	100 000
16	MH	x	x	-	-	-	0.10	0.20	100 000
17	DET	x	x	-	-	-	0.20	0.30	100 000
18	MH	x	x	-	-	-	0.20	0.30	100 000
19	DET	x	x	-	-	-	0.33	0.30	100 000
20	MH	x	x	-	-	-	0.33	0.30	100 000
Different SH Demand Requirements									
21	DET	x	-	-	x	-	0.01	0.10	-
22	MH	x	-	-	x	-	0.01	0.10	-
23	DET	x	x	-	x	-	0.01	0.10	100 000
24	MH	x	x	-	x	-	0.01	0.10	100 000
Different HW Demand Requirements									
25	DET	x	-	-	-	x	0.01	0.10	-
26	MH	x	-	-	-	x	0.01	0.10	-
27	DET	x	-	-	-	x	0.01	0.10	-
28	MH	x	-	-	-	x	0.01	0.10	-
29	DET	x	-	-	-	x	0.01	0.10	-
30	MH	x	-	-	-	x	0.01	0.10	-
Increased Waste Heat and Larger TES									
31	DET	x	x	x	-	-	0.01	0.10	80 000
32	MH	x	x	x	-	-	0.01	0.10	80 000
33	DET	x	x	x	-	-	0.01	0.10	200 000
34	MH	x	x	x	-	-	0.01	0.10	200 000
35	DET	x	x	x	-	-	0.01	0.10	330 000
36	MH	x	x	x	-	-	0.01	0.10	330 000
Investment Analysis of Larger TES									
37	DET	-	x	x	-	-	-	-	80 000
38	MH	-	x	x	-	-	-	-	80 000
39	DET	-	x	x	-	-	-	-	330 000
40	MH	-	x	x	-	-	-	-	330 000

9.1 The Base Case

Case 1 and Case 2 represent the Base Case (BC) for the deterministic model and multi-horizon model, respectively, where neither TES nor DSM is included. The results, used as a benchmark for comparison in this chapter, are found in Table 9.2.

Table 9.2: The BC for the two model types.

Case Model	1 DET	2 MH
Total production [kWh]	504 588	504 588
Peak production [kWh/h]	3 016	3 016
CO ₂ emissions [kWh]	26 063	27 411
Fuel cost [NOK]	139 847	143 435
Total operational cost [NOK]	172 982	176 571

The total heat production amount is the same for both models since the deterministic model is analyzed with the weighted average SH demand. The constraints in the multi-horizon model are defined per scenario and must be satisfied for each operational scenario. In scenarios with high SH demand, the multi-horizon model has higher peak loads than the weighted average SH demand in the deterministic model and must produce more heat, e.g., from expensive technologies to fulfill the SH demand constraints for the high demand scenario. The difference in peaks yields different production mixes for the deterministic and the multi-horizon model as the multi-horizon model's production mix is the weighted average from the scenarios. The deterministic model can more easily avoid production from expensive production technologies, which is why some of the deterministic outputs differ from the multi-horizon model. Compared to the multi-horizon model, the fuel cost is 3% lower in the deterministic model, and the CO₂ emissions are 5% lower. The reduction in fuel cost and CO₂ emissions explain why the total operational cost in the deterministic model is lower (2%) than in the multi-horizon model.

It can be challenging to interpret the results for a year, as we only analyze 12 representative days, representing each month in a year. However, obtaining annual estimates can give the DHO insight into the long-term operation of the DHG. It can be reasonable to multiply the total operational cost with 30 to get the annual operational cost (i.e., the operational cost for 360 days), assuming 30 days per month. The BC's total annual operational cost is approximately 5.19 million NOK for the deterministic model and 5.30 million NOK for the multi-horizon model.

9.2 The Base Case with TES

This section explores the addition of a TES to the BC discussed in Section 9.1 to explore the value of including a TES at Leangen when no DSM actions are possible. The results for the cases can be found in Table 9.3.

Table 9.3: The BC with a TES.

Case Model	3 DET	4 MH
Inputs		
Max TES level [kWh]	100 000	100 000
Outputs		
Max actual TES level [kWh]	20 504	20 504
Total production [kWh]	510 598	510 489
Peak production [kWh/h]	2 851	2 701
CO ₂ emissions [kWh]	22 019	23 373
Fuel cost [NOK]	128 551	132 111
Total operational cost [NOK]	161 687	165 247
Δ in operational cost from BC [%]	-7	-6
Δ in CO ₂ emissions from BC [%]	-16	-15
Δ in peak production from BC [%]	-5	-10

Storing cheap heat from waste incineration in the summer and withdrawing it in the winter reduces the total operational cost in both the deterministic model and the multi-horizon model. Utilization of a TES in Case 3 and Case 4 reduces the operational cost by 6-7%, by better exploiting the cheapest production technologies to accommodate fluctuating heat demand. The production capacity of waste incineration in the summer restricts the maximum TES level in Case 3 and Case 4. Explaining why the deterministic and multi-horizon models have the same maximum TES levels (20 504 kWh). The four problem instances investigated in Table 8.7 in Chapter 8 have shown that this only applies if there is restricted access to low-cost heat production during the summer.

From Table 9.3, it is clear that the production amount is almost the same for the deterministic model and the multi-horizon model. However, the total peak production in the deterministic model (Case 3) is higher than in the multi-horizon model (Case 4). The peak production for both cases appears in hour 7:00 in March. The deterministic model empties the storage in the middle of February, while the storage in the multi-horizon model is not emptied until the middle of April, as seen in Figure 9.1. As a result, the deterministic model has to produce more heat from LPG than the multi-horizon in hour

7:00 in March to cover the SH peak demand, while the multi-horizon withdraws some heat from the storage to reduce the peak production. Consequently, the total peak production is approximately 6% higher in the deterministic model.

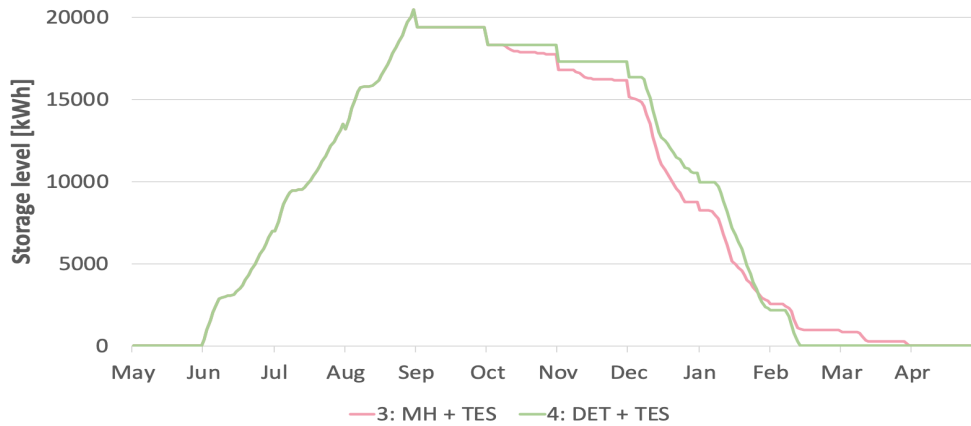


Figure 9.1: Storage level for the deterministic model and the multi-horizon model.

In Figure 9.2, the differences in production mix are depicted for the BCs without TES (cases 1-2) and with TES (cases 3-4). The most significant difference between the deterministic model with TES (Case 3) and the multi-horizon model with TES (Case 4) is the LPG production. The multi-horizon model produces more heat from LPG, as the combination of TES and production from other heat technologies is not enough to cover the SH demand in high demand scenarios. This explains the higher total operational cost as LPG has the highest production cost. Even though the models store the same amount of heat in the adding period, the uncertainty in September for the multi-horizon model causes small differences in the total production from waste incineration (See Figure 9.8). In the multi-horizon model, the production mix is affected by different SH demand scenarios, while the deterministic model uses the weighted average SH demand.

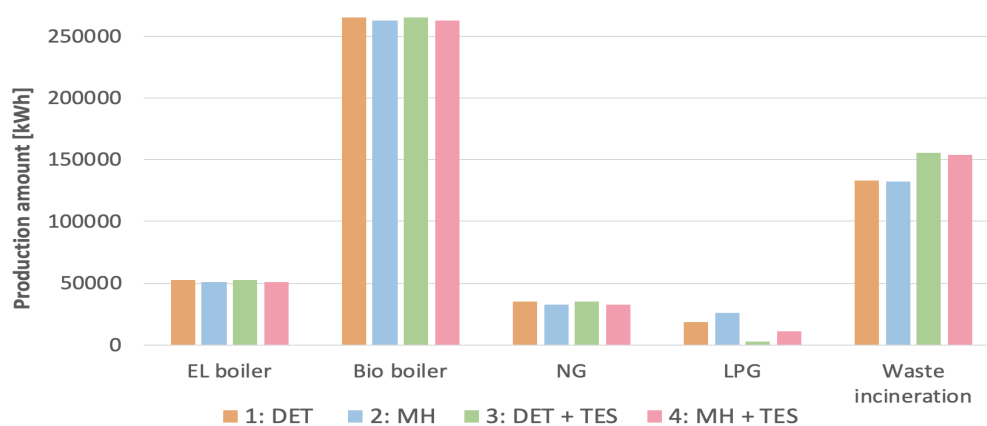


Figure 9.2: Production mix for the BCs with and without TES.

Compared to the BCs without TES, Case 3 and Case 4 manage to reduce LPG production by storing heat from the surplus waste incineration production, as seen in Figure 9.2. There is also some difference in how the deterministic and multi-horizon model manages the TES. As discussed in the previous section, peak loads are higher for the multi-horizon model than for the deterministic model resulting in the multi-horizon model producing more heat from expensive technologies. When a TES is present, the deterministic model manages almost to eliminate the use of LPG (Case 3), which is the most expensive production technology. Thereby, the fuel cost and thus, the total operational cost is reduced more in Case 3. The amount of LPG in the deterministic model (Case 4) is 75% less than in the multi-horizon model (Case 3). It is clear from the figure that the reduced LPG production in Case 3 and Case 4 is mostly covered by the increased waste incineration withdrawn from the TES.

9.3 Different Deficit and Curtailment Costs

This section investigates how deficit and curtailment costs affect the optimal operation of the DHG by analyzing cases with different deficit costs and curtailment costs. Test cases with different deficit and curtailment costs were analyzed for the models, but only four different sets of costs are presented. The presented costs indicate costs that cause important differences in the production mix. The cases 5-12 (Section 9.3.1) are without a TES, while the cases 13-20 include a TES (Section 9.3.2).

Table 9.4 is presented to understand how the deficit and curtailment cost affect the shifts and curtailment in cases 5-12 in Section 9.3.1, and cases 13-20 in Section 9.3.2. The table illustrates decisions the DHO faces on whether production should happen in the current hour or if it should be shifted or curtailed, depending on DSM costs. Each row in the table presents the available heat production technology in the current hour with its production cost and suitable replacements (shift technology). In addition, the table presents the shift and curtail cost. A shift indicates moving the heat production to an earlier or later period, so the current production technology is replaced by a cheaper technology. Therefore, the shift cost is the sum of the shift technology's production cost and the deficit cost. Curtailment implies that the heat amount is not produced or delivered at all, and thus the curtail cost is the sum of the deficit cost and curtailment cost. Hourly deficit costs and daily curtailment costs can be inserted in the table to find the optimal decisions for specific cases. It is important to keep in mind that the DHO needs to fulfill the specified demand requirements, and therefore the amount that can be shifted or curtailed is limited.

Table 9.4: Cost for different DSM decisions.

Current technology	Production cost [NOK/kWh]	Shift technology	Shift cost [NOK/kWh]	Curtail cost [NOK/kWh]
LPG	0.7510	Bio boiler	0.3239+deficit cost	deficit cost + curtailment cost
LPG	0.7510	NG	0.3415+deficit cost	deficit cost + curtailment cost
LPG	0.7510	EL boiler	(0.3736-0.5529)+deficit cost	deficit cost + curtailment cost
EL boiler	0.3736-0.5529	Bio boiler	0.3239+deficit cost	deficit cost + curtailment cost
EL boiler	0.3736-0.5529	NG	0.3415+deficit cost	deficit cost + curtailment cost
NG	0.3415	Bio boiler	0.3239+deficit cost	deficit cost + curtailment cost

9.3.1 Without TES

Table 9.5 depicts different values for hourly SH deficit cost and SH curtailment cost. The table also presents how the different costs affect production, the amount of deficit and curtailment, and the total operational cost.

Table 9.5: Results from different deficit and curtailment costs without TES.

Case Model	5 DET	6 MH	7 DET	8 MH	9 DET	10 MH	11 DET	12 MH
Inputs								
Hourly SH deficit cost [NOK/kWh]	0.01	0.01	0.10	0.10	0.20	0.20	0.33	0.33
SH curtailment cost [NOK/kWh]	0.10	0.10	0.20	0.20	0.30	0.30	0.30	0.30
Outputs								
Total production [kWh]	497 793	497 808	497 793	497 808	499 742	500 224	500 718	501 410
Peak production [kWh/h]	2 973	2 879	2 837	2 907	2 833	2 939	2 937	2 949
CO ₂ emissions [kWh]	23 751	25 008	23 751	25 031	23 970	25 401	24 363	25 696
SH deficit [kWh]	10 522	10 088	9 242	8 386	6 471	5 290	3 870	3 197
SH curtailment [kWh]	6 795	6 780	6 795	6 780	4 846	4 364	3 870	3 178
Total operational cost [NOK]	166 377	170 833	167 922	172 306	169 328	173 609	170 019	174 145
Total operational cost excl. DSM [NOK]	165 524	169 986	164 959	169 433	165 611	170 369	166 304	171 088
Δ in operational cost from BC [%]	-4	-3	-3	-2	-2	-2	-2	-1
Δ in CO ₂ emissions from BC [%]	-9	-9	-9	-9	-8	-7	-7	-6
Δ in peak production from BC [%]	-1	-5	-6	-4	-6	-3	-3	-2

The changes in total production are related to changes in SH curtailment. Table 9.5 indicates that the total production amount decreases compared to the BC (Table 9.2) as much as the curtailed amount increases. For the lowest deficit and curtailment cost (0.01 NOK/kWh and 0.10 NOK/kWh, respectively), the deterministic model (Case 5) only reduces the peak production by 1% compared to the BC (Case 1). It is worth mentioning that our problem only focuses on reducing the total operational cost rather than peak production. Hence, the peak production in the deterministic model increases with lower deficit costs due to fluctuating electricity prices, making it preferable to shift more production to low-cost hours, resulting in a higher peak production. In addition,

peak production in the deterministic model (Case 5, 7 and 9) decreases with the increasing deficit and curtailment costs up to a cost point (Case 11). As a result of high penalty costs for the deficit and curtailment in Case 11, it is no longer preferable to shift delivered heat, only curtail, resulting in the increase in peak production compared to Case 7 and Case 9. The multi-horizon model behaves differently, as indicated in Table 9.5. The peak production increases with the increasing deficit and curtailment costs because of different SH demand scenarios. This indicates that the utilization of the deterministic model leads to differences in production decisions compared to the multi-horizon model when no TES is included.

It is evident from the cases in Table 9.5 that higher deficit and curtailment costs eventually result in lower shift and curtailment activities. According to Table 9.4, it is always cheaper to curtail than to shift heat in cases 5-12 as the curtail cost is lower than the shift cost for all the possible shifted technologies. However, some of the SH demand is only shifted since the curtailed amount is restricted not to be higher than 2% of the daily SH demand (Section 6.2.11). Therefore, in some hours, shifts are also preferred. With an hourly deficit cost of 0.33 NOK/kWh, it is no longer preferred to shift heat production from the bio boiler to waste incineration in September. However, it is still optimal to reduce LPG production in the other months. Therefore, all shifted SH is curtailed in Case 11, while in Case 12, nearly all of the shifted heat is curtailed due to higher peak loads in the multi-horizon model, where only 2% of the daily SH demand can be curtailed (Table 9.5).

It is cost-optimal to replace NG by the bio boiler in cases 5-8 due to low hourly deficit costs (Table 9.4). Shifting production from the EL boiler depends on the fluctuating electricity prices. With an hourly deficit cost of 0.20 NOK/kWh or lower (cases 5-10), the production from the EL boiler can be shifted to the bio boiler or NG, depending on the hourly electricity price. If the hourly deficit cost is equal or above 0.43 NOK/kWh, then the hourly deficit for SH demand is no longer desirable. In Table 9.4, it can be seen that the production cost of LPG is 0.7510 NOK/kWh. The cheapest possible replacement technology is the bio boiler (see production mix in Section 6.2.2). However, the bio boiler's shift cost becomes 0.7539 NOK/kWh, which is higher than the production cost of LPG. Following this, it is not optimal to shift any production with shift cost higher than the production cost of the most expensive technology.

The deterministic model manages to reduce the production of LPG more than the multi-horizon model, as seen in Figure 9.3 and Figure 9.4. The figures show the reduction in production amount compared to the BC for the two models. The difference between the two models adds value to the discussion on whether the deterministic model is a good

enough model compared to the multi-horizon model. The deterministic model increases NG production (Figure 9.3), while the multi-horizon model reduces it (Figure 9.4). The increased NG production in the deterministic model results from the ability to reduce a larger part of LPG production. The reason for this is the higher peak loads in the multi-horizon model. The production from the EL boiler is reduced for the lowest deficit and curtailment costs in both models (cases 5-8) but increased compared to the BC for the higher costs (cases 9-12), resulting from the production cost of the EL boiler compared to shift and curtail costs (Table 9.4). Accordingly, when the hourly deficit cost is low compared to production costs, the models use DSM to avoid production from expensive heat technologies.

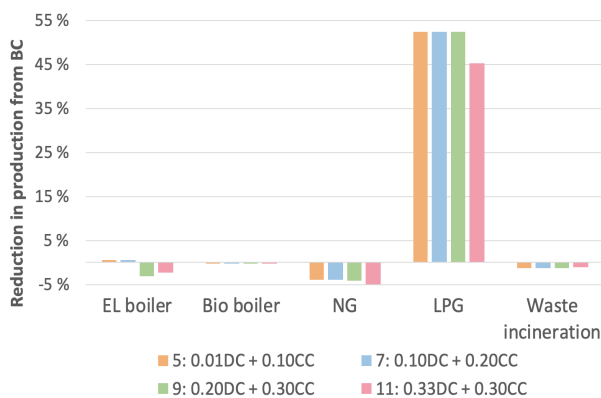


Figure 9.3: Production mix for the deterministic model.

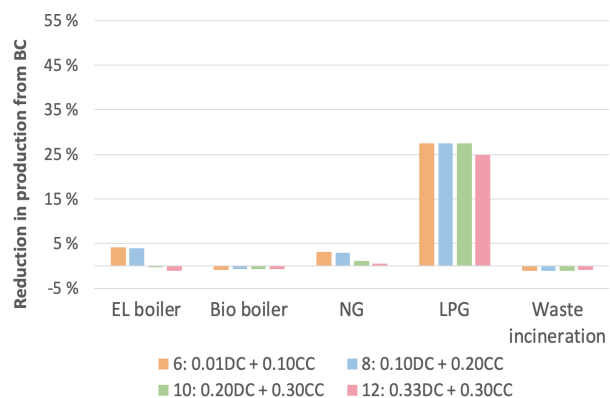


Figure 9.4: Production mix for the multi-horizon model.

To summarize, the total operational cost when DSM is included is highly dependent on the assumed hourly deficit cost, curtailment cost, and production costs. When the hourly deficit cost and curtailment cost are low, the models shift and curtail to eliminate the use of expensive production technologies, resulting in reduced total operational cost. Shifts and curtailment happen as long as deficit or curtailment is optimal compared to production in the current hour. When the hourly deficit cost increases and the shift cost exceeds the LPG production cost, DSM is no longer desirable.

9.3.2 With TES

Table 9.6 presents the results for different hourly SH deficit costs and curtailment costs when including a TES. The table also presents how the different costs affect production, the amount of deficit and curtailment, and the total operational cost.

Table 9.6: Results from different deficit and curtailment costs with TES.

Case Model	13 DET	14 MH	15 DET	16 MH	17 DET	18 MH	19 DET	20 MH
Inputs								
Hourly SH deficit cost [NOK/kWh]	0.01	0.01	0.10	0.10	0.20	0.20	0.33	0.33
SH curtailment cost [NOK/kWh]	0.10	0.10	0.20	0.20	0.30	0.30	0.30	0.30
Max TES level [kWh]	100 000	100 000	100 000	100 000	100 000	100 000	100 000	100 000
Outputs								
Max actual TES level [kWh]	20 853	20 853	20 853	20 853	20 504	20 601	20 504	20 504
Total production [kWh]	503 020	503 891	503 066	503 891	506 056	506 609	509 815	509 001
Peak production [kWh/h]	2 421	2 672	2 421	2 677	2 527	2 690	2 527	2 690
CO ₂ emissions [kWh]	20 752	21 393	20 757	21 417	21 091	21 871	21 569	22 326
SH deficit [kWh]	10 761	10 259	8 496	8 739	4 276	4 579	526	1 762
SH curtailment [kWh]	7 170	7 155	7 170	7 155	3 997	4 323	526	1 762
Total operational cost [NOK]	156 358	160 303	157 947	161 843	159 210	163 140	159 518	163 525
Total operational cost excl. DSM [NOK]	155 462	159 413	154 946	158 823	156 356	160 063	159 013	161 833
Δ in operational cost from BC [%]	-10	-9	-9	-8	-8	-8	-8	-7
Δ in CO ₂ emissions from BC [%]	-20	-22	-20	-22	-19	-20	-17	-19
Δ in peak production from BC [%]	-20	-11	-20	-11	-16	-11	-16	-11

The total operational cost reduction is significantly larger for all cases with a TES compared to without a TES. The highest total operational cost reduction is 9-10% with a TES compared to 3-4% without a TES (Table 9.6 and Table 9.5). The results also show a reduction in peak production, which allows the DHO to decrease the needed capacity in the grid and install fewer expensive peak production technologies, thus reducing the infrastructure investment cost. The SH deficit in cases 13-17 is roughly 6% higher compared to cases 5-8, while the SH curtailment is roughly 5% higher. Comparing the results from Table 9.6 to Table 9.5 indicate that the difference in DSM decisions between the cases with and without TES is highest when the deficit and curtailment costs are high. The highest difference is found when the hourly deficit cost is 0.33 NOK/kWh, and the curtailment cost is 0.30 NOK/kWh. In Case 19, the SH deficit and curtailment are reduced by 86% compared to Case 11, while in Case 20, it is reduced by approximately 45% compared to Case 12. The reason for this is that DSM techniques are not as effective with a TES as without a TES. DSM techniques with a TES are mainly used to reduce LPG production as the TES level is not large enough (when including heat losses) to eliminate LPG on its own. In addition, the combination of DSM and TES reduces delivered heat during the summer in order to store more heat for succeeding periods.

In Case 19 and Case 20, the amount of SH deficit and curtailment are equal, implying that all shifts are curtailed. This is caused by the hourly deficit and curtailment cost at 0.33 and 0.30 NOK/kWh, respectively (Table 9.4). The same reason as stated in Section 9.3.1 applies here, where it is preferred to curtail LPG rather than shift to other technologies.

In Figure 9.5 and Figure 9.6, the reduction in production from the technologies compared to the BC is presented for the deterministic and multi-horizon model with a TES, respectively.

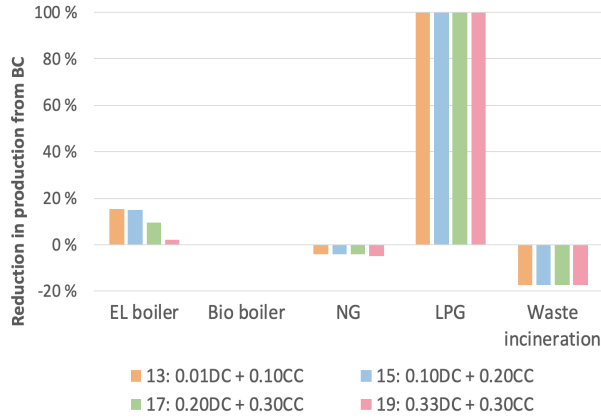


Figure 9.5: Production mix for the deterministic model with a TES.

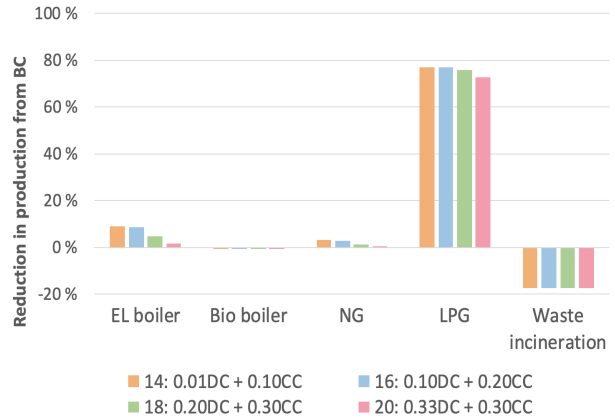


Figure 9.6: Production mix for the multi-horizon model with a TES.

With a combination of DSM and TES, the LPG production is eliminated in the deterministic model (as opposed to only having a TES in Case 3, Figure 9.2). This is possible due to increased production and storage of waste incineration in the summer. The lower the deficit and curtailment costs, the better the model reduces EL boiler production, mainly due to fluctuating electricity prices, which can be seen in both models. However, the multi-horizon model does not manage to eliminate LPG production due to higher SH peak loads but reduces it significantly compared to the BC. This difference is also seen in Figure 9.3 and Figure 9.4. The reduction of expensive and polluting production technologies also gives a reduction of up to 22% in CO₂ emissions compared to the BC.

9.4 Different SH Demand Requirements

In this section, we explore the value of lower hourly and daily demand requirements for SH target demand, i.e., the ability to shift and curtail a higher amount of delivered heat. The lower hourly demand requirement is set to 80%, the lower intervals to 90%, and the lower daily requirement to 95%. The upper hourly demand requirement is set to 120%, while the other upper bounds are kept as presented in Section 6.2.11. The effects on costs and production from changing the SH demand requirements in the deterministic and multi-horizon model are presented in Table 9.7.

Table 9.7: Results from changing SH demand requirements.

Case Model	21 DET	22 MH	23 DET	24 MH
Inputs				
Lower/Upper hourly SH demand requirement [%]	80/120	80/120	80/120	80/120
Lower interval SH demand requirement [%]	90	90	90	90
Lower daily SH requirement [%]	95	95	95	95
Max TES level [kWh]	-	-	100 000	100 000
Outputs				
Max actual TES level [kWh]	-	-	21 377	21 377
Total production [kWh]	488 032	488 070	492 981	493 810
Peak production [kWh/h]	2 801	2 835	2 421	2 715
CO ₂ emissions [kWh]	21 616	22 966	19 388	19 488
SH deficit [kWh]	22 527	23 061	23 464	23 702
SH curtailment [kWh]	16 556	16 518	17 493	17 455
HW deficit [kWh]	21 380	22 357	21 653	22 752
Total operational cost [NOK]	161 382	165 927	152 559	155 777
Total operational cost excl. DSM [NOK]	159 314	163 857	150 378	153 598
Δ in operational cost from BC [%]	-7	-6	-12	-12
Δ in CO ₂ emissions from BC [%]	-17	-16	-26	-29
Δ in peak production from BC [%]	-7	-6	-20	-10

The BC's total operational cost is reduced by 6-7% without a TES (Case 21 and Case 22), and 12% with a TES (Case 23 and Case 24) in Table 9.7. The peak production in Case 23 and Case 24 differ by a lot, resulting from different decisions made in the deterministic and multi-horizon model. Evidently, due to higher peak loads in the multi-horizon model, as discussed in Section 9.1. The amount of SH and HW deficit and SH curtailment is slightly higher in the cases with a TES (Case 23 and Case 24). In these cases, more deficit and curtailment are used in the summer to store more heat for utilization in later peak hours. The TES level in Case 23 and Case 24 is approximately 4% higher than in the BC. This contributes to reducing production from expensive heat technologies in the cold months, thus reducing operational costs. The TES store the same amount in the deterministic and multi-horizon model, but empty the TES differently, as seen in Figure 9.7.

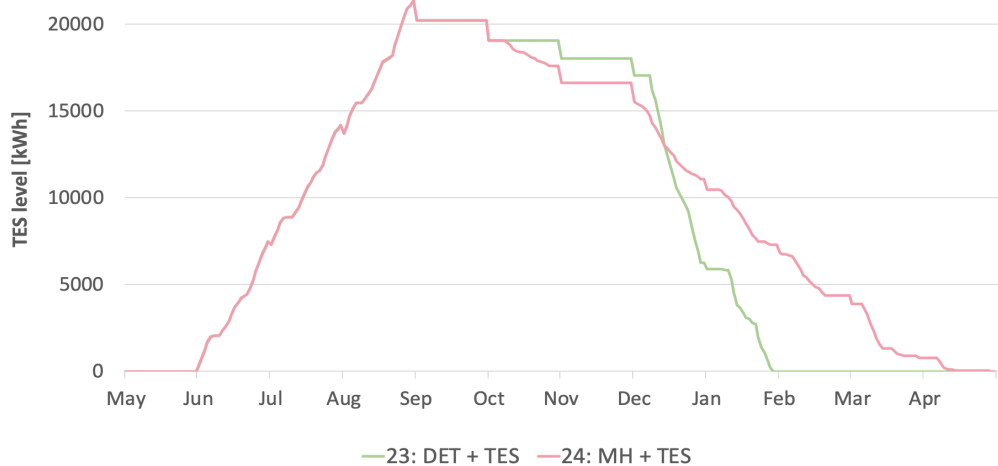


Figure 9.7: TES level for changed SH demand requirements.

The deterministic model empties the TES earlier than the multi-horizon model. The TES has a monthly heat loss of 5.5%, and since the multi-horizon model empties the TES in later months, it results in higher total heat production. Another reason for the difference in storage behavior is the higher peak loads in the multi-horizon model. The multi-horizon model manages to reduce LPG production by 44% without a TES (Case 22) and 87% with a TES (Case 24). In comparison, the deterministic model reduces it by 87% without a TES (Case 21), while the model with a TES (Case 23) eliminates LPG production by emptying the storage earlier. Figure 9.8 shows the percentage difference in production mix for cases 21-24 compared to their respective BC (Case 1 and Case 2), depending on whether it is the deterministic or multi-horizon model.

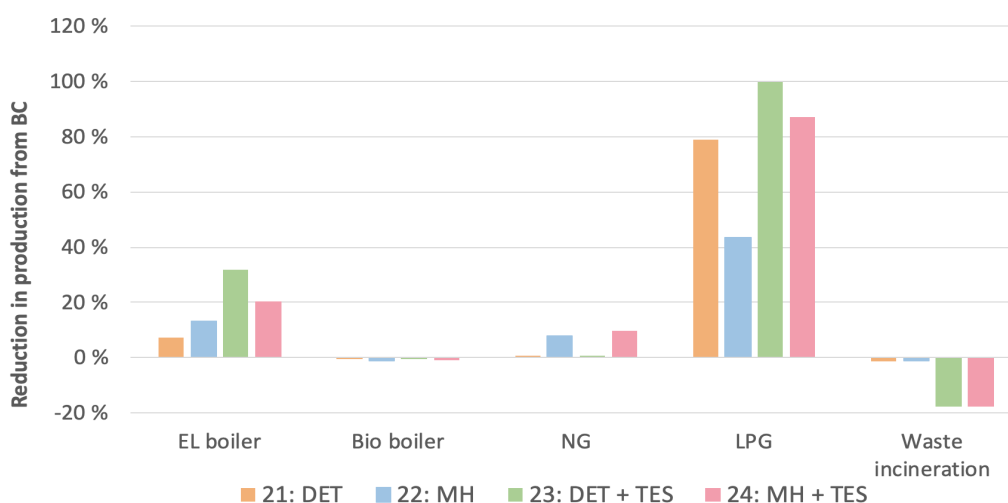


Figure 9.8: Difference in production mix from BC.

The production amount from all peak technologies (EL boiler, NG, and LPG) is reduced in all cases. Waste incineration is increased by 1-2% without a TES (Case 21 and Case 22), compared to 18% with a TES (Case 23 and Case 24). This is explained by the ability to store heat from waste incineration in the TES during the summer in Case 23 and Case 24. Therefore, storing waste incineration has a substantial effect on reducing LPG production and delivered heat during peak hours. This can be seen in Figure 9.9, which presents the total delivered heat (SH and HW) for cases 21-24 compared to the total target heat demand for the planning horizon. The delivered heat in May is relatively flat because of high waste incineration capacity, free local waste heat, and no uncertainty in SH demand.

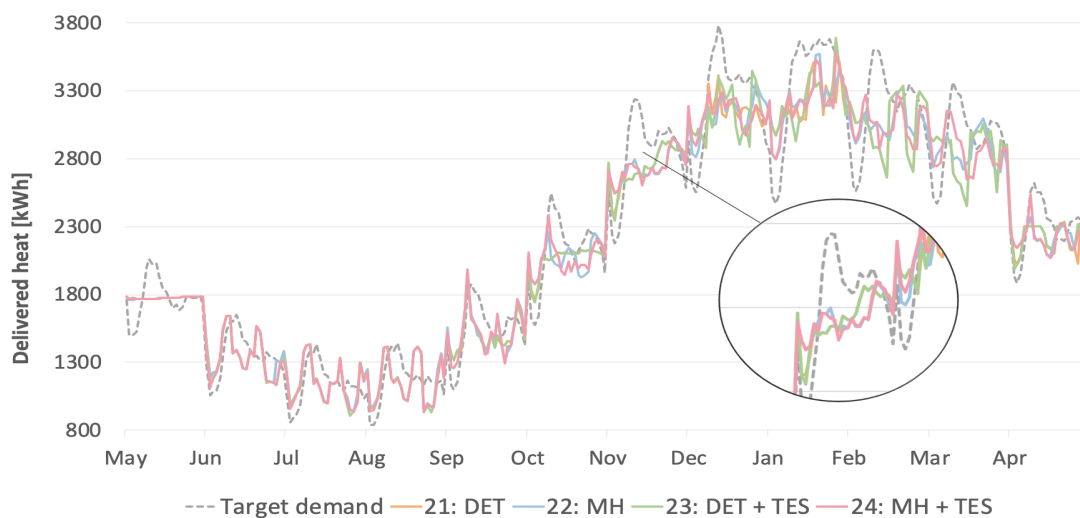


Figure 9.9: Total delivered heat versus target demand.

In all cases, it is preferred to reduce delivered heat in peak hours if it is possible to reduce production from expensive technologies (Figure 9.9). The reduction of expensive technologies reduces the capacities needed for the available production technologies, leading to lower investment costs for the DHG infrastructure. The zoomed-in part indicates November, where we can see that demand is not met during peak hours, but shifted to off-peak hours. Expensive production technologies drive peak cutting and demand shifting. It is also evident from Figure 9.9 that the DHG with only DSM techniques manage to reduce the delivered heat peak just as much as a combination of DSM and TES.

9.5 Different HW Demand Requirements

All previous cases that allow DSM has allowed a 20% hourly deficit/surplus on HW demand. This section analyzes the effects of different HW demand requirements since the hourly minimum HW heat amount that needs to be delivered is uncertain due to uncertainty regarding the number of hot water tanks and their capacities at Leangen. Some of these effects are changes in costs, heat delivery, and electricity use for the deterministic and the multi-horizon model. The cases are analyzed without a TES to highlight cost reductions and the correlation between HW demand requirements and electricity use.

Case 25 and Case 26 represent the deterministic and multi-horizon model, with a 20% hourly deficit/surplus allowed, while Case 27 and Case 28 have a lower bound of 20% and an upper bound of 180% for the target HW demand. Case 29 and Case 30 are analyzed with a capacity approach, where it is assumed that the Heat Pumps (HPs) for HW have high enough capacity to deliver the highest demand for HW that occurs during the planning horizon. Therefore, the lower bound is set to 0 kWh and the upper bound to 1 270 kWh. HW curtailment for a day is assumed to be unrealistic due to safety (see Section 6.2.9), and therefore not included in any cases.

Table 9.8: Change of HW demand requirements with no TES.

Case Model	25 DET	26 MH	27 DET	28 MH	29 DET	30 MH
Inputs						
Lower/Upper HW demand requirement	80/120%	80/120%	20/180%	20/180%	0/1 270 kWh	0/1 270 kWh
Outputs						
Peak production [kWh/h]	2 973	2 879	3 368	3 133	3 016	2 978
Peak delivered heat [kWh/h]	3 699	3 645	4 065	3 829	3 742	3 690
Peak delivered HW [kWh/h]	1 318	1 318	1 896	1 853	1 270	1 270
SH deficit [kWh]	10 522	10 087	7 249	7 721	7 124	8 153
SH curtailment [kWh]	6 795	6 780	6 622	6 607	6 622	6 607
HW deficit [kWh]	20 584	21 521	44 576	53 064	43 254	48 875
Total operational cost [NOK]	166 377	170 833	165 072	169 757	165 082	169 787
Total operational cost excl. DSM [NOK]	165 504	169 965	164 227	168 900	164 239	168 930
Electricity cost for HP HW [NOK]	26 188	26 187	25 929	25 874	25 941	25 905
Electricity cost for EL boiler [NOK]	24 882	23 406	24 940	23 286	24 941	23 303
CO ₂ emissions [kWh]	23 751	25 008	23 553	24 784	23 553	24 780

Table 9.8 shows that the multi-horizon model yields higher total operational costs than the deterministic model for all the listed cases. The table also shows lower electricity costs for the multi-horizon model compared to the deterministic model. Lower electricity costs are due to a higher HW deficit, which is shifted to hours with low electricity prices. To investigate different HW demand requirements, we find it more interesting to analyze

results from the model that take the most advantage of DSM for HW. In addition, the multi-horizon model has different scenarios representing days with high and low demand, which give a more realistic representation of the real world and more relevant to the application of DSM. Therefore, the remainder of this section will contain further analysis of the results obtained from the multi-horizon model.

Comparing Case 28 and 30 against Case 26 in Table 9.8 shows that the HW deficit is 147% and 127% higher in Case 28 and Case 30, respectively. The differences in electricity costs and total operational cost are relatively small for the cases in Table 9.8, despite significant differences in HW deficit. Meaning that DSM is frequently used, but the economic advantage of adjusting heat delivery according to the electricity prices is rather small. The explanation for this is that we use averaged electricity prices (Section 6.2.2), which results in small variations in the electricity prices within a month. It is important to emphasize that the hourly deficit cost for HW is almost zero (0.001 NOK/kWh), and a significantly higher hourly deficit cost can result in no utilization of DSM for HW at all.

Figure 9.10 depicts the target HW demand and the delivered HW for the multi-horizon cases. It can be seen that neither of the cases follows the demand pattern. The delivered HW peak is 4% and 46% higher than the BC in Case 26 and 28, respectively, while the delivered peak for Case 30 equals the BC peak. The symmetrical bounds in HW requirements result in a high variation in delivery, with high delivery peaks in cases with high deficit/surplus percentages allowed, as in Case 28. Indicating that the upper bound needs to be further restricted, as high peaks are unfortunate for the grid infrastructure due to capacity limitations. On the other hand, as seen in Table 9.8, SH deficit and curtailment amounts are lower in cases that allow large amounts of hourly HW deficit (Case 28 and Case 30). One reason for this could be that a large HW shift releases capacity from cheaper production technologies so they instead can be used to cover SH demand. Another aspect is that delivered HW is zero in some hours for Case 30, which indicates that in some periods, the HPs for HW need to be turned on and off several times a day, which can cause wear on the HPs.

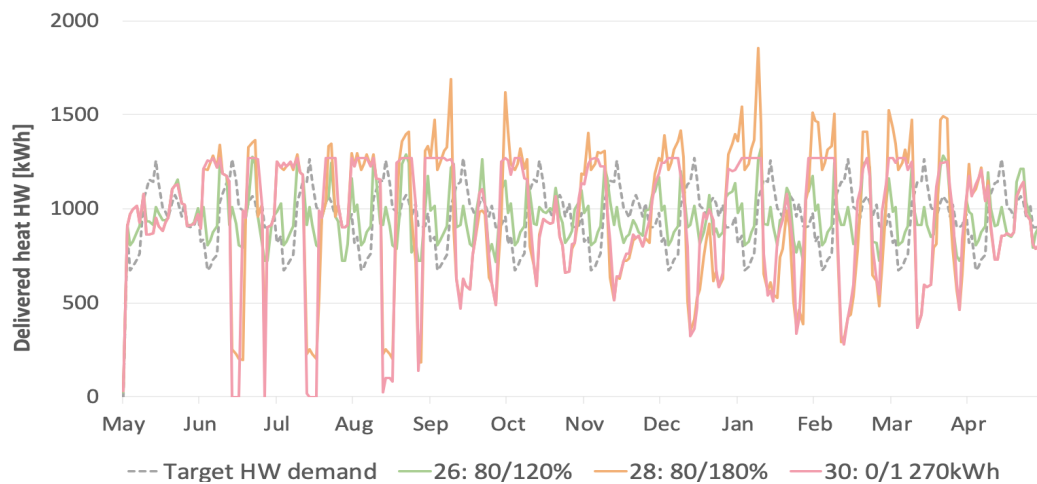


Figure 9.10: Delivered HW versus target HW demand in the multi-horizon model.

The highest delivered HW peak occurs in January. Therefore, Figure 9.11 analyzes January further for the multi-horizon cases. The figure depicts the correlation between electricity use and the electricity price. The DHO uses electricity to operate the centralized HP for waste heat, the decentralized HPs for HW, and the EL boiler. Case 28 and Case 30 manage to adjust the use of electricity to the electricity price far better than Case 26 due to less strict bounds. Case 30 has the flattest peaks because the capacity limit of 1 270 kWh for the decentralized HPs (i.e., for HW) is reached for several hours in January. The supply of 1 270 kWh of HW requires 254 kWh of electricity for HPs due to a COP of 5.

Figure 9.12 illustrates how the high allowed surplus in Case 28 makes it possible to take advantage of low electricity prices. The figure shows the hourly production from the HPs for HW and the hourly production from the EL boiler as it is also affected by the HW demand requirements. The operation of the centralized HP for waste heat is not affected by the HW demand requirements but is included to illustrate how much of the total electricity cost it stands for.

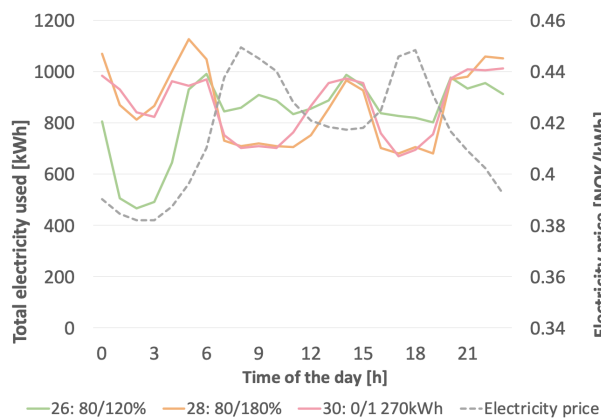


Figure 9.11: Electricity used in January for the multi-horizon cases.

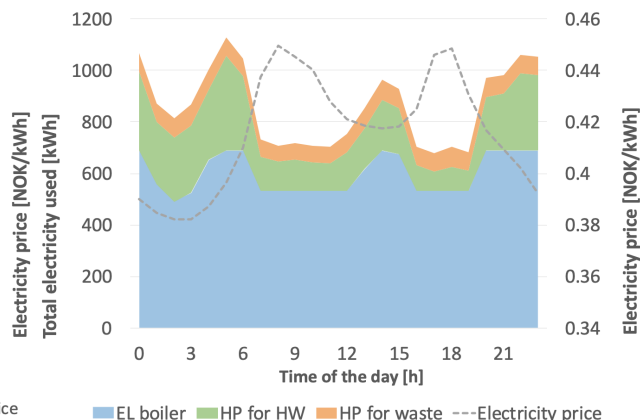


Figure 9.12: Electricity used by HPs and EL boiler in January for Case 28.

Figure 9.11 and Figure 9.12 indicate why the total operational cost difference is relatively small for the multi-horizon cases, but the effect is evident in all the cases 25-30. Price variations in electricity can only be used within a month due to no allowed daily HW curtailment. The variation in hourly electricity price in January is only 0.07 NOK/kWh. The variations in the other months are small, due to the averaged prices, with May having the highest variation of 0.10 NOK/kWh. High fluctuations in electricity prices ensure that more heat is shifted between hours, but this is also highly dependent on hourly deficit costs. The very low hourly HW deficit cost is another reason why the total operational cost difference is small.

9.6 Increased Waste Heat and Larger TES

The total operational cost could be further reduced if more waste heat was available. In this thesis, we can only store heat from controllable technologies. Therefore, we explore the effect of more available waste incineration and a larger TES in this section. It is generally a surplus of heat from waste incineration in Trondheim during the summer because the demand is relatively low compared to the production. Therefore, it might be valuable to have a larger TES that can store this surplus heat. In all cases in this section, the production capacity for waste incineration is increased to 5 000 kWh per hour in the summer months, i.e., June, July, and August. Three different storage sizes are investigated to analyze how the size of the TES can affect the operation of the DHG at Leangen. The maximum TES level for the cases is set out in Table 9.1. For reference, a new residential area in Furuset is planned with a low-temperature DHG and a 10 GWh TES (Granås 2018). In this thesis, three days represent the three summer months where we can store heat, and therefore scaling down a 10 GWh storage would approximately

equal a 330 000 kWh storage in our problem. However, a storage of this size can be expensive. If Leangen were to have a smaller storage with a yearly capacity of 6 GWh, it would equal a TES of 200 000 kWh in our problem. An even smaller TES with a yearly capacity of 2.5 GWh (approximately the same amount as the total waste heat supply from Leangen ice rink) would approximately equal an 80 000 kWh TES in our problem. The effects on production and costs are presented in Table 9.9.

Table 9.9: Models analyzed with three different storage sizes.

Case Model	31 DET	32 MH	33 DET	34 MH	35 DET	36 MH
Inputs						
Max TES level [kWh]	80 000	80 000	200 000	200 000	330 000	330 000
Outputs						
Max actual TES level [kWh]	80 000	80 000	200 000	200 000	245 001	242 511
Total production [kWh]	517 266	517 400	550 328	550 372	572 020	570 689
Peak production excl. waste incineration [kWh/h]	2 407	2 211	2 049	1 900	1 465	1 491
CO ₂ emissions [kg]	16 068	15 934	9 784	8 455	7 953	7 963
SH deficit [kWh]	8 065	8 371	7 074	7 003	6 699	6 511
SH curtailment [kWh]	6 795	6 780	6 795	6 780	6 517	6 329
HW deficit [kWh]	22 090	22 699	23 081	23 223	23 247	23 167
Total operational cost [NOK]	137 100	138 358	108 515	108 900	100 111	100 966
Total operational cost excl. DSM [NOK]	136 250	137 506	107 674	108 061	99 304	100 182
Δ in operational cost from BC [%]	-21	-22	-37	-38	-42	-43
Δ in CO ₂ emissions from BC [%]	-38	-42	-62	-69	-69	-71
Δ in peak production from BC [%]	-20	-27	-32	-37	-51	-51

The total heat demand at Leangen for the planning horizon is 646 352 kWh, so a TES of approximately 245 000 kWh (Case 35 and Case 36) would cover roughly 38% of the total demand. The total amount of waste heat from the Leangen ice rink in the planning horizon is 141 764 kWh, which covers 22% of the total demand. The remaining 40% needs to be covered by controllable sources such as a bio boiler, EL boiler, NG, and LPG. If the TES is 80 000 kWh (Case 31 and Case 32), it only covers 12% of the total demand, and thus the controllable sources must cover the remaining 66%. This difference can also be seen in the total operational cost compared to the BC. The smallest TES size reduces the operational cost by 21-22%, while the largest TES reduces it by 42-43%. Evidently, the larger the storage, the greater the savings in operational cost. However, the investment costs for the different storage sizes are not included. Therefore larger storage sizes might not be as profitable as smaller storage sizes when considering this.

With a maximum level of 330 000 kWh (Case 35 and Case 36), the TES only stores around 245 000 kWh in both models, even though the waste incineration capacity is not maxed out, and is very cheap compared to other heat technologies. However, the TES has a monthly heat loss of 5.5%, and therefore it is not optimal to store heat for several months unless the production cost is very high. The storage reduces the most expensive controllable technologies, first LPG, followed by the EL boiler, NG and the bio boiler, seen in Figure 9.13.

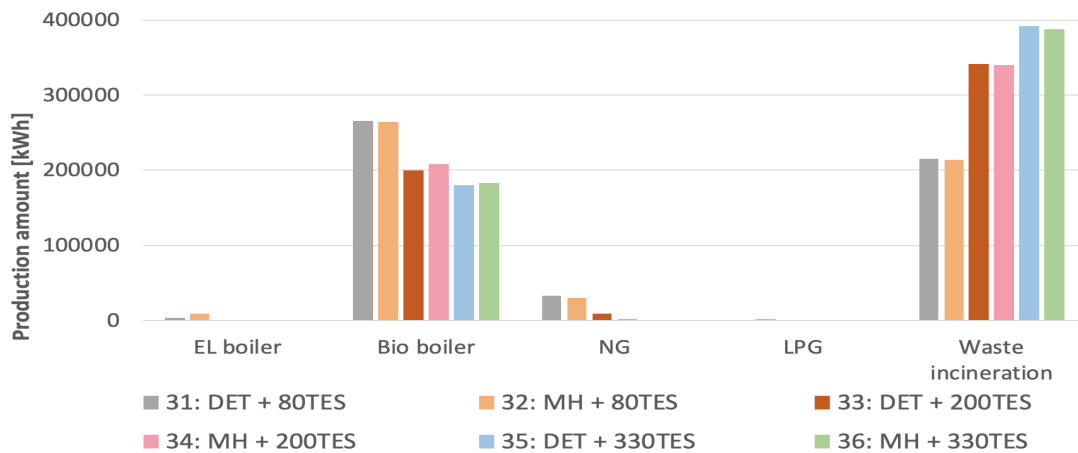


Figure 9.13: Production mix for cases with increased waste heat and different TES sizes.

Figure 9.13 indicates that the production mix is closely related to the TES level. The production from all controllable technologies (e.g., EL boiler, bio boiler, NG, and LPG) decreases with the increasing TES level. Simultaneously, waste incineration production increases in order to fill the TES. This is further indicated by the total operational cost reduction in Table 9.9, where the largest TES leads to a 27% lower total operational cost than the smallest TES.

Figure 9.14 shows the TES level alongside the TES behavior for the deterministic and multi-horizon model. On average, the deterministic model tends to empty the storage earlier than the multi-horizon model. The higher peak loads might explain this for the multi-horizon model. Despite this, Figure 9.14 shows that the TES level and behavior for the deterministic model and the multi-horizon model are very similar. So for large amounts of "free" storage (e.g., stored waste incineration), the deterministic model can be adequate compared to the multi-horizon model.

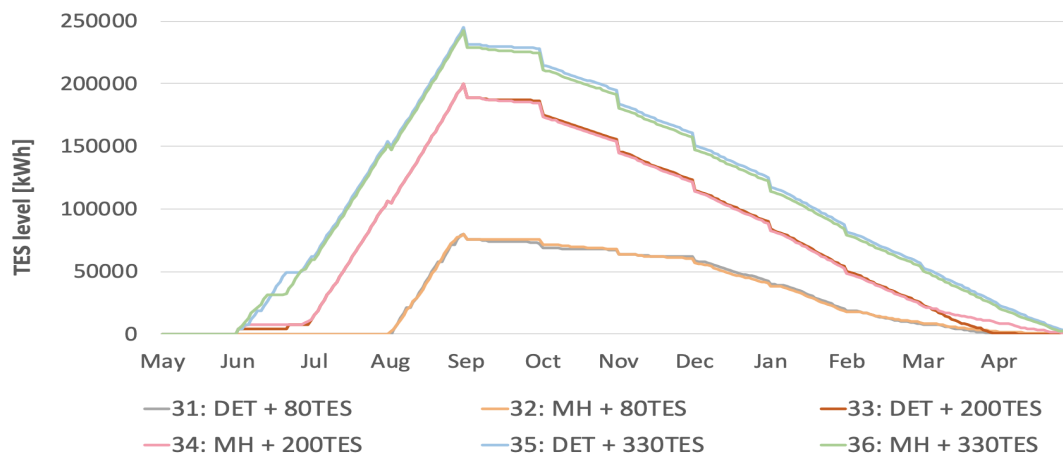


Figure 9.14: TES level for cases with increased waste heat and different TES sizes.

9.7 Investment Cost Analysis of TES

The cases investigated so far do not consider investment costs related to a TES. In this section, an analysis of storage investment costs is done to get more insight into the profitability of a TES in the DHG at Leangen. As mentioned in Section 3.2, borehole TES is a well-suited storage technology for DHGs. This section provides an investment analysis of two different TES sizes. A borehole TES with a storage capacity of 2.5 GWh/year, equivalent to 80 000 kWh in our problem, has an investment cost of approximately 8-10 million NOK. A larger TES of 7.5 GWh/year, equivalent to a maximum actual TES level of approximately 250 000 kWh in our problem, can be estimated to cost 20-25 million NOK¹. In this section, we look at the pay-back period for the two storage sizes to find out how long it will take for the original investment to be repaid for different storage sizes. The pay-back period is used to calculate the amount of time it takes before the TES becomes profitable by dividing the investment cost by the annual savings. DSM is not included in order to find the savings in operational costs only caused by the TES. Table 9.10 presents the effects on costs and production from the cases with increased waste heat and larger storage sizes.

¹ Source: ballpark estimates given in personal communication, Randi Ramstad, Asplan Viak, 08/05/20

Table 9.10: Profitability analysis of the different TES sizes.

Case Model	37 DET	38 MH	39 DET	40 MH
Inputs				
Max TES level [kWh]	80 000	80 000	330 000	330 000
Outputs				
Max actual TES level [kWh]	80 000	80 000	249 724	246 095
Total operational cost [NOK]	140 098	141 567	101 110	102 095
Δ in operational cost from BC [%]	-19	-20	-42	-42
Investment Analysis				
Investment cost [mill NOK]	8-10	8-10	20-25	20-25
Savings from BC [NOK]	32 884	35 004	71 872	74 476
Savings in a year [NOK]	1 000 222	1 064 705	2 186 107	2 265 312
Pay-back period	8-10	8-9	9-11	9-11

One drawback of the pay-back period is that it does not account for the time value of money; therefore, the pay-back period for longer investments is disposed to inaccuracy. Besides, the method is strictly limited to the amount of time required to earn back initial investment costs, and the rate of return on investment could encounter abrupt changes (Black et al. 2009). Due to the lack of exact investment costs for different TES sizes and uncertainty connected to the savings in operational cost, the results will be rough estimates regardless of the profitability method. Therefore, the pay-back method is sufficient for this investment analysis instead of a more sophisticated economic analysis.

For the TES with a capacity of 2.5 GWh/year (Case 37 and Case 38), the pay-back time is approximately 8-10 years, and the DHO will receive a profit from the TES in the following years. The TES with a capacity of 7.5 GWh/year (Case 39 and Case 40) has a pay-back time of 9-11 years. It is important to emphasize that the investment costs used here are very rough cost estimates, and the actual costs depend on the desired temperature level, geological conditions, and location. However, based on the rough estimates in this thesis, the largest TES has approximately the same profitability as the smallest TES. The pay-back period is up to one year longer for the largest TES. The pay-back period is similar for the small and large TES, given that there is a significant surplus of waste heat that can be stored in the summer. The obtained results are specific for this case study with all the assumptions made in Chapter 6, and therefore, not directly applicable to other DHGs.

Borehole TESs usually have a life expectancy of more than 100 years (Acworth 2019). Therefore, a large TES at Leangen could be a profitable long-term solution if there is much excess waste heat (with the right temperature for storing) in the surrounding area or the main grid in Trondheim. Also, if the supply of renewable energy increases in the future, a TES is a good approach to capture irregular energy supply.

9.8 Comparison of DSM and TES

In this section, a comparison of DSM and TES is done based on the results obtained from the cases analyzed with the multi-horizon model. The multi-horizon model is chosen since it considers uncertainty in SH demand.

An aspect that makes the comparison challenging is the deficit penalty costs and SH demand requirements, which should somehow reflect consumer comfort zones and the impact heat demand adjustments (i.e., shifted and curtailed loads) have on them. With moderate demand requirements as described in Chapter 6, the results show that LPG is reduced by 27% without a TES (Case 6) compared to the BC and 77% with a TES (Case 14). With higher allowed deficit and surplus demand (Section 9.4), the multi-horizon model manages to reduce LPG production by 44% without a TES (Case 22) and 87% with a TES (Case 24). In comparison, the LPG production in Case 4, which includes a TES but not DSM, is reduced by 59% compared to the BC. This indicates that the consumer comfort zones and the consumer tolerance for SH shift and curtailment can significantly affect the reduction in peak production technologies. The TES contributes to achieving the highest reduction in LPG production. In addition, the analysis indicates that DSM techniques (i.e., shift and curtailment) are more used in cases with no TES. However, the combination of DSM and TES can provide further value to the TES (see Case 14 versus Case 4) as implementing DSM does not involve any investment costs.

The value of waste heat and waste incineration in the DHG is analyzed in Section 9.6. A large TES is not useful in the DHG unless there is a large amount of low-cost heat production technologies available in the summer. This was investigated in Chapter 8 (see Table 8.7) and in Chapter 9 (see Table 9.9). A large TES can lead to a significant reduction in installed peak production technologies if a high amount of surplus waste incineration is available in the summer. By comparing the production mix in Case 4 (Figure 9.2) with Case 36 (Figure 9.13), it is seen that all the peak technologies are eliminated in Case 36 with the large storage, while LPG is only reduced compared to the BC, but none of the peak technologies are eliminated in Case 4. By reducing peak production technologies, i.e., controllable technologies such as LPG, the DHO has the

opportunity to install fewer expensive peak production technologies and, therefore, also reduce the infrastructure investment cost. Moreover, this will reduce CO₂ emissions as peak production technologies are often less climate-friendly.

The results also show that including DSM, TES, or both affect the total operational cost. The inclusion of a TES (Case 4) reduces the total operational cost by 6 % compared to the BC by storing surplus waste heat incineration in the adding period and withdrawing in periods with high peak loads. The TES contributes to avoiding production from expensive production technologies, here LPG. The application of DSM without a TES also reduces the total operational cost, although lower than with the inclusion of only a TES. The total operational cost is reduced by up to 4% with only DSM (Case 6). However, the reduction is more significant when a TES is included, by up to a 10% reduction in total operational cost.

9.9 Data Limitations

In this section, we discuss how some of the data assumptions affect the obtained results for the case study at Leangen. More specifically, we discuss the practical implications of the main assumptions made in Chapter 6. These assumptions include; choice of the planning horizon length and representation, the production mix, and the production costs.

9.9.1 Planning Horizon

The analysis are done for a stylized planning horizon of 12 days representing 24 hours of a typical day in each month. We chose twelve days to capture the fluctuations in SH heat demand throughout the year. We consider the insight we gain from analyzing 12 representative days to be sufficient to indicate the value of DSM and TES. Despite this, it is important to keep in mind that a more accurate representation of the year may give numerical results that differ from the results presented in this chapter. Another approach is to use the models for operational planning of independent time periods, e.g., one week. However, this approach makes it hard to model the seasonal TES, as it requires assumptions about the storage level at the beginning and end of the week. Due to the seasonal TES, we find it more valuable to analyze a whole year.

9.9.2 Production Mix

It is important to emphasize that the production mix at Leangen strongly affects most of the results presented in this chapter and the previous chapter. The lack of available data means that we have to make several assumptions regarding the capacities of the production technologies used to cover the local heat demand at Leangen. It is challenging to know which production technologies will be completely exploited in the Trondheim DHG and which will have excess capacity. In addition, the capacities need to be limited to prevent the models from only utilizing the cheapest production technologies. The utilization of buffers to ensure the feasibility of all demand scenarios makes it even more complicated to find appropriate scaled-down capacities. We have attempted to make the production mix as realistic as possible by distinguishing between production technologies used to cover the base load, peak load, and buffer load in different months. The production mix is also designed to be affected by the use of DSM and TES to ensure interesting analyses. To summarize, the production mix we use to investigate Leangen is highly stylized and can be very different from the real production mix that will be used.

9.9.3 Production Costs

The production costs for the bio boiler, NG, LPG, and waste incineration are obtained from Sidelnikova et al. (2015) and assumed to be constant in this analysis. The costs are published by The Norwegian Water Resources and Energy Directorate. The fuel costs and variable costs are given for different heat boilers for some capacities. The capacity of the boilers does not fully match the real installed capacities in the Trondheim DHG, so the nearest given capacity is used. In reality, the fuel prices for production technologies can vary with time and can be affected by contracts. The production costs for the electric boiler used in this thesis are time-dependent and based on historical spot power prices in Trondheim, in addition to Sidelnikova et al. (2015). The electricity price has higher fluctuations in reality as the spot prices in this thesis are averaged for each month and every hour. Given this, the real production costs in the future DHG at Leangen can be significantly different from those used in this thesis.

Chapter 10

Concluding Remarks and Future Research

10.1 Concluding Remarks

In this thesis, we define and develop a deterministic optimization model and two stochastic optimization models to find the optimal operation of a low-temperature District Heating Grid (DHG). The models optimize the operation over a year's planning horizon using 12 representative days while taking into account the uncertainty in Space Heating (SH) demand. The objective is to minimize expected operational costs by utilizing a seasonal TES and DSM techniques, as these features increase the degree of demand-side flexibility, which can help reduce costs. Unmet demand, through load shifting and curtailment, is penalized with a cost. Similarly, we penalize CO₂ emissions.

The stochastic problem is first solved using a multistage traditional scenario tree-based stochastic model. Due to a large number of scenarios, each problem instance has a calculation time of approximately 9 hours. A multi-horizon stochastic model is developed to reduce the number of scenarios and hence the calculation time. The multi-horizon model provides a satisfactory solution close to the traditional stochastic model's solution, with a calculation time of approximately 25 seconds.

A comprehensive case study of the planned residential area at Leangen, in Trondheim, has been performed in this thesis. The main focus has been to evaluate the applicability of a seasonal TES and DSM techniques, providing a thorough analysis of the value of including these two features in the DHG from an operational aspect. However, from this analysis, we can conclude that a seasonal TES will have a significant impact on annual operational cost and reduction of generation by expensive and polluting peak technologies such as LPG. Following this, fewer expensive peak production technologies need to be installed in the DHG, reducing the infrastructure cost. In addition, implementing DSM techniques increase the advantage of the storage. Production from LPG is reduced by 59% when only a TES is included, while production is reduced by up to 77% with a combination of DSM and TES. The potential reduction in operational cost is less when only DSM techniques are included (up to 4%) than when only a TES is included (6-7%). The combination of a

TES and application of DSM provides savings of up to 22% in CO₂ emissions, 11% peak production, and 9% lower operational cost. However, implementing DSM is probably more applicable for many urban areas as implementing DSM is cheaper and less space demanding than having a large seasonal TES, which may be impossible for many urban areas. In addition, we find DSM techniques to be valuable for the reduction of delivered heat peaks in the grid. The reduction of these peaks, so-called peak-flattening of the heat curve, relieves the load on the infrastructure and allows reduced needed grid capacity to supply heat to end-users.

If more excess heat from waste incineration would be available in the summer months than in our initial analysis, an even larger storage could be profitable. The availability of a large storage and application of DSM provides savings of up to 71% in CO₂ emissions, 51% peak production, and 43% lower operational cost. It allows removing the most expensive production technologies from the production mix, which would also save investment and maintenance costs from these technologies, but at the expense of higher investment cost in the storage. The larger the storage, the less added value DSM techniques have at the grid level, although there are still benefits at the individual building level as Heat Pump (HP) capacities can be lower. Overall, for smaller storages, implementing DSM techniques increase the advantage of the storage. Although a storage facility is not planned for the Leangen area, our analysis shows rather short payback periods of nine to eleven years and orders of magnitude lower than the technical lifetime of such storages. Therefore, the business case for a seasonal TES at Leangen would be interesting to investigate.

The cases were analyzed with both the deterministic model and the multi-horizon model to evaluate the added uncertainty in the multi-horizon model. The output results in the deterministic model and the expected output results in the multi-horizon model give similar output values for total operational cost, deficit, and curtailment. However, the two models' production mix is slightly different as the multi-horizon considers scenarios with three different SH demand levels and can provide valuable planning for a day with high SH demand, while the deterministic model can only plan for a weighted average SH demand. The deterministic model is appropriate if there is a high amount of free storage.

Although the analysis indicates that it is desirable to combine a TES and DSM in a DHG, it is hard to quantify the exact value of DSM and TES as the models do not include investment costs for the TES and the investment analysis done in Section 9.7 is a rough estimate. In addition, the assumed DSM penalties do not directly affect the operational costs of DHGs in reality. Furthermore, the total operational cost is highly dependent on input data, and several of the data inputs in this thesis are highly stylized and can be different from the real data for the future DHG at Leangen.

10.2 Future Research

During the work on the proposed problem presented in this thesis, we have identified several aspects that can be studied advantageously to a larger extent. In this section, we summarize the various aspects that we consider to be of interest in future research.

The first direction that we find interesting to follow is to obtain a better representation of the planning horizon and demand uncertainty to see how this affects the value of using the stochastic models instead of the deterministic model. The investigated planning horizon could get a more accurate representation by introducing more representative days (e.g., one for each week through the year). In order to achieve this for the traditional stochastic model, it is necessary to reduce the model's memory use. Another interesting aspect is to add more SH demand scenarios in each representative day in the multi-horizon model to investigate the impacts it will have on the results. Uncertainty in HW demand may also be considered. Still, this uncertainty should not necessarily be represented by temperature scenarios, as demand is not affected by ambient temperatures, but rather by consumer demand patterns. Another approach is to compare the models for operational planning of independent time periods, e.g., one week with or without storage possibility, and including demand uncertainty in each day. The operational planning of independent time periods could also be linked to real weather forecasts for short-term periods.

For the case study at Leangen, an area of improvement is to obtain more accurate and realistic data for the future DHG. It is crucial to establish a better correlation between the demand at Leangen and the heat production from different production technologies in the main DHG to make the production mix at Leangen more realistic. More accurate cost data and demand requirements for the different user profiles should be applied, which involves testing combinations of demand requirements and time-dependent penalty costs for both SH and HW. In addition, different combinations of user profiles in a consumer node/area could be tested to see if it is possible to exploit the composition of different consumption patterns to smooth out peaks for delivered heat and production. In order to provide a better basis for comparing the value of TES and DSM, the operation of different TES solutions should be evaluated, and the investment costs for the seasonal TES should receive more focus. If more representative estimates of investment and production costs are provided, then more sophisticated investment analyses, which account for depreciation and interest rates for TES with different sizes and properties, could be implemented.

There are also several extensions of the model formulation that we find interesting to follow. A natural extension is to combine tactical and operational planning by adding separate investment periods before the operational periods, where investment in seasonal

storage, local boilers, and DHG infrastructure is possible. Another interesting extension of the mathematical models is to connect the DHG and a power grid to optimize the combined grid. The model formulations can be further developed by allowing prosumers, which can lead to a valuable contribution to future smart grid development. The model implementations should then be reformulated, so prosumers are categorized as both production and consumer nodes.

Currently, our models only focus on reducing the total operational cost rather than peak production and the amount of delivered heat in peak hours. If the models should be applied to a DHG with production or pipeline capacity challenges, one possibility is to reward the models for production and delivery shift from on-peak hours to off-peak hours. The reward could be combined with a penalty cost for decreasing consumer comfort.

Bibliography

- Acworth, I. (2019). *Investigating groundwater*. IAH - International Contributions to Hydrogeology. CRC Press.
- Adamo, L., Cammarata, G., Fichera, A., & Marletta, L. (1997). Improvement of a district heating network through thermoeconomic approach. *Renewable Energy*, *10*(2), 213–216.
- Asplan Viak. (2018). Leangen bolig as, energi og miljø - fagutredning, utgave: 1.02.
- Bachmaier, A., Narmsara, S., Eggers, J.-B., & Herkel, S. (2015). Spatial distribution of thermal energy storage systems in urban areas connected to district heating for grid balancing. *Energy Procedia*, *73*(100), 3–11.
- Balijepalli, V., Pradhan, V., Khaparde, S., & Shereef, R. (2011). Review of demand response under smart grid paradigm, 236–243.
- Basecq, V., Michaux, G., Inard, C., & Blondeau, P. (2013). Short-term storage systems of thermal energy for buildings: A review. *Advances in Building Energy Research*, *7*(1), 66–119. Retrieved from <http://www.tandfonline.com/doi/abs/10.1080/17512549.2013.809271>
- Birge, J. R., & Louveaux, F. (2011). *Introduction to stochastic programming*. Springer Series in Operations Research and Financial Engineering, New York, NY: Springer New York.
- Black, J., Hashimzade, N., & Myles, G. (2009). A dictionary of economics. Oxford University Press. Retrieved from <http://www.oxfordreference.com/view/10.1093/acref/9780199237043.001.0001/acref-9780199237043-e-2287>
- Bøeng, A. C. (2019). Økt forbruk av fjernvarme. SSB.
- Boshell, F., & Veloza, O. (2008). Review of developed demand side management programs including different concepts and their results, 1–7.
- Byggteknisk forskrift [TEK07]. (2007). Retrieved from https://dibk.no/globalassets/byggeregler/tidligere_regelverk/veiledning_til_teknisk_forskrift_4.utg.2007.pdf
- Byggteknisk forskrift [TEK17]. (2017). Retrieved from <https://dibk.no/byggereglene/byggteknisk-forskrift-tek17/>
- Cai, H., Ziras, C., You, S., Li, R., Honoré, K., & Bindner, H. W. (2018). Demand side management in urban district heating networks. *Applied Energy*, *230*, 506–518.

- Capone, M., Guelpa, E., & Verda, V. (2019). Optimal operation of district heating networks through demand response. *International Journal of Thermodynamics*, 22(1), 35–43.
- Celebi, M. E., Kingravi, H. A., & Vela, P. A. (2013). A comparative study of efficient initialization methods for the k-means clustering algorithm. *Expert systems with applications*, 40(1), 200–210.
- Ciulla, G., & D’Amico, A. (2019). Building energy performance forecasting: A multiple linear regression approach. *Applied Energy*, 253.
- Council of European Union. (2018). Council regulation (EU) no 844/2018. Retrieved from https://eur-lex.europa.eu/legal-content/EN/TXT/?uri=uriserv%3AOJ.L_.2018.156.01.0075.01.ENG
- Dantzig, G. B. (2004). Linear programming under uncertainty. *Management Science*, 50(12), 1764–1769.
- de Oliveira, V., Jäschke, J., & Skogestad, S. (2016). Optimal operation of energy storage in buildings: Use of the hot water system. *Journal of Energy Storage*, 5, 102–112.
- Di Domenica, N., Lucas, C., Mitra, G., & Valente, P. (2009). Scenario generation for stochastic programming and simulation: A modelling perspective. *IMA Journal of Management Mathematics*, 20(1), 1–38.
- Dinçer, I., & Rosen, M. (2010). *Thermal energy storage: Systems and applications, second edition*. John Wiley and Sons.
- Dorotić, H., Pukšec, T., & Duić, N. (2019). Multi-objective optimization of district heating and cooling systems for a one-year time horizon. *Energy*, 169, 319–328.
- Dupačová, J., Consigli, G., & Wallace, S. W. (2000). Scenarios for multistage stochastic programs. *Annals of operations research*, 100(1-4), 25–53.
- Enøk i bygninger : Effektiv energibruk* (3. utg.). (2007). Oslo: Gyldendal undervisning.
- ENOVA. (2016). Kjøpsveileder Pelletskjel. Accessed: 2018-02-11. Retrieved from <https://www.enova.no/privat/alle-energitiltak/biovarme/biokjel/>
- UN-Environment. (2017). Global status report 2017. Retrieved from [https://www.worldgbc.org/sites/default/files/UNEP%5C%20188_GABC_en%5C%20\(web\).pdf](https://www.worldgbc.org/sites/default/files/UNEP%5C%20188_GABC_en%5C%20(web).pdf)
- European Committee for Standardization. (2012). Recommendations for prevention of legionella growth in installations inside buildings conveying water for human consumption. *CEN/TR*, 16355, 2012.
- Fortum. (2019). Prismodeller - fjernvarme. Retrieved September 11, 2019, from <https://www.fortum.no/fjernvarme/prismodeller>
- Gao, L., Cui, X., Ni, J., Lei, W., Huang, T., Bai, C., & Yang, J. (2017). Technologies in smart district heating system. *Energy Procedia*, 142, 1829–1834.

- Granås, S. (2018). Skal lagre 10 gwh fra sommer til vinter. Retrieved from <https://www.teknisknyheter.no/forside/aktuelt/skal-lagre-10-gwh-fra-sommer-til-vinter>
- Guelpa, E., Marincioni, L., Deputato, S., Capone, M., Amelio, S., Pochettino, E., & Verda, V. (2019). Demand side management in district heating networks: A real application. *Energy*, *182*, 433–442.
- Hansen, L. P. (2017). Time-series econometrics in macroeconomics and finance. *Journal of Political Economy*, *125*(6), 1774–1782.
- Hellemo, L. (2016). Managing uncertainty in design and operation of natural gas infrastructure. Trondheim: Norwegian University of Science et al.
- Henseler, J., Ringle, C., & Sinkovics, R. (2009). The use of partial least squares path modeling in international marketing. (Vol. 20, pp. 277–319). doi:10.1108/S1474-7979(2009)0000020014
- Higle, J. L. (2005). Stochastic programming: Optimization when uncertainty matters.
- Hoffmann, R. (1987). Damodar gujarati. basic econometrics. mcgraw-hill, 1978. *Brazilian Review of Econometrics*, *7*, 83.
- Hohmann, M., Warrington, J., & Lygeros, J. (2019). A two-stage polynomial approach to stochastic optimization of district heating networks. *Sustainable Energy, Grids and Networks*, *17*, 100177. Retrieved from <http://www.sciencedirect.com/science/article/pii/S2352467718302601>
- Huang, Y.-H., Wu, J.-H., & Hsu, Y.-J. (2016). Two-stage stochastic programming model for the regional-scale electricity planning under demand uncertainty. *Energy*, *116*. doi:10.1016/j.energy.2016.09.112
- IEA. (2019). World energy outlook 2019. Retrieved from <https://www.iea.org/reports/world-energy-outlook-2019>
- IRENA. (2013). *Thermal energy storage: Technology brief*. ASHRAE.
- Jain, A. K. (2010). Data clustering: 50 years beyond k-means. *Pattern recognition letters*, *31*(8), 651–666.
- Jie, P., Zhu, N., & Li, D. (2015). Operation optimization of existing district heating systems. *Applied Thermal Engineering*, *78*, 278–288.
- Kall, P. (1997). Stochastic programming. Chichester: John Wiley.
- Kauko, H. (2018). Lttg+. Retrieved from <https://www.sintef.no/prosjekter/lttg/>
- Kauko, H., Kvalsvik, K. H., Rohde, D., Hafner, A., & Nord, N. (2017a). Dynamic modelling of local low-temperature heating grids: A case study for norway. Retrieved from <http://hdl.handle.net/11250/2451662>
- Kauko, H., Kvalsvik, K. H., Rohde, D., Hafner, A., & Nord, N. (2017b). Dynamic modelling of local low-temperature heating grids: A case study for norway. Retrieved from <http://hdl.handle.net/11250/2451662>

- Kaut, M. (2003). Scenario tree generation for stochastic programming : Cases from finance. Trondheim: Department of Mathematical Sciences, Faculty of Information Technology, Mathematics, Electrical Engineering, Norwegian University of Science, and Technology.
- Kaut, M., Midthun, K., Werner, A., Tomasgard, A., Hellemo, L., & Fodstad, M. (2014). Multi-horizon stochastic programming. *Computational Management Science*, 11(1-2), 179–193.
- Kemp, I. C. (2012). Fundamentals of energy analysis of dryers. In *Modern drying technology* (Chap. 1, pp. 1–45). doi:[10.1002/9783527631681.ch1](https://doi.org/10.1002/9783527631681.ch1)
- Kim, T. K. (2015). T test as a parametric statistic. *Korean journal of anesthesiology*, 68(6), 540.
- King, A. J., & Wallace, S. W. (2012). Modeling with stochastic programming.
- Kontu, K., Vimpari, J., Penttinen, P., & Junnila, S. (2018). City scale demand side management in three different-sized district heating systems. *Energies*, 11(12). Retrieved from <http://search.proquest.com/docview/2316421382/>
- Lambert, R., Maier, S., Polak, J., & Shah, N. (2016). Optimal phasing of district heating network investments using multi-stage stochastic programming. *International Journal of Sustainable Energy Planning and Management*, 9, 57–74.
- Lee, J., & Elmasri, R. (1998). An eer-based conceptual model and query language for time-series data. (Vol. 1507, pp. 21–34). Springer Verlag.
- Lefter, R. C., Popescu, D., & Untăroiu, A. (2014). Method for redesign of district heating networks within transition from the 2nd to the 3rd generation. *Applied Mechanics and Materials*, 657(Engineering Solutions and Technologies in Manufacturing), 689–693.
- Leško, M., Bujalski, W., & Futyma, K. (2018). Operational optimization in district heating systems with the use of thermal energy storage. *Energy*, 165(PA), 902–915.
- Lettenbichler, S., & Provaggi, A. (2019). 100 % renewable energy districts: 2050 vision. Retrieved from <https://www.euroheat.org/publications/100-renewable-energy-districts-2050-vision/>
- Li, D., Chiu, W.-Y., & Sun, H. (2016). Microgrid: Advanced control methods and renewable energy system integration. Elsevier Science.
- Li, H., & Nord, N. (2018). Transition to the 4th generation district heating - possibilities, bottlenecks, and challenges. *Energy Procedia*, 149, 483–498.
- Liew, V. (2004). Which lag selection criteria should we employ? *Economics Bulletin*, 3, 1–9.

- Lindberg, K., Bakker, S., & Sartori, I. (2019). Modelling electric and heat load profiles of non-residential buildings for use in long-term aggregate load forecasts. *Utilities Policy*, *58*, 63–88. doi:[10.1016/j.jup.2019.03.004](https://doi.org/10.1016/j.jup.2019.03.004)
- Liu, P., Fu, Y., & Kargarian, A. (2014). Multi-stage stochastic optimal operation of energy-efficient building with combined heat and power system. *Electric Power Components and Systems*, *42*. doi:[10.1080/15325008.2013.862324](https://doi.org/10.1080/15325008.2013.862324)
- Lloyd, S. (1982). Least squares quantization in pcm. *IEEE Transactions on Information Theory*, *28*(2), 129–137.
- Lund Hagem Arkitekter. (2019). Tungavegen 1 forslag til reguleringsplan åpent møte 24.01.2019. Retrieved from <https://www.koteng.no/leangenbolig/>
- Lund, H. (2018). Renewable heating strategies and their consequences for storage and grid infrastructures comparing a smart grid to a smart energy systems approach. *Energy*, *151*, 94–102.
- Lund, H., Werner, S., Wiltshire, R., Svendsen, S., Thorsen, J. E., Hvelplund, F., & Mathiesen, B. V. (2014). 4th generation district heating (4gdh). *Energy*, *68*, 1–11.
- Mangold, D., & Deschaintre, L. (2015). Seasonal thermal energy storage - report on state of art and necessary further r+d. Retrieved from <http://task45.iea-shc.org/publications>
- Marañón-Ledesma, H., & Tomasgard, A. (2019). Analyzing demand response in a dynamic capacity expansion model for the european power market. *Energies*, *12*(15). Retrieved from <http://search.proquest.com/docview/2316982721/>
- Neath, A. A., & Cavanaugh, J. E. (1997). Regression and time series model selection using variants of the schwarz information criterion. *Communications in Statistics - Theory and Methods*, *26*(3), 559–580. Retrieved from <http://www.tandfonline.com/doi/abs/10.1080/03610929708831934>
- Nordell, B. (1994). Borehole heat store design optimization. Luleå tekniska universitet, Institutionen för samhällsbyggnad och naturresurser, Arkitektur och vatten. Luleå: Luleå tekniska universitet.
- NordPool. (2020). Historical market data- elspot prices -hourly. Accessed: 2020-02-14. Retrieved from <https://www.nordpoolgroup.com/historical-market-data/>
- Norsk Fjernvarme. (2015). Fjernvarme: Et trygt og miljøvennlig alternativ. Retrieved from <https://docplayer.me/1401563-Fjernvarme-et-trygt-og-miljovennlig-alternativ.html>
- Norsk Fjernvarme. (2018). Om energikildene-omgivelsesvarme. Accessed: 2020-02-28. Retrieved from <https://www.fjernkontrollen.no/content/om-energikildene/>
- Norsk Fjernvarme. (2019). Energikilder trondheim 2019. Accessed: 2019-11-17. Retrieved from <https://www.fjernkontrollen.no/trondheim/>
-

- Norwegian Energy Act § 5-5*. (1990, June 29). Retrieved September 8, 2019, from <https://lovdata.no/dokument/NL/lov/1990-06-29-50>
- NOVAP. (2018). Om varmpumper- slik virker en varmpumpe. Accessed: 2020-02-28. Retrieved from <https://www.varmpumpeinfo.no/verdt-a-vite-om-varmpumper/slik-virker-en-varmpumpe>
- NOVAP. (2020). Om varmpumper- nyttige begreper. Accessed: 2020-02-28. Retrieved from <https://www.varmpumpeinfo.no/verdt-a-vite-om-varmpumper/nyttige-begreper>
- NVE. (2015). Konesjonsbehandling av fjernvarme. Retrieved September 8, 2019, from <https://www.nve.no/konesjonssaker/konesjonsbehandling-av-fjernvarme/>
- Olje- og energidepartementet. (2019). Energibruken i ulike sektorer. Energifakta Norge. Retrieved from <https://energifaktanorge.no/norsk-energibruk/energibruken-i-ulike-sektorer/>
- Ottesen, S. Ø., & Tomasgard, A. (2015). A stochastic model for scheduling energy flexibility in buildings. *Energy*, *88*(100), 364–376.
- Ottesen, S. Ø., Tomasgard, A., & Fleten, S.-E. (2016). Prosumer bidding and scheduling in electricity markets. *Energy*, *94*(100), 828–843.
- Palensky, P., & Dietrich, D. (2011). Demand side management: Demand response, intelligent energy systems, and smart loads. *IEEE Transactions on Industrial Informatics*, *7*(3), 381–388.
- Palmer, P. B., & O’Connell, D. G. (2009). Regression analysis for prediction: Understanding the process.
- Pedhazur, E. J. (1982). Multiple regression in behavioral research : Explanation and prediction. New York: Holt, Rinehart and Winston.
- Popela, P., Novotný, J., Roupec, J., Hrabec, D., & Olstad, A. (2014). Two-stage stochastic programming for engineering problems. *Engineering Mechanics*, *21*, 335–353.
- ProgramByggerne. (2020). Simien. Retrieved June 3, 2020, from <http://www.programbyggerne.no/>
- Regjeringen. (2018). *co₂ avgiften*. Retrieved from <https://www.regjeringen.no/no/tema/okonomi-og-budsjett/skatter-og-avgifter/veibruksavgift-pa-drivstoff/co2-avgiften/id2603484/>
- Rønneseth, Ø., & Sartori, I. (2019). Is it possible to supply norwegian apartment blocks with 4th generation district heating? *Energies*, *12*(5). Retrieved from <http://search.proquest.com/docview/2316650820/>
- Rutz, D., Winterscheid, C., Pauschinger, T., Grimm, S., Roth, T., Doračić, B., . . . Hummelshøj, R. (2019). *Upgrading the performance of district heating networks*. Renewable Energies.

-
- Sachs, J., & Sawodny, O. (2016). Multi-objective three stage design optimization for island microgrids. *Applied Energy*, *165*(100), 789–800.
- Sameti, M., & Haghghat, F. (2019). Optimization of 4th generation distributed district heating system: Design and planning of combined heat and power. *Renewable Energy*, *130*, 371–387.
- Sarbu, I., & Sebarchievici, C. (2016). *Solar heating and cooling systems: Fundamentals, experiments and applications*. Elsevier Science.
- Sarbu, I., & Sebarchievici, C. (2018). A comprehensive review of thermal energy storage. *Sustainability (Switzerland)*, *10*.
- Schmidt, D., Kallert, A., Blesl, M., Svendsen, S., Li, H., Nord, N., & Sipilä, K. (2017). Low temperature district heating for future energy systems. *Energy Procedia*, *116*, 26–38. 15th International Symposium on District Heating and Cooling, DHC15-2016, 4-7 September 2016, Seoul, South Korea. doi:<https://doi.org/10.1016/j.egypro.2017.05.052>
- Seljom, P., & Tomasgard, A. (2015). Short-term uncertainty in long-term energy system models – a case study of wind power in denmark. *Energy Economics*, *49*. doi:[10.1016/j.eneco.2015.02.004](https://doi.org/10.1016/j.eneco.2015.02.004)
- Shapiro, A., & Philpott, A. (2007). A tutorial on stochastic programming.
- Sidelnikova, M., Weir, D. E., Groth, L. H., Nybakke, K., Stensby, K. E., Langseth, B., . . . Qureishy, T. H. (2015). Kostnader i energisektoren - kraft, varme og effektivisering.
- Sinha, A., Malo, P., & Kuosmanen, T. (2015). A multiobjective exploratory procedure for regression model selection. *Journal of Computational and Graphical Statistics*, *24*(1), 154–182. Retrieved from <http://www.tandfonline.com/doi/abs/10.1080/10618600.2014.899236>
- SINTEF. (2018). Low-temperature thermal grids with surplus heat utilization – lttg+.
- Skar, C., Doorman, G., Pérez-Valdés, G. A., & Tomasgard, A. (2016). A multi-horizon stochastic programming model for the european power system.
- SSB. (2018). Fjernvarme og fjernkjøling. Retrieved from <https://www.ssb.no/statbank/table/09469/chartViewColumn/>
- Su, Z., Egging, R., Huppmann, D., & Tomasgard, A. (2015). A multi-stage multi-horizon stochastic equilibrium model of multi-fuel energy markets. *CenSES Working paper*, *2*.
- Tanaka, I., & Ohmori, H. (2016). Scenario generation with clustering for optimal allocation of renewable dg. In *2016 IEEE Innovative Smart Grid Technologies - Asia (ISGT-Asia)* (pp. 966–971).
- Tereshchenko, T. (2016). Energy planning of future district heating systems with various energy sources. Trondheim: Norwegian University of Science et al.
-

- Trochim, W. (2007). The research methods knowledge base.
- Trondheim Kommune Byplankontoret. (2018). Planbeskrivelse leangen. Retrieved from <https://www.dropbox.com/sh/5gi1873bphn67yu/AACddQ-0MuTzQsVQzO4LCOJYa?dl=0&preview=1.+Planbeskrivelse.pdf>
- Tvärne, A. (2018). Värmeförsörjning i furuset med utnyttjande av säsongslager i systemet. Unpublished.
- Vesterlund, M., Toffolo, A., & Dahl, J. (2017). Optimization of multi-source complex district heating network, a case study. *Energy*, *126*, 53–63.
- Von Rhein, J., Henze, G. P., Long, N., & Fu, Y. (2019). Development of a topology analysis tool for fifth-generation district heating and cooling networks. *Energy Conversion and Management*, *196*, 705–716.
- Wahlroos, M., Pärssinen, M., Manner, J., & Syri, S. (2017). Utilizing data center waste heat in district heating – impacts on energy efficiency and prospects for low-temperature district heating networks. *Energy*, *140*(P1), 1228–1238.
- Wooldridge, J. (2003). *Introductory econometrics: A modern approach*.
- Zhou, M., Gao, Y., & Li, G. (2008). Study on improvement of available transfer capability by demand side management, 545–550.
- Zinko, H., Agency, I. E., & voor Energie en Milieu, N. O. (2005). *Improvement of operational temperature differences in district heating systems: Iea r & d programme on district heating and cooling*. ZW Energiteknik.

Appendices

Appendix A

Traditional Stochastic Model

A.1 Indices, sets, parameters and variables

Indices and Sets:

$e \in E$	Set of all heat production technologies.
$E^C \subset E$	Subset of heat technologies of type controllable.
$E^U \subset E$	Subset of heat technologies of type uncontrollable.
$g \in G$	Set of demand types.
$i, j \in N$	Set of all nodes.
$N^P \subset N$	Subset of nodes of type heat central.
$N^B \subset N$	Subset of nodes of type branching.
$N^C \subset N$	Subset of nodes of type consumer.
$t \in T^S$	Set of strategic time periods.
$h, h' \in T^O$	Set of operational time periods.
$p \in P$	Set of all user profiles.
$\omega \in \Omega$	Set of all operational scenarios

Parameters:

$C_{ghh'p}$	Unit deficit cost for not meeting demand type g in the operational period from h to h' for user profile p [NOK/kWh].
C^A	Unit cost for adding heat to the TES [NOK/kWh].
C_e^E	CO_2 emission cost for technology e [NOK/ kg CO_2].
C_{eth}^F	Unit fuel costs of technology e in strategic period t at operational period h [NOK/kWh].
C_{ij}^T	Pipeline transportation costs from node i to node j [NOK/kWh].
COP^C	Coefficient of Performance for the centralized HP.
COP^D	Coefficient of Performance for the decentralized HPs.
$D_{githp\omega}$	Target heat demand of type g at node i in strategic period t at operational period h for user profile p in scenario ω [kWh].
F_{ij}^{MAX}	Capacity limit for the pipeline from node i to j [kWh].
$L_{gihh'p}$	Minimum percentage of demand type g at node i that must be satisfied in the operational period from h to h' for user profile p .
O_e	CO_2 factor for technology e [kg CO_2 /kWh].
Q_{it}^{-MAX}	Capacity limit for adding heat to the TES at node i in strategic period t [kWh].
Q_{it}^{+MAX}	Capacity limit for withdrawing heat from the TES at node i in strategic period t [kWh].
S_i^{START}	Initial storage level in the TES at the beginning of the planning horizon [kWh].
S_i^{MAX}	Capacity limit for stored heat (total inventory) in the TES at node i [kWh].
S_i^{END}	Planned storage level in the TES at the end of the planning horizon [kWh].
R_{ip}	Percentage of target demand at node i that user profile p stands for.
$U_{gihh'p}$	Maximum percentage of demand type g at node i that must be satisfied in the operational period from h to h' for user profile p .
X_{eith}	Uncontrollable heat from technology e available at node i in strategic period t in operational period h [kWh].
X_{eith}^{MAX}	Production capacity limit for technology e at node i in strategic period t in operational period h [kWh].
η_{ij}	Efficiency ratio (1-loss rate) for heat flow from node i to node j .
η^A	Efficiency ratio for adding heat to the TES.
η_i^S	Efficiency ratio for the stored heat in the from strategic period t to strategic period $t + 1$.
π_ω	Probability of operational scenario ω .
$\phi_{th\omega}$	Is 1 if the variables in strategic period t , operational period h and scenario ω equal the variables in scenario $\omega + 1$, otherwise it is 0.

Variables:

$f_{ijth\omega}$	Heat amount that is transported from node i to node j in strategic period t in operational period t in scenario ω [kWh].
$q_{ith\omega}^-$	Heat amount that is added to the TES at node i in strategic period t in operational period h in scenario ω [kWh].
$q_{ith\omega}^+$	Heat amount that is withdrawn from the TES at node i in strategic period t in operational period h in scenario ω [kWh].
$s_{ith\omega}$	Heat amount stored in the TES at node i in strategic period t at the end of operational period h in scenario ω [kWh].
$x_{eith\omega}$	Heat amount produced by technology e at node i in strategic period t in operational period h in scenario ω [kWh].
$y_{githp\omega}$	Delivered heat amount for demand type g in node i in strategic period t in operational period h for user profile p in scenario ω [kWh].
$z_{githh'p\omega}$	Amount of deficit load for demand type g in node i in strategic period t in the operational period from h to h' for user profile p in scenario ω [kWh].

A.2 Objective function

$$\begin{aligned}
\min \sum_{t \in T^S} \sum_{\substack{h, h' \in T^O \\ \wedge h' \geq h}} & \left(\sum_{e \in E} \sum_{i \in N} (C_{eth}^F + C_e^E O_e) x_{eith} \right. \\
& + \sum_{i \in N} \sum_{j \in N} C_{ij}^T f_{ijth} \\
& + \sum_{i \in N^C} \sum_{p \in P} C_{ghh'p} z_{githh'p} \\
& + \sum_{i \in N} C^A q_{ith}^- \\
& + \sum_{i \in N} \sum_{p \in P} C_{(EL),th}^P \frac{y_{(HW),ithp}}{COPD} \\
& \left. + \sum_{i \in N} C_{(EL),th}^P \frac{X_{eith}}{COPC} \right)
\end{aligned} \tag{A.1}$$

A.3 Constraints

Demand

$$z_{gihh'p\omega} \geq \sum_{\tau=h}^{h'} (R_{ip} D_{git\tau p\omega} - y_{git\tau p\omega}), \quad \forall g \in G, i \in N^C, t \in T^S(h, h'), \in T^O \wedge h' \geq h, p \in P, \omega \in \Omega \quad (\text{A.2})$$

$$\sum_{\tau=h}^{h'} y_{git\tau p\omega} \geq L_{gihh'p} R_{ip} D_{githp\omega}, \quad \forall g \in G, i \in N^C, t \in T^S, (h, h') \in T^O \wedge h' \geq h, p \in P, \omega \in \Omega \quad (\text{A.3})$$

$$\sum_{\tau=h}^{h'} y_{git\tau p\omega} \leq U_{gihh'p} R_{ip} D_{githp\omega}, \quad \forall g \in G, i \in N^C, t \in T^S, (h, h') \in T^O \wedge h' \geq h, p \in P, \omega \in \Omega \quad (\text{A.4})$$

Production

$$x_{eith\omega} \leq X_{eith}^{MAX}, \quad \forall e \in E^C, i \in N^P, t \in T^S, h \in T^O, \omega \in \Omega \quad (\text{A.5})$$

Nodal heat balance

$$\sum_{e \in E^C} x_{eith\omega} + \sum_{e \in E^U} X_{eith} + \sum_{j \in N} \eta_{ji} f_{jith\omega} + q_{ith\omega}^+ = \sum_{g \in G} \sum_{p \in P} y_{githp\omega} + \sum_{j \in N} f_{ijth\omega} + q_{ith\omega}^-, \quad \forall i \in N, t \in T^S, h \in T^O, \omega \in \Omega \quad (\text{A.6})$$

Pipeline

$$f_{ijth\omega} \leq F_{ij}^{MAX}, \quad \forall (i, j) \in N, t \in T^S, h \in T^O, \omega \in \Omega \quad (\text{A.7})$$

Storage

$$s_{ith\omega} = s_{it(h-1)\omega} + \eta^A q_{ith\omega}^- - q_{ith\omega}^+ \quad \forall i \in N, t \in T^S \setminus \{1\}, h \in T^O, \omega \in \Omega \quad (\text{A.8})$$

$$s_{it,1,\omega} = \eta_t^S s_{i(t-1)t_{last}^O, \omega} + \eta^A q_{it,1,\omega}^- - q_{it,1,\omega}^+ \quad \forall i \in N, t \in T^S, \omega \in \Omega \quad (\text{A.9a})$$

$$s_{i,1,1,\omega} = \eta_1^S S_i^{START} + \eta^A q_{i,1,1,\omega}^- - q_{i,1,1,\omega}^+ \quad \forall i \in N, \omega \in \Omega \quad (\text{A.9b})$$

$$s_{ith\omega} \leq S_i^{MAX}, \quad \forall i \in N, t \in T^S \setminus \{t_{last}^S\}, h \in T^O \setminus \{t_{last}^O\}, \omega \in \Omega \quad (\text{A.10a})$$

$$s_{i,t_{last}^S, t_{last}^O, \omega} \leq S_i^{END}, \quad \forall i \in N, \omega \in \Omega \quad (\text{A.10b})$$

$$\eta^A q_{ith\omega}^- \leq Q_{it}^{-MAX}, \quad \forall i \in N, t \in T^S, h \in T^O, \omega \in \Omega \quad (\text{A.11})$$

$$q_{ith\omega}^+ \leq Q_{it}^{+MAX}, \quad \forall i \in N, t \in T^S, h \in T^O, \omega \in \Omega \quad (\text{A.12})$$

Non-anticipativity

$$f_{ijth\omega} = f_{ijth(\omega+1)}, \quad \forall i \in N, j \in N, t \in T^S, h \in T^O, \omega \in \Omega \wedge \phi_{th\omega} = 1 \quad (\text{A.13})$$

$$q_{ith\omega}^+ = q_{ith(\omega+1)}^+, \quad \forall i \in N, t \in T^S, h \in T^O, \omega \in \Omega \wedge \phi_{th\omega} = 1 \quad (\text{A.14})$$

$$q_{ith\omega}^- = q_{ith(\omega+1)}^-, \quad \forall i \in N, t \in T^S, h \in T^O, \omega \in \Omega \wedge \phi_{th\omega} = 1 \quad (\text{A.15})$$

$$s_{ith\omega} = s_{ith(\omega+1)}, \quad \forall i \in N, t \in T^S, h \in T^O, \omega \in \Omega \wedge \phi_{th\omega} = 1 \quad (\text{A.16})$$

$$x_{eith\omega} = x_{eith(\omega+1)}, \quad \forall e \in E^C, i \in N^P, t \in T^S, h \in T^O, \omega \in \Omega \wedge \phi_{th\omega} = 1 \quad (\text{A.17})$$

$$y_{githp\omega} = y_{githp(\omega+1)}, \quad \forall g \in G, i \in N^C, t \in T^S, h \in T^O, p \in P, \omega \in \Omega \wedge \phi_{th\omega} = 1 \quad (\text{A.18})$$

$$z_{githh'p\omega} = z_{githh'p(\omega+1)}, \quad \forall g \in G, i \in N^C, t \in T^S, h \in T^O, p \in P, \omega \in \Omega \wedge \phi_{th\omega} = 1 \quad (\text{A.19})$$

Non-negativity

$$\begin{aligned} f_{ijth\omega}, q_{ith\omega}^-, q_{ith\omega}^+, s_{ith\omega}, x_{eith\omega}, y_{githp\omega}, z_{githh'p\omega} \geq 0, \\ \forall (i, j) \in N, e \in E, t \in T^S, (h, h') \in T^O, p \in P, g \in G, \omega \in \Omega \end{aligned} \quad (\text{A.20})$$

Appendix B

Multi-horizon Stochastic Model

B.1 Indices, sets, parameters and variables

Indices and Sets:

$e \in E$	Set of all heat production technologies.
$E^C \subset E$	Subset of heat technologies of type controllable.
$E^U \subset E$	Subset of heat technologies of type uncontrollable.
$g \in G$	Set of demand types.
$i, j \in N$	Set of all nodes.
$N^P \subset N$	Subset of nodes of type heat central.
$N^B \subset N$	Subset of nodes of type branching.
$N^C \subset N$	Subset of nodes of type consumer.
$t \in T^S$	Set of strategic time periods.
$h, h' \in T^O$	Set of operational time periods.
$p \in P$	Set of all user profiles.
$\omega \in \Omega$	Set of all operational scenarios

Parameters:

$C_{ghh'p}$	Unit deficit cost for not meeting demand type g in the operational period from h to h' for user profile p [NOK/kWh].
C^A	Unit cost for adding heat to the TES [NOK/kWh].
C_e^E	CO_2 emission cost for technology e [NOK/ kg CO_2].
C_{eth}^F	Unit fuel costs of technology e in strategic period t at operational period h [NOK/kWh].
C_{ij}^T	Pipeline transportation costs from node i to node j [NOK/kWh].
COP^C	Coefficient of Performance for the centralized HP.
COP^D	Coefficient of Performance for the decentralized HPs.
$D_{githp\omega}$	Target heat demand of type g at node i in strategic period t at operational period h for user profile p in scenario ω [kWh].
F_{ij}^{MAX}	Capacity limit for the pipeline from node i to j [kWh].
$L_{gihh'p}$	Minimum percentage of demand type g at node i that must be satisfied in the operational period from h to h' for user profile p .
O_e	CO_2 factor for technology e [kg CO_2 /kWh].
Q_{it}^{-MAX}	Capacity limit for adding heat to the TES at node i in strategic period t [kWh].
Q_{it}^{+MAX}	Capacity limit for withdrawing heat from the TES at node i in strategic period t [kWh].
S_i^{START}	Initial storage level in the TES at the beginning of the planning horizon [kWh].
S_i^{MAX}	Capacity limit for stored heat (total inventory) in the TES at node i [kWh].
S_i^{END}	Planned storage level in the TES at the end of the planning horizon [kWh].
R_{ip}	Percentage of target demand at node i that user profile p stands for.
$U_{gihh'p}$	Maximum percentage of demand type g at node i that must be satisfied in the operational period from h to h' for user profile p .
X_{eith}	Uncontrollable heat from technology e available at node i in strategic period t in operational period h [kWh].
X_{eith}^{MAX}	Production capacity limit for technology e at node i in strategic period t in operational period h [kWh].
η_{ij}	Efficiency ratio (1-loss rate) for heat flow from node i to node j .
η^A	Efficiency ratio for adding heat to the TES.
η_i^S	Efficiency ratio for the stored heat in the from strategic period t to strategic period $t + 1$.
π_ω	Probability of operational scenario ω .

Variables:

$f_{ijth\omega}$	Heat amount that is transported from node i to node j in strategic period t in operational period t in scenario ω [kWh].
$q_{ith\omega}^-$	Heat amount that is added to the TES at node i in strategic period t in operational period h in scenario ω [kWh].
$q_{ith\omega}^+$	Heat amount that is withdrawn from the TES at node i in strategic period t in operational period h in scenario ω [kWh].
$s_{ith\omega}$	Heat amount stored in the TES at node i in strategic period t at the end of operational period h in scenario ω [kWh].
$x_{eith\omega}$	Heat amount produced by technology e at node i in strategic period t in operational period h in scenario ω [kWh].
$y_{githp\omega}$	Delivered heat amount for demand type g in node i in strategic period t in operational period h for user profile p in scenario ω [kWh].
$z_{githh'p\omega}$	Amount of deficit load for demand type g in node i in strategic period t in the operational period from h to h' for user profile p in scenario ω [kWh].

B.2 Objective function

$$\begin{aligned}
\min \sum_{t \in T^S} \sum_{\substack{h, h' \in T^O \\ \wedge h' \geq h}} & \left(\sum_{e \in E} \sum_{i \in N} (C_{eth}^F + C_e^E O_e) x_{eith} \right. \\
& + \sum_{i \in N} \sum_{j \in N} C_{ij}^T f_{ijth} \\
& + \sum_{i \in N^C} \sum_{p \in P} C_{ghh'p} z_{githh'p} \\
& + \sum_{i \in N} C^A q_{ith}^- \\
& + \sum_{i \in N} \sum_{p \in P} C_{(EL),th}^P \frac{y_{(HW),ithp}}{COPD} \\
& \left. + \sum_{i \in N} C_{(EL),th}^P \frac{X_{eith}}{COPC} \right)
\end{aligned} \tag{B.1}$$

B.3 Constraints

Demand

$$z_{gihh'p\omega} \geq \sum_{\tau=h}^{h'} (R_{ip} D_{git\tau p\omega} - y_{git\tau p\omega}), \quad \forall g \in G, i \in N^C, t \in T^S(h, h'), \in T^O \wedge h' \geq h, p \in P, \omega \in \Omega \quad (\text{B.2})$$

$$\sum_{\tau=h}^{h'} y_{git\tau p\omega} \geq L_{gihh'p} R_{ip} D_{githp\omega}, \quad \forall g \in G, i \in N^C, t \in T^S, (h, h') \in T^O \wedge h' \geq h, p \in P, \omega \in \Omega \quad (\text{B.3})$$

$$\sum_{\tau=h}^{h'} y_{git\tau p\omega} \leq U_{gihh'p} R_{ip} D_{githp\omega}, \quad \forall g \in G, i \in N^C, t \in T^S, (h, h') \in T^O \wedge h' \geq h, p \in P, \omega \in \Omega \quad (\text{B.4})$$

Production

$$x_{eith\omega} \leq X_{eith}^{MAX}, \quad \forall e \in E^C, i \in N^P, t \in T^S, h \in T^O, \omega \in \Omega \quad (\text{B.5})$$

Nodal heat balance

$$\sum_{e \in E^C} x_{eith\omega} + \sum_{e \in E^U} X_{eith} + \sum_{j \in N} \eta_{ji} f_{jith\omega} + q_{ith\omega}^+ = \sum_{g \in G} \sum_{p \in P} y_{githp\omega} + \sum_{j \in N} f_{ijth\omega} + q_{ith\omega}^-, \quad \forall i \in N, t \in T^S, h \in T^O, \omega \in \Omega \quad (\text{B.6})$$

Pipeline

$$f_{ijth\omega} \leq F_{ij}^{MAX}, \quad \forall (i, j) \in N, t \in T^S, h \in T^O, \omega \in \Omega \quad (\text{B.7})$$

Storage

$$s_{ith\omega} = s_{it(h-1)\omega} + \eta^A q_{ith\omega}^- - q_{ith\omega}^+ \quad \forall i \in N, t \in T^S \setminus \{1\}, h \in T^O, \omega \in \Omega \quad (\text{B.8})$$

$$s_{it,1,\omega} = \eta_t^S \sum_{\omega \in \Omega} s_{i(t-1)t_{last}^O \omega} \cdot \pi_\omega + \eta^A q_{it,1,\omega}^- - q_{it,1,\omega}^+ \quad \forall i \in N, t \in T^S, \omega \in \Omega \quad (\text{B.9a})$$

$$s_{i,1,1\omega} = \eta_1^S s_i^{START} + \eta^A q_{i,1,1\omega}^- - q_{i,1,1\omega}^+ \quad \forall i \in N, \omega \in \Omega \quad (\text{B.9b})$$

$$\sum_{e \in E^U} X_{eith\omega} \geq q_{ith\omega}^+, \quad \forall i \in N, t \in T^S, h \in T^O, \omega \in \Omega \quad (\text{B.10})$$

$$s_{ith\omega} \leq S_i^{MAX}, \quad \forall i \in N, t \in T^S \setminus \{t_{last}^S\}, h \in T^O \setminus \{t_{last}^O\}, \omega \in \Omega \quad (\text{B.11a})$$

$$s_{i,t_{last}^S,t_{last}^O \omega} \leq S_i^{END}, \quad \forall i \in N, \omega \in \Omega \quad (\text{B.11b})$$

$$\eta^A q_{ith\omega}^- \leq Q_{it}^{-MAX}, \quad \forall i \in N, t \in T^S, h \in T^O, \omega \in \Omega \quad (\text{B.12})$$

$$q_{ith\omega}^+ \leq Q_{it}^{+MAX}, \quad \forall i \in N, t \in T^S, h \in T^O, \omega \in \Omega \quad (\text{B.13})$$

Non-negativity

$$f_{ijth\omega}, q_{ith\omega}^-, q_{ith\omega}^+, s_{ith\omega}, x_{eith\omega}, y_{githp\omega}, z_{githh'p\omega} \geq 0, \\ \forall (i, j) \in N, e \in E, t \in T^S, (h, h') \in T^O, p \in P, g \in G, \omega \in \Omega \quad (\text{B.14})$$

Appendix C

Averaged electricity price

Hour of the day	January	February	March	April	May	June	July	August	September	October	November	December
00 - 01	0,3902	0,3941	0,3931	0,3728	0,3546	0,3853	0,3953	0,3970	0,3981	0,4251	0,4033	0,4016
01 - 02	0,3847	0,3898	0,3862	0,3601	0,3401	0,3748	0,3852	0,3860	0,3911	0,4196	0,3964	0,3963
02 - 03	0,3820	0,3882	0,3834	0,3513	0,3296	0,3676	0,3797	0,3788	0,3864	0,4169	0,3918	0,3931
03 - 04	0,3822	0,3883	0,3832	0,3465	0,3218	0,3628	0,3758	0,3784	0,3860	0,4163	0,3904	0,3927
04 - 05	0,3873	0,3921	0,3856	0,3482	0,3186	0,3602	0,3757	0,3850	0,3921	0,4215	0,3963	0,3958
05 - 06	0,3963	0,4004	0,3953	0,3643	0,3378	0,3691	0,3860	0,4030	0,4095	0,4321	0,4070	0,4035
06 - 07	0,4101	0,4129	0,4110	0,3905	0,3708	0,3861	0,4068	0,4328	0,4299	0,4484	0,4208	0,4160
07 - 08	0,4376	0,4447	0,4385	0,4185	0,3943	0,3982	0,4217	0,4509	0,4494	0,4697	0,4371	0,4549
08 - 09	0,4496	0,4635	0,4573	0,4372	0,4160	0,4062	0,4326	0,4637	0,4584	0,4788	0,4472	0,4742
09 - 10	0,4452	0,4521	0,4442	0,4372	0,4191	0,4096	0,4357	0,4648	0,4567	0,4734	0,4496	0,4684
10 - 11	0,4403	0,4412	0,4340	0,4317	0,4212	0,4108	0,4356	0,4628	0,4553	0,4689	0,4467	0,4610
11 - 12	0,4280	0,4293	0,4259	0,4271	0,4174	0,4098	0,4336	0,4570	0,4522	0,4684	0,4471	0,4538
12 - 13	0,4210	0,4202	0,4182	0,4189	0,4103	0,4065	0,4305	0,4516	0,4455	0,4673	0,4464	0,4481
13 - 14	0,4185	0,4150	0,4132	0,4112	0,4036	0,4036	0,4278	0,4462	0,4415	0,4681	0,4447	0,4456
14 - 15	0,4174	0,4112	0,4076	0,4044	0,3998	0,4009	0,4259	0,4421	0,4376	0,4680	0,4461	0,4448
15 - 16	0,4182	0,4104	0,4050	0,4002	0,3943	0,3990	0,4239	0,4416	0,4373	0,4738	0,4527	0,4519
16 - 17	0,4249	0,4118	0,4040	0,3982	0,3891	0,3982	0,4223	0,4433	0,4386	0,4863	0,4564	0,4765
17 - 18	0,4460	0,4262	0,4087	0,4048	0,3930	0,4024	0,4259	0,4491	0,4501	0,4979	0,4551	0,4907
18 - 19	0,4484	0,4447	0,4148	0,4110	0,3990	0,4060	0,4286	0,4539	0,4593	0,4822	0,4464	0,4685
19 - 20	0,4308	0,4394	0,4193	0,4133	0,4014	0,4077	0,4298	0,4591	0,4566	0,4657	0,4384	0,4422
20 - 21	0,4168	0,4208	0,4204	0,4094	0,3951	0,4061	0,4300	0,4566	0,4405	0,4542	0,4306	0,4300
21 - 22	0,4092	0,4123	0,4167	0,4091	0,3899	0,4045	0,4286	0,4438	0,4291	0,4473	0,4259	0,4213
22 - 23	0,4022	0,4044	0,4080	0,4005	0,3851	0,4038	0,4208	0,4256	0,4180	0,4391	0,4181	0,4139
23 - 00	0,3922	0,3953	0,3958	0,3811	0,3650	0,3931	0,4055	0,4049	0,4027	0,4283	0,4075	0,4041

Figure C.1: Electricity price (NOK/kWh).

Appendix D

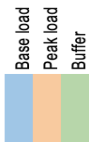
Production mix in Trondheim

Energy Sources	Jan	Feb	Mar	Apr	May	Jun	Jul	Aug	Sep	Oct	Nov	Des
Waste incineration	52 000	52 000	50 000	49 000	41 000	29 232	25 507	26 309	38 494	48 000	52 200	53 000
Bio gas boiler	400	400	400	400	350	350	350	350	350	397	400	400
Bio boiler	6 300	6 300	5 000	1 000	0	0	0	0	0	1 300	6 000	6 300
Bio oil boiler	1 700	1 200	500	0	0	0	0	0	0	100	1 000	2 500
Heatpump	0	0	0	0	0	0	0	0	0	0	0	0
Electric boiler	4 700	12 500	13 000	1 528	977	450	150	1 050	950	2 400	12 555	13 000
NG	5 000	2 000	2 000	0	0	0	0	0	0	0	800	1 000
LPG	24 000	8 000	6 225	2 500	0	0	0	0	0	500	1 200	7 900
Oil boiler	435	400	300	0	0	0	0	0	0	0	300	491
Sum	94 535	82 801	77 425	54 428	42 327	30 032	26 007	27 709	40 294	53 597	75 755	84 591

Figure D.1: Production mix in Trondheim for 2019 in MWh.

Appendix E

Production mix at Leangen



Energy sources	Jan	Feb	Mar	Apr	May	Jun	Jul	Aug	Sep	Oct	Nov	Dec
Waste incineration	0	0	0	0	1568	1468	1317	1162	1043	0	0	0
Bio gas boiler	0	0	0	0	0	0	0	0	0	0	0	0
Bio boiler	1733	1684	1900	1636	0	0	0	0	0	1179	1397	1521
Bio oil boiler	0	0	0	0	0	0	0	0	0	0	0	0
Electric boiler	688	516	507	413	10000	0	0	0	10000	522	565	552
NG	0	0	0	413	10000	0	0	0	10000	522	565	0
LPG	10000	10000	10000	10000	0	0	0	0	0	10000	10000	10000
Oil boiler	0	0	0	0	0	0	0	0	0	0	0	0
Maximum	3023.9	2717.1	2812.8	2364.6	1859.2	1467.0	1316.6	1161.9	1364.2	2125.4	2473.2	2702.8
Minimum	1732.8	1684.1	1900.1	1635.7	1295.2	880.0	739.8	521.6	630.4	1178.7	1397.0	1520.7
Average	2421.0	2199.7	2406.7	2048.7	1567.3	1175.3	1030.3	839.1	1042.2	1700.2	1962.5	2072.6
Difference (avg - min)	688.3	515.6	506.6	413.0	272.1	285.4	290.5	317.5	411.9	521.5	565.5	551.9

Figure E.1: Proposed production mix at Leangen in kWh.

Appendix F

Regression

F.1 Optimal lag length for apartments

The starts in Table F.1 show the optimal number of lags for each of the eight criteria.

Table F.1: Optimal lag length for apartments.

	LL	LR	df	p	FPE	AIC	HQIC	SBIC
0	-35784.6				5.8e-12	8.1746	8.1779	8.1843
1	31386.7	1.3e+05*	144	0.000	1.3e-18	-7.13192*	-7.08896*	-7.00585*
2	.	.	144	.	0*	.	.	.

Source: Stata.

F.2 Regression functions

F.2.1 Apartments

$$\begin{aligned} Y = & -0.6035Temp + 1.1546D_1 - 0.7694D_2 - 0.8871D_3 - 0.8039D_5 + \\ & 0.8696D_6 + 1.3876D_7 + 1.6830D_8 + 1.5984D_9 + 2.5046D_{10} + \\ & 3.2528D_{11} + 3.7098D_{12} + 3.9462D_{13} + 3.0721D_{14} + 3.0671D_{15} + \\ & 3.0459D_{16} + 3.6014D_{17} + 3.4388D_{18} + 3.8516D_{19} + 3.5184D_{20} + \\ & 2.8995D_{21} + 1.7998D_{22} + 1.5795D_{23} - 0.3454D_{26} - 1.3348D_{27} - \\ & 2.1126D_{28} - 2.4057D_{29} - 1.9780D_{30} - 2.0507D_{31} - 2.4323D_{32} \\ & -1.6573D_{33} - 1.6573D_{34} - 0.6640 \end{aligned} \tag{F.1}$$

F.2.2 Shops

$$\begin{aligned}
Y = & -0.9683Temp - 0.3547D_2 - 0.4766D_3 + 1.5567D_6 + 2.8659D_7 + \\
& 4.1055D_8 + 4.7388D_9 + 5.4444D_{10} + 5.7972D_{11} + \\
& 5.7447D_{12} + 5.7350D_{13} + 5.5947D_{14} + 5.5239D_{15} + \\
& 5.0885D_{16} + 4.8151D_{17} + 4.2629D_{18} + 3.8893D_{19} + \\
& 3.1014D_{20} + 2.2050D_{21} + 1.1927D_{22} + 0.7377D_{23} - 0.4701D_{25} - \\
& 1.7704D_{26} - 2.2935D_{27} + 1.8249D_{28} - 0.5186D_{29} - \\
& 0.5646D_{30} - 2.1880D_{31} - 1.8860D_{32} - 0.6082D_{33} + 11.0999
\end{aligned} \tag{F.2}$$

F.2.3 Kindergarten

$$\begin{aligned}
Y = & -1.1635Temp + 0.6355D_5 + 3.6276D_6 + 7.1697D_7 + \\
& 9.9623D_8 + 8.9623D_9 + 8.0376D_{10} + 8.2628D_{11} + \\
& 7.7871D_{12} + 7.1686D_{13} + 7.3883D_{14} + 7.3660D_{15} + \\
& 6.6103D_{16} + 4.5019D_{17} + 3.0142D_{18} + 2.8177D_{19} + \\
& 2.4715D_{20} + 2.3902D_{21} + 1.4415D_{22} + 1.1398D_{23} - \\
& 0.365D_{25} - 1.0980D_{26} - 1.2830D_{27} + 1.2119D_{28} - \\
& 0.6896D_{29} - 0.5609D_{30} - 1.5536D_{31} - 0.9748D_{32} + 14.0999
\end{aligned} \tag{F.3}$$

F.2.4 Nursing home

$$\begin{aligned}
Y = & -0.9744Temp + 0.2648D_1 + 0.6292D_3 + 0.7159D_4 + \\
& 1.8527D_5 + 2.5660D_6 + 3.0431D_7 + 4.4130D_8 + \\
& 4.8592D_9 + 5.0284D_{10} + 5.3328D_{11} + 5.2635D_{12} + \\
& 5.34126D_{13} + 5.3063D_{14} + 5.0394D_{15} + 4.7160D_{16} + \\
& 4.5064D_{17} + 3.6446D_{18} + 3.0852D_{19} + 1.8059D_{20} + \\
& 1.8059D_{21} + 1.3860D_{22} + 1.1398D_{23} - 0.2766D_{25} - \\
& 0.1050D_{26} + 1.5811D_{27} - 1.7224D_{28} - 1.6021D_{29} - \\
& 1.5840D_{30} - 1.9027D_{31} - 1.2602D_{32} - 0.4055D_{33} + 13.7175
\end{aligned} \tag{F.4}$$

F.2.5 Office

$$\begin{aligned} Y = & -0.84739Temp + 0.8785D_4 + 1.9660D_5 + 3.8097D_6 + \\ & 5.4705D_7 + 6.1393D_8 + 6.3925D_9 + 6.2753D_{10} + \\ & 6.3805D_{11} + 6.3890D_{12} + 6.2500D_{13} + 6.0930D_{14} + \\ & 5.8191D_{15} + 5.3324D_{16} + 4.7586D_{17} + 3.8588D_{18} + \\ & 2.7488D_{19} + 2.1137D_{20} + 1.6473D_{21} + 1.2139D_{22} - \\ & 0.3210D_{25} - 1.1250D_{26} - 1.4547D_{27} - 1.3697D_{28} - \\ & 0.8060D_{29} - 0.8169D_{30} - 1.5704D_{31} - 1.1628D_{32} - \\ & 0.2055D_{33} + 9.6832 \end{aligned} \tag{F.5}$$

Appendix G

Temperature scenarios

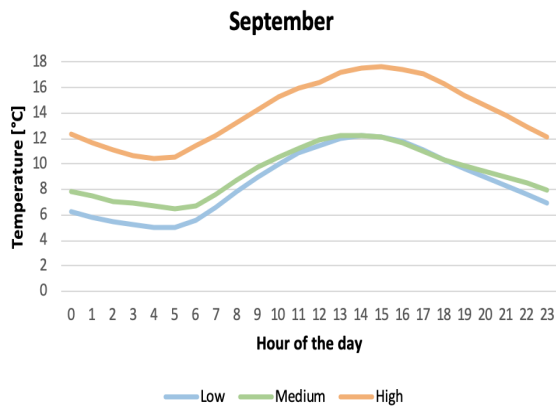


Figure G.1: Scenarios for September.

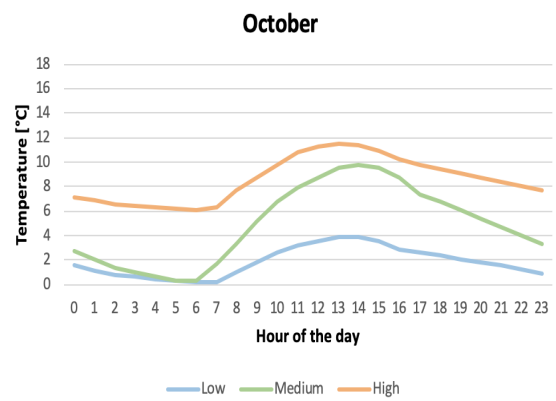


Figure G.2: Scenarios for October.

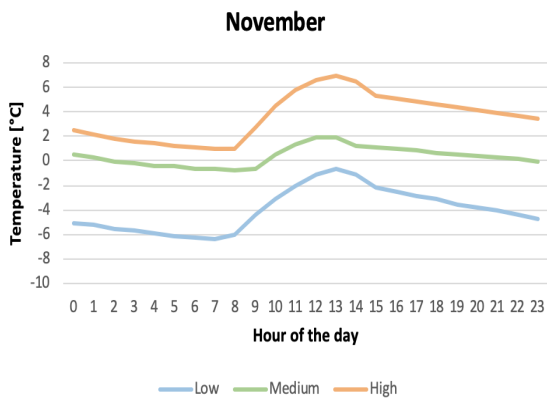


Figure G.3: Scenarios for November.

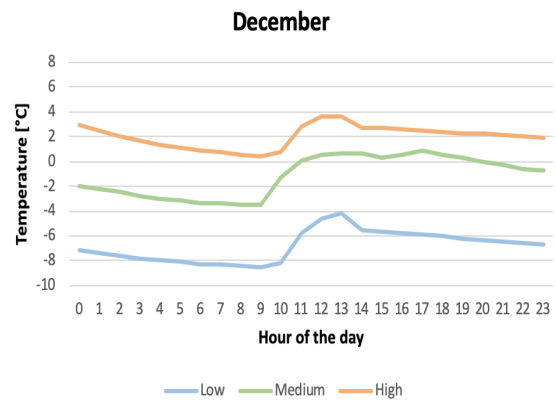


Figure G.4: Scenarios for December.

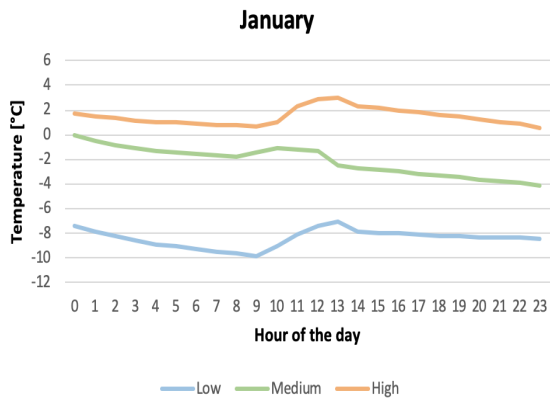


Figure G.5: Scenarios for January.

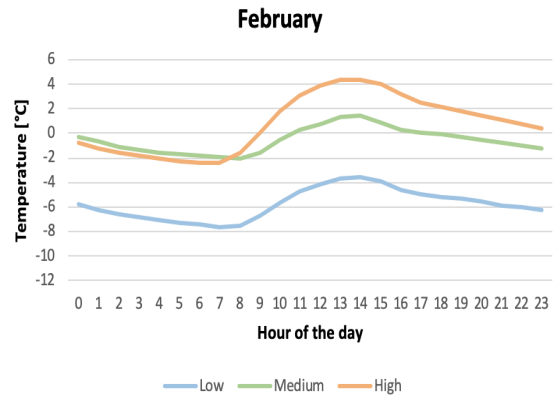


Figure G.6: Scenarios for February.

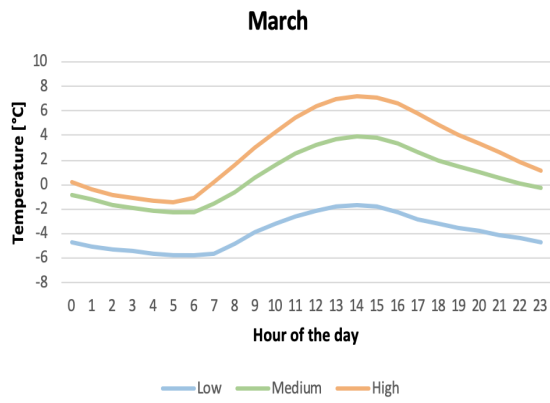


Figure G.7: Scenarios for March.

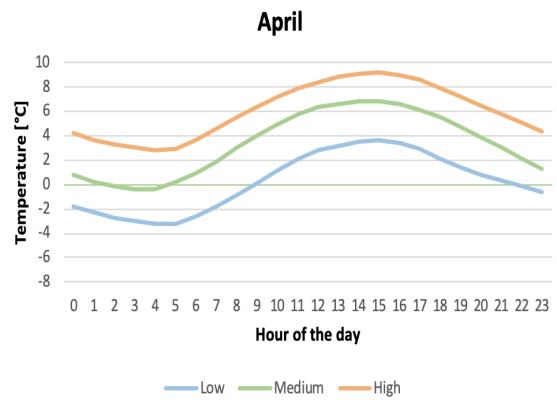


Figure G.8: Scenarios for April.

